Asphaltenes Conversion by S-Alkylation and C-Alkylation Reactions

by

Mohan Shyam Pathak

A thesis submitted in partial fulfillment of the requirements for the degree of

Master of Science

in
Chemical Engineering

Department of Chemical and Materials Engineering
University of Alberta

Abstract

Asphaltenes, defined as the fraction of crude oil soluble in toluene and insoluble in C_5 to C_7 paraffinic solvents, constitute the lowest value fraction of heavy oil. Sulfur is the most abundant heteroatom in asphaltenes. The present work explores two approaches for upgrading asphaltenes using chemical reactions focused on aliphatic C-S bonds, which are approximately 30 % of the C-S bonds in asphaltenes.

The first approach in the present work investigated the sulfur alkylation enabled scission of C-S bonds using methyl iodide at 75 °C under nitrogen environment. Reaction of selected organosulfur compounds (acyclic thioethers, cyclic thioethers and thiophene) with methyl iodide was conducted to confirm the chemistry of C-S bond cleavage by S-alkylation. Successful C-S bond cleavage in aliphatic thioethers motivated an attempt to use the same reaction with *n*-pentane precipitated asphaltenes from Athabasca bitumen. Solid product from the reaction was analyzed to contain above 10 wt% iodine. This solid product was further analyzed using thermogravimetric analysis. The reaction affected the thermal behavior of the product in the temperature range 250–350 °C, which was mainly due to iodine-related loss in this temperature range. Reaction of methyl iodide did not increase the yield of paraffin soluble products from asphaltenes.

The second approach explored C-S bond scission concomitant with C-alkylation in organosulfur compounds by 1-hexene in presence of an amorphous silica-alumina catalyst, SIRAL®40. The presence of an acid catalyst facilitated C-S bond scissions in some thioether bonds. Tetrahydrothiophene and diphenyl sulfide was found to be fairly stable at the reaction conditions of 325 °C temperature and self-generated pressure. Benzyl phenyl sulfide and dibenzyl sulfide

were completely converted to products at the reaction conditions employed in this study. C-S bond scission in dibenzyl sulfide led to the formation of sulfur free molecules when the acid catalyst was present. In case of benzyl phenyl sulfide existing C-S bonds were broken and some new C-S bonds were formed, which included the formation of diphenyl sulfide. Detection of H_2S in gas product indicated the C-S bond scission and sulfur elimination in case of alkyl sulfide, dibenzyl sulfide and benzyl phenyl sulfide.

Key words: Asphaltenes, Aliphatic sulfur, Thiophenic sulfur, C-S bond scission, Oilsands bitumen upgrading, Methyl iodide, SIRAL$^{®}$40

Acknowledgement

Table of Contents

List of tables

List of figures

Abbreviations

Abbreviation	Meaning
ABC	Asphaltenic Bottom Cracking
ASA	Amorphous Silica Alumina
ASTM	American Society for Testing and Materials
BPS	Benzyl Phenyl Sulfide
Cal	California
Can	Canada
DBS	Dibenzyl Sulfide
DBT	Dibenzothiophene
DMF	Dimethylformamide
DnBS	Di-*n*-Butyl Sulfide
DSC	Differential Scanning Calorimeter
FE-SEM	Field Emission - Scanning Electron Microscopy
Fr	France
FT-ICR-MS	Fourier Transform Ion Cyclotron resonance Mass Spectroscopy
GC	Gas Chromatography
GC-MSD	Gas Chromatography – Mass Selective Detector
GPC	Gel Permeation Chromatography
HP	High Purity
HPLC	High Performance Liquid Chromatography
Kw	Kuwait
MCR	Micro Carbon Residue
NIST	National Institute of Standards and Technology
NMR	Nuclear Magnetic Resonance
SEC	Size Exclusion Chromatography
SEM	Scanning Electron Microscopy
Tex	Texas
TGA	Thermogravimetric Analysis

THF	Tetrahydrofuran
THT	Tetrhydrothiophene
UHP	Ultra-High Purity
VPO	Vapor Pressure Osmometry
XANES	X-Ray Near Edge Structure
XPS	X-Ray Photoelectron Spectroscopy
XRF	X-Ray Fluorescence

1. Introduction

1.1. Background

Operationally crude oil can be classified into four fractions namely Saturates, Aromatics, Resins and Asphaltenes. Saturates, Aromatics and Resins are the *n*-pentane soluble material that are classified based on solubility and adsorption according to the ASTM D 2007 standard test method. The relative content of these fractions in a crude oil are highly dependent upon the oil reserve.[1] The properties and relative abundance of these fractions also depends upon the methods employed for separating these fractions.[2] Asphaltenes is defined as the fraction of crude oil soluble in toluene and insoluble in *n*-alkane solvents. Asphaltenes is ultra-complex and heaviest fraction of crude oil. Presence of this fraction poses problems at every stage of oil processing.[3]

Asphaltenes used in this study has been separated from oil sand bitumen using normal pentane as solvent during the solvent deasphalting processing step. Therefore the term "nC_5-Asphaltene" is used for asphaltene material used in this study to signify that it was produced by nC_5 precipitation. During processing of heavy oils, if the asphaltenes are not removed before processing, there is a risk that the asphaltenes fraction can precipitate from the oil phase.

Asphaltenes in heavy oil limits the conversion that can be achieved employing currently available technologies both in thermal and catalytic categories. Conversion of heavy oil into useable products is achieved by employing processes categorized broadly as thermal and heterogeneous catalytic processes. Thermal processes (visbreaking, delayed coking and fluid coking) employ temperatures in the range of 430 to 500 °C. Heterogeneous catalytic processes (fluid catalytic cracking, fixed bed hydrocracking and slurry residue hydroconversion) employ high temperature in presence of solid catalysts. Hydrocracking and hydroconversion processes

use hydrogen too. Heavy oils, when processed at high temperatures, are prone to liquid-liquid phase separation. Asphaltenes plays key role in this phase separation. This phase separation ultimately leads to formation of coke.[4]

Heavy oil from oil sands bitumen contains around 15 wt% *n*-pentane precipitated asphaltenes.[1] Using available coking technologies, only 30% of asphaltenes can be thermally converted to liquid products and rest of the asphaltenes ends up as less valuable petroleum coke. The formation of coke from oil sands bitumen is considered a loss due to the high sulfur and metals content of the coke.

Canadian oil sand bitumen production totaled nearly 2.5 million barrels per day (0.4×10^6 m^3/day) in 2016.[5] Therefore loss of production that can potentially be attributed to formation of coke is equivalent to 262,500 barrel per day. Asphaltenes in conventional crude oils has the same fate. Therefore the extent of loss of material to petroleum coke is huge if entire oil production around the world is considered.

Self-aggregation is considered important in asphaltene behavior (phase separation) during its processing at high temperature. The interaction (attractive) forces between asphaltenes molecules cause aggregation and likely contribute to insolubility in paraffinic solvents.

Asphaltene conversion strategies attempted by many researchers have been focused on cleaving C-C bonds[6, 7, 8] in cracking or forming new C-C bonds in alkylation.[9] Researchers have observed that C-S bond cleavage may also lead to asphaltene transformation.[10, 11, 12, 13]

One example of asphaltene degradation is hydrodesulfurization of asphaltenes over proprietary catalyst in a hydrogen rich environment with little increase in hydrogen content of product.[11] Desulfurization with little hydrogen addition indicate that C-S bond cleavage is the main reaction

taking place. Therefore cleavage of C-S bond can be considered as an important reaction in the conversion of the asphaltenes.

The present work explores the two strategies employed for C-S bond cleavage in asphaltenes, namely S-alkylation and C-alkylation, i.e. alkyl addition to sulfur and addition to carbon respectively. The S-alkylation method has been explored by Shaw.[10] C-alkylation enabled C-S bond cleavage and it was speculated to be the origin of asphaltenes to oil conversion by Mao.[13]

S-alkylation is widely used in the rubber industry. Successful application of methyl iodide in cleaving C-S bond in vulcanized rubber[14] inspired use of methyl iodide for reaction with asphaltenes. Significant reduction in molecular weight has been reported by reacting asphaltenes with methyl iodide.[10] It was hypothesized that the product resulting from reaction between asphaltenes and methyl iodide is lower temperature boiling hydrocarbons as compared to starting asphaltenes. The work presented in this thesis explores the S-alkylation reaction of asphaltenes and with model organosulfur compounds representing compound classes with C-S bonds present in asphaltenes.

C-alkylation of asphaltene using propylene over silica-alumina catalyst has resulted in measurable conversion of asphaltenes into maltenes (13-23 wt%). It was speculated that this conversion was the result of C-S bond scission during the alkylation reaction. At the same time alkylation was observed to increase the hydrogen content of the asphaltenes.[13] Further study is needed to support this observation. Therefore model organosulfur compounds were used in this work and reacted with 1-hexene over a silica-alumina catalyst to explore this chemistry.

It was envisioned that the work performed in this study can be implemented in processing plant for converting asphaltenes into oil for further processing into finished product. The asphaltenes

from deasphalting unit will be dissolved into a suitable solvent and fed to the reactor using alkylation reaction. The reactor effluent will be separated for solvent recycle and obtaining the product from asphaltene conversion. This implementation scheme will vary depending upon the existing processing plant configuration.

1.2. Objective

The objective of this work was to explore C-S bond scission in organosulfur compounds and asphaltenes using two approaches. The first approach was the reaction with methyl iodide and the second approach was reaction with an olefin in the presence of an acid catalyst.

1.3. Scope of work

The present work is mainly focused on the reactions involving C-S bonds in asphaltenes and representative model organosulfur compounds. The structure of the thesis is as follows:

Chapter 2: Literature review of previous research related to this study.

Chapter 3: Model organosulfur compound reactions with methyl iodide. The purpose of this work was to confirm the reaction chemistry of methyl iodide and C-S bonds in thioethers.

Chapter 4: Reaction of asphaltenes with methyl iodide via S-alkylation reaction. Work presented in this chapter was an applied study to evaluate the same reaction chemistry as in Chapter 3 for the material of interest, i.e. nC$_5$-asphaltenes.

Chapter 5: Model organosulfur compound alkylation with 1-hexene in the presence of an amorphous silica-alumina (SIRAL®40) catalyst. This work was used for exploring the C-S bond scission chemistry by reaction with 1-hexene in presence of SIRAL®40.

Chapter 6: Final Conclusion. This chapter presents the major findings from individual chapters.

1.4. References

1. Gray, M. R. Upgrading Oilsands Bitumen and Heavy Oil, 1st Edition; The University of Alberta Press: Edmonton, Alberta, **2015**.

2. Aske, N.; Kallevik, H.; Sjöblom, J. Determination of Saturate, Aromatic, Resin, and Asphaltenic (SARA) Components in Crude Oils by Means of Infrared and Near-Infrared Spectroscopy. *Energy Fuels* **2001**, 15, 1304-1312.

3. Mullins, O. C.; Sheu, E. Y.; Fine Particle Society; American Chemical Society; American Chemical Society Structures and Dynamics of Asphaltenes; Plenum Press: New York, **1998**.

4. Wiehe, I. A. A phase-separation kinetic model for coke formation. *Ind. Eng. Chem. Res.* **1993**, 32, 2447-2454.

5. Alberta Energy Facts and statistics (http://www.energy.alberta.ca/OilSands/791.asp)

6. Kenneth A. Gould, K. A. Chemical Depolymerization of Petroleum Asphaltenes. *Fuel* **1978**, 57, 756-762.

7. Speight, J. G.; Moschopedis, S. E. On the Polymeric Nature of Petroleum Asphaltenes. *Fuel* **1980**, 59, 440-442.

8. Savage, P. E.; Klein, M. T. Asphaltene Reaction Pathways. 2. Pyrolysis of n-pentadecylbenzen. *Ind. Eng. Chem. Res.* **1987**, 26, 488-494.

9. Prado, G. H. C.; Klerk, A. D. Alkylation of Asphaltenes Using a FeCl3 Catalyst. Energy *Fuels* **2015**, 29, 4947−4955.

10. Shaw, J. E. Molecular Weight Reduction of Petroleum Asphaltenes by Reaction with Methyl Iodide-Sodium Iodide. *Fuel* **1989**, 68, 1218-1220.

11. Asaoka, S.; Nakata, S.; Shiroto, Y.; Takeuchi, C. Asphaltene Cracking in Catalytic Hydrotreating of Heavy Oils 2. Study of Changes in Asphaltene Structure during Catalytic Hydroprocessing. *Ind. Eng. Chem. Pro. Des. Dev.* **1983**, 22, 242-248.

12. Papayannakos, N. Kinetics of Catalytic Hydrodesulfurization of a Deasphalted Oil and of the Asphaltenic and Non-Asphaltenic Fractions of a Petroleum Residue. *Appl. Catal.* **1986**, 24, 99-107

13. Mao, X. Alkylation of Asphaltenes. MSc Thesis, University of Alberta, Edmonton, AB, Canada, **2015**.

14. Selker M. L.; Kemp A. R. Reaction of Methyl Iodide with Sulfur Compounds. *Ind. Eng. Chem.* **1944**, 36 (January), 16-20.

2. Literature Review

2.1. Introduction

This chapter provides background information on asphaltenes, which is the industrial feed material of interest. The remainder of the literature review is focused on reactions leading to C-S bond cleavage, and focused on two reactions in particular:

(i) Reaction of iodomethane with aliphatic sulfur leading to C-S bond cleavage.

(ii) Alkylation of sulfur by olefins over an acid catalyst with concomitant C-S bond cleavage.

2.2. Asphaltenes: characterization and structure

As Francis Crick[1] stated "If you want to understand function, study structure", numerous attempts has been performed at deciphering the structure of asphaltenes.

Asphaltenes is defined as the fraction of liquid oil that is soluble in toluene but is separated by precipitation on adding a large quantity of *n*-alkane solvents.[2] Standard test method ASTM D6560 uses *n*-heptane as solvent for determining asphaltene content in petroleum crude oil or petroleum products.[3] However, the asphaltenes fraction can also be defined by precipitation with other paraffinic solvents. Asphaltenes is named prefixed with the solvent used for separating the asphaltenes from oil. For example if *n*-heptane is used as solvent then the asphaltenes is termed as "C_7-asphaltenes".

Asphaltenes constitute the heaviest fraction of liquid oils as obtained after fractionating oil using solvents. It is a complex mixture of compounds of hydrogen, carbon and heteroatoms. A large number of researchers have strived to understand the general structure of asphaltenes. Mullins[4]

and Wiehe[5] presented an extensive collection of work on the asphaltenes physical behavior. A single measurement is not sufficient to assign a generalized structure to asphaltenes. Therefore a combination of results obtained from elemental composition measurement, molecular weight measurement, optical absorption and a range of spectroscopic methods have enabled researchers to come closer to defining the main structural elements in asphaltenes.

Siskin[6] has reported analysis results for C_7 asphaltenes from various crude oil sources. Results from elemental composition measurement, X-ray Photoelectron Spectroscopy (XPS) and solid-state ^{13}C NMR methods have been reported and are presented here.

Table 2.1 Elemental composition of C_7- asphaltenes[6]

C_7 asphaltene source	Elements, wt%					Metal, wppm	
	C	H	S	N	O	Ni	V
Campana	87.6	8.2	0.5	1.5	2.2	54	81
Heavy Canadian (Cold Lake)	84.7	7.9	4.5	1.2	1.6	320	697
Lloydminster-Wainwright	80.0	8.0	7.9	1.3	2.7	417	1100
Maya	82.3	7.9	6.6	1.2	1.8	724	1468
Mid-Continent US	84.9	8.6	3.8	1.0	1.6	188	309
San Joaquin Valley	84.5	8.3	2.3	2.6	2.3	594	540

The elemental composition is presented in table 2.1. Hydrogen to carbon atomic ratio in C_7 asphaltenes was found to be in the range of 1.1 to 1.2. This indicated that asphaltenes is a hydrogen poor fraction compared to the oils from which it was derived. Majority of heteroatom in asphaltenes is sulfur.

Results from XPS and solid state ^{13}C NMR analysis provided information about the type of carbon (aromatic versus methyl). Number of hydrogen and sulfur atoms per 100 carbon atoms are presented as shown in table 2.2. The number of aromatic carbons per cluster as measured using solid-state ^{13}C NMR method is also shown in table 2.2. Presenting the number of atoms per 100 carbon atoms in asphaltene provides an easily comprehensible structural perspective on the molecules present in the asphaltenes fraction. The cluster in this case is defined as the fused condensed multiple aromatic rings.

Table 2.2 Number of hydrogen, sulfur and aromatic carbon atoms per 100 carbon atoms in C$_7$ asphaltenes[6]

| Asphaltenes source | Number of atoms per 100 carbon atoms in C$_7$ asphaltenes | | | | |
| | Elemental | XPS | Solid-state ^{13}C NMR | | |
	Hydrogen	Sulfur	Aromatic Carbon	Methyl Carbon	Aromatic Carbons per cluster
Campana	112	0.3	49	10.5	21
Mid-Continent US	122	1.1	36	12.6	17
San Joaquin Valley	118	1.0	39	14.3	19
Lloydminster-Wainwright	120	3.4	36	14	14
Maya	115	2.7	49	12.7	22
Heavy Canadian (Cold Lake)	112	2.2	45	13.3	19

Measurement of molecular weight has been estimated using numerous methods. The average molecular weight for molecules in the asphaltene fraction has been reported to vary in wide range from 700-10000 g/mol depending upon method employed to measure it and also the source

of asphaltenes. Methods used were, among other, Vapor Pressure Osmometry (VPO), Gel Permeation Chromatography (GPC), and Mass Spectrometry (MS).

Molecular weight measurements using the VPO method have been reported by Wiehe[5] and Moschopedis.[7] It has also been reported that VPO overestimates the molecular weight because of suspected aggregation of asphaltenes during measurement. While using VPO, the measured molecular weight depends upon solvent, technique and temperature of measurement.[5]

Use of Fourier transform ion cyclotron resonance mass spectrometry (FT-ICR-MS) for analysis of petroleum macromolecules has been able to resolve nearly 17000 compounds. Using mass spectrometry the average molecular weight has been reported to be less than 1000 g/mol.[5]

Time-resolved fluorescence depolarization and molecular diffusion measurements has been used by Mullins and coauthors for measuring average molecular weight of asphaltenes and they reported the result to be in order of 700 g/mol.[4]

The relative number of constituent atoms as presented in tables 2.1 and 2.2 coupled with the average molecular weight of asphaltene can be used for speculating about a generalized asphaltenes structure. Based on different assumed average molecular weights of asphaltenes, the number of total carbon atoms, and sulfur atoms can be calculated per molecule. One sample calculation was done for asphaltenes derived from Canadian heavy. The calculation results are presented in table 2.3. It indicated that on average at least one sulfur atom is present in every molecule, assuming that the distribution of heteroatoms is even across all molecules. Sulfur is the most abundant heteroatom in asphaltenes (table 2.1) and therefore C-S bonds are expected to play an important role in asphaltenes behavior.

Table 2.3 Sample calculation for average number of carbon, and sulfur atoms in a typical C_7-asphaltenes molecule derived from Canadian heavy crude oil.

Molecular weight	Carbon	sulfur
700	49.4	1.1
1000	70.5	1.5
1500	100.5	2.2

The number of aromatic carbon per cluster, as presented in table 2.2, illustrates another aspect of asphaltenes structure. This indicates the presence of four to five ring polynuclear aromatics in an average cluster in asphaltenes. Combining the information in table 2.2 on total number of aromatic carbons and number of aromatic carbon per cluster, it indicates the presence of two or more polynuclear aromatic clusters in the asphaltenes.

Optical absorption and fluorescence emission measurements with molecular orbital calculations has been used with an aim of identifying the number of rings in asphaltenes. These studies have concluded that asphaltenes molecules contains about 7 to 10 aromatic rings. These findings were used to support the proposed island structure of asphaltenes.[4,5] A similar finding has been reported for studies done on Maya Asphaltenes.[8]

Speight speculated that asphaltenes contain on an average of 1 to 4 ring systems and a maximum of 6 aromatics rings each.[9] This is in line with conclusion drawn from information in table 2.2 regarding number of clusters in asphaltene molecules.

^{13}C NMR and X-ray studies showed that carbon distribution typically contained 40% of the carbon as aromatics and remaining carbon as aliphatic carbon. Nearly 90% of hydrogen was

found on the aliphatic carbon, especially as methylene groups. X-ray diffraction studies indicated that asphaltenes occurred as stacked layers of poly-nuclear aromatic ring systems.[10] Island-type structures were observed using atomic force microscopy for coal derived asphaltenes; the structures had one poly-nuclear aromatic core and alkyl chains as pendent groups.[11]

2.3. Sulfur atom in asphaltenes

Numerous attempts have been made to determine the type of sulfur bonds present in asphaltenes. There is a wide range of observations regarding the bonds between carbon and sulfur in asphaltenes derived from oils sands resources. Payzant et al.[12] reported that bitumen from Northern Alberta contains only cyclic sulfide and thiophenes.

Zhao et al.[13] studied the reactivity of sulfur species in Athabasca bitumen pitch using XPS (X-ray photoelectron spectroscopy) methodology. Using the sulfur reactivity data, thiophenic and aliphatic sulfur content was reported. Without oxidation of sample, no sulfoxide or sulfone species were reported in the Athabasca bitumen samples. About 65-80% of the total sulfur exist as thiopehens and remainder being sulfide species.

Asphaltenes precipitated from a Saudi Arabian black oil using *n*-pentane solvent was analysed for sulfur speciation using XANES by Pomerantz.[14] Thiophenic sulfur was found to be the dominant species in each sample. About 90% of the total sulfur was reported as thiophenic sulfur and sulfide species were about 5%. Remainder of the sulfur species detected were elemental sulfur, sulfone, sulfoxide and sulfate.

The presence of sulfur bridges in Athabasca asphaltenes has been inferred from the formation of synthetic asphaltenes after reaction between cholesterol and sulfur at 170 °C for 7 days in a

nitrogen environment. The formation of synthetic asphaltenes was attributed to aromatization and condensation of smaller molecules with sulfur acting as bridge.[15]

Hofmann[16] performed reduction of C_7 asphaltenes (14 wt% sulfur content) derived from Rozel Point crude oil using lithium in ethyl amine (Li/EtNH$_2$) at a temperature 0 °C for a reaction time of over 18 hours. Specificity of Li/EtNH$_2$ reductive cleavage of aliphatic C-S bonds was demonstrated before analyzing the asphaltenes' reduction product. Alkane molecules formed after reduction of the asphaltenes indicated the presence of sulfide linkages in the asphaltenes. When two clusters of fused aromatic rings are connected by a sulfur between them, such linkage is termed as sulfide linkage. However, it was inconclusive whether the alkanes were from the asphaltenes matrix or from a macromolecular fraction that trapped alkanes. Nevertheless, this study provided confirmation of sulfide linkages in asphaltenes.

Siskin[6] performed XPS analysis for sulfur speciation on C_7 asphaltenes precipitated from six crudes for which elemental analysis is given in table 2.1. The sulfur speciation result is presented in table 2.4. Nearly 30 mol % of the total sulfur was present as aliphatic sulfur in all asphaltenes analyzed in this study, except the asphaltenes obtained from mid-continent US.

Table 2.4. Sulfur speciation of asphaltenes sulfur[6]

Asphaltenes source	Aliphatic Sulfur (mol %)	Thiophenic Sulfur (mol %)
Campana	31	69
Mid-Continent US	16	84
San Joaquin Valley	37	63
Lloydminster-Wainwright	29	71
Maya	32	68
Heavy Canadian (Cold Lake)	30	70

Similarly Geoffrey et al.[17] has analyzed C_7 asphaltenes derived from eight different crudes selected across the globe and reported sulfur speciation results using XANES (X-ray Near Edge Structure). The eight locations selected were California (Cal), Texas (Tex), Canada (Can), Kuwait (Kw1, Kw2, Kw3) and France (Fr1, Fr2). The XANES results are shown in table 2.5 in the order of decreasing thiophenic sulfur.

Table 2.5. Sulfur speciation of asphaltenes (%) using XANES[17]

Asphaltenes	Thiophene	Sulfide	Sulfoxide	Sulfone	Sulfate
Fr2	67	20	11	1	<1
Fr1	64	25	9	1	2
Kw1	61	35	3	<1	<1
Can	60	32	8	<1	<1
Kw3	56	34	7	2	<1
Kw2	52	43	4	2	<1
Tex	51	38	4	3	4
Cal	36	16	44	3	<1

Combining the results presented in table 2.4 and 2.5 helps to conclude that nearly 30% of total sulfur in asphaltenes from Canadian oil sands is aliphatic. Aliphatic sulfur could be in either cyclic or acyclic form. The actual location of C-S bond in asphaltenes will determine the effectiveness of the C-S bond cleavage as a strategy for asphaltenes conversion. For example, if the C-S bond in asphaltene is between two clusters in asphaltenes, then cleavage of C-S bond will result in a significant reduction in the molecular weight of the fragments produced from the conversion of the asphaltenes molecule.

Peng et. al.[18] used *n*-pentane for precipitating asphaltenes from Athabasca bitumen and reacted the C_5 asphaltenes with in situ generated nickel boride (Ni_2B) in THF (tetrahydrofuran) and methanol solvent. The desulfurization reaction proceeded with C-S bond cleavage on both sides of sulfur atom. Molecules with significantly lower molecular weight were created as a result of

this reaction. The presence of C-S linkages was demonstrated. Based on the results of this study an asphaltenes molecular structure was proposed as consisting of multiple polyaromatic cores that are linked via sulfide linkages.

Kemp-Jones[15] performed a study on the role of sulfur in asphaltenes formation in nature. Material with properties similar to asphaltenes was created by reacting smaller molecules of biological origin with sulfur. Reaction of Cholesterol with sulfur under nitrogen at 170^0C for seven days produced material (synthetic asphaltene) with properties similar to Athabasca asphaltenes. The hydrogen to carbon atomic ratio in synthetic asphaltenes was measured to be equal to 1.24 and sulfur content was measured to be equal to nearly 17 wt%. The high sulfur content was attributed to the presence of disulfide in the synthetic asphaltenes. Similar spectra were obtained when both synthetic asphaltenes and Athabasca asphaltenes were analyzed using IR (Infrared), ^{13}C NMR (nuclear magnetic resonance) and UV (Ultraviolet) spectroscopy methods. It was inferred that "sulfur plays an important role in asphaltenes formation in nature".[15]

Therefore, following on the literature that was discussed, cleaving C-S bond in asphaltene is expected to transform asphaltenes into smaller molecules with lower molecular weight.

2.4. Asphaltenes conversion by C-S bond cleavage

Desulfurization with an Asphaltenic Bottom Cracking (ABC) process at 360 to 430 °C temperature and 8.8 to 17.7 MPa pressure over bed of proprietary catalyst has been reported to lower the molecular weight and encourage the depolymerisation of asphaltenes without excessive hydrogen consumption. It was claimed that this type of upgradation of asphaltenes is not due to hydrogen addition based on the unchanged hydrogen content of the product.[19]

Similar results has been reported by Nickos, regarding formation of lower molecular weight asphaltenes molecules resulting from hydrodesulfurization performed on atmospheric residue from Greek Thasos crude oil at temperatures in the range 350 to 400 °C and 5 MPa pressure over CoMo/Al$_2$O$_3$ catalyst under hydrogen environment.[20]

Takeuchi et al.[21] reported that desulfurization of asphaltenes does not necessarily require hydrogenation of polyaromatic ring before removing the sulfur. This reaction proceeds mainly by hydrogenolysis of sulfur to convert sulfur into H$_2$S and the hydrogenation of the fragments generated after sulfur removal.

These studies indicate that cleavage of C-S bond is effective enough for producing products from asphaltenes that have lower molecular weights. Extensive hydrogen addition is not a mandatory requirement for transforming asphaltenes, although stoichiometric requirements must be met, despite some of the claims made.

Shaw[22] and Mao[23] have both speculated that asphaltenes conversion by C-S bond cleavage should be possible. The approaches to C-S bond cleavage proposed by them are explained in sections 2.5 and 2.6.

2.5. C-S bond cleavage by C-alkylation

2.5.1. C-S bond cleavage enabled conversion by alkylation over acid catalysts

Alkylation of industrially precipitated C$_5$ asphaltenes has been performed by reaction with ethylene, propylene and 1-hexene in presence of acid catalysts phosphoric acid, aluminum chloride, hydrochloric acid, and amorphous silica-alumina catalyst (SIRAL® 40). Reaction between propylene and asphaltenes in presence of SIRAL®40 at 325 °C resulted in about 20%

conversion of asphaltenes into maltenes.[23] The conversion of asphaltenes into maltenes was attributed to C-S bond cleavage.

Given the availability of olefin in thermal cracked naphtha generated during oil sand bitumen processing, this result has generated interest in studying this reaction further. Sections 2.5.2 and 2.5.3 deals with the selection and justification of an appropriate olefin and catalyst for this work. Additional information on the reaction chemistry corresponding to C-Alkylation is discussed in Chapter 5.

2.5.2. Selection of olefin

There is similarity in the total olefin content of naphtha obtained from both thermal and catalytic process. Thermally cracked naphtha from a delayed coker process contains 35-45 % olefins.[24] A similar amount (35 %) of olefins is also found in naphtha obtained from a fluid catalytic cracking process.[25] The branching of the olefins is significantly different depending upon the source of naphtha between thermal or catalytic process.

To illustrate the composition of a cracked naphtha, the composition of a catalytically cracked naphtha stream is given in table 2.6. This naphtha was produced by a fluid catalytic cracking unit that was operated at a riser outlet temperature of 482 °C with a synthetic silica-alumina catalyst. The feed material was a gas oil generated from mixed crude source. More than half of total olefins are found in the hydrocarbons containing five or six carbon atoms.[25]

Table 2.6 Composition of naphtha obtained from fluid catalytic cracking unit[25]

Hydrocarbon type	C_4 and lighter	C_5	C_6	C_7	C_8	C_9 and heavier	Total
Paraffin	2.26	6.83	5.23	3.56	2.86	13.93	34.67
Olefin	3.95	10.92	8.48	4.59	2.31	4.75	35.00
Cycloolefin	……	0.4	0.77	2.27	0.87	2.03	6.34
Aromatic	……	……	0.21	2.32	5.41	16.05	23.99
Total	6.21	18.15	14.69	12.74	11.45	36.76	100

Cady[26] has compared the composition of virgin, catalytic and thermal naphtha. Branching of olefins is higher in naphtha obtained from catalytic processes as compared to that obtained from thermal cracking. 1-Hexene is the most abundant olefin among C_6 olefins in thermally cracked naphtha. Therefore 1-hexene was selected as model olefin for the experimental work in this thesis (Chapter 5).

2.5.3. Selection of acid catalyst

Silica-alumina, or only silica, or only alumina supported catalysts have been the work horses for refining industry. These materials are widely used as part of catalysts used in hydrocracking, hydrotreating, fluidised catalytic cracking, reforming and isomerization processes. These materials may exist in both amorphous or in crystalline form.

The Brønsted acid character of silica-alumina materials is exploited to facilitate the alkylation reaction. Strongest acidity of the catalyst is not always favorable for the reaction, because it

could slow down desorption of product intermediates from catalyst surface. Therefore weaker acid sites are preferred having enough acidity to facilitate desired reaction.[27] Amorphous silica-alumina (ASA) catalysts are moderate acidity catalysts.[28] This is because amorphous silica-alumina catalyst promotes the reactions owing to its both Lewis and Brønsted type acid characteristics.[27]

Brønsted acid characteristics of acid catalysts are not favorable with respect to direct C-S bond cleavage, because most sulfides are resistant to the proton catalyzed C-S bond cleavage, as expected from the poor donor capability of sulfur atom towards the proton.[29] However, in olefin alkylation, Brønsted acid characteristics are needed for protonation of the olefins. Thus, SIRAL®40, which has Brønsted acid character has been selected as acid catalyst for use in this study.

2.6. C-S bond cleavage by S-alkylation

2.6.1. C-S bond cleavage during reaction between asphaltenes and methyl iodide

Shaw[22] explored the reduction of asphaltene molecular weight by C-S bond cleavage enabled by sulfonium intermediate. Four different crude oils, namely, Maya, Hondo, Oriente, and Midway Sunset were selected. *n*-Pentane was used as solvent for precipitating asphaltenes from all these four crude oils. Asphaltenes thus obtained was reacted with methyl iodide and sodium iodide in tetrahydrofuran (THF) and dimethylformamide (DMF) solvents at 75 °C under nitrogen environment for 24 hours. The product mixture was extracted with chloroform and washed with demineralised water. Product was obtained after solvent evaporation. The molecular weight of the starting material and product asphaltenes was determined using Vapor Pressure Osmometry (VPO) and Size Exclusion Chromatography (SEC). A significant reduction in molecular weight

(up to 70%) of the asphaltenes has been reported by reaction with methyl iodide.[22] This reduction in molecular weight has been reported along with a slight reduction in sulfur content of asphaltenes product. This reaction is proposed to follow the route of sulfonium salt as intermediate. Significant ingress of iodine in asphaltenes is also reported. Shaw[32] proposed the reaction as shown in figure 2.1.

$$R-S-R' + CH_3I \xleftrightarrow{\text{DMF}} R-\overset{\overset{\displaystyle CH_3}{|}}{\underset{\underset{\displaystyle I^-}{+}}{S}}-R' \xleftrightarrow[\text{NaI}]{\text{DMF}} R-S-CH_3 + R'\text{-I}$$
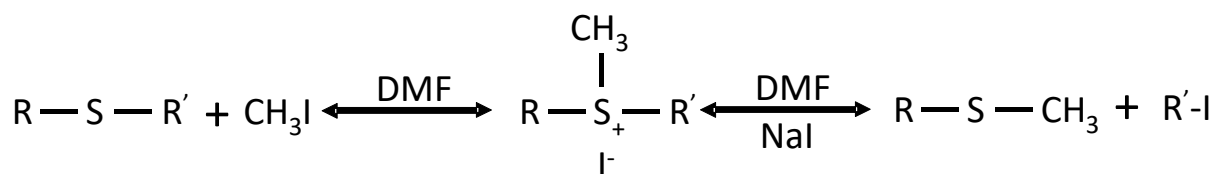
Figure 2.1 Reaction of methyl iodide with sulfides

2.6.2. S-alkylation mechanism and C-S bond cleavage via sulfonium intermediate

Oae[29] presented a comprehensive study on organic chemistry of sulfur. Carbon and sulfur bonds in sulfides are generally stable towards nucleophilic reagents. However when the sulfur atoms donates electrons to an electrophilic reagent, i.e. the sulfur is the nucleophile, the C-S bond of sulfides becomes susceptible to cleavage.

The sulfur atom in a sulfide molecule is weakly nucleophilic and reacts with alkyl halides readily. This reaction is promoted by polar solvents, such as methanol and dimethylformamide. The rate of reaction decreases with increasing chain length of the alkyl halide. So, methyl halide is most reactive. Iodide is more reactive than other halide members. Therefore methyl iodide is the preferred reagent for reaction with alkyl sulfides.

Methyl iodide reacts with organic sulfides via an ionic sulfonium iodide intermediate with positive charge on sulfur. Sulfonium species consists of two covalent bonds, one coordinative bond and one ionic bond (see Figure 2.1). The positive charge on sulfur in sulfonium salts produces a strong dipole moment and thus the C-S bonds weakens. The positive charge on sulfur enables it to accept the C-S bond electrons and thus transferring positive charge on to the carbon attached to sulfur. Among three C-S bonds, one C-S bond breaks. The C-S bond that breaks is the bond for which formation of most stable carbonium ion is produced.[29]

The sulfonium salt formation is in equilibrium with its components under all conditions. Pressure drives the equilibrium to the right and elevation of temperature has the opposite effect.[30] The reaction path given in figure 2.1 indicates the reduction in number of gas molecules while moving from left to right. Therefore as per Le Chatelier's principle the equilibrium is driven to the right side of reaction as pressure is increased.
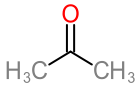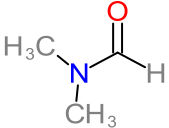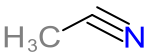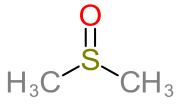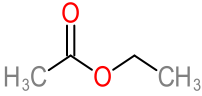
Methionine contains nitrogen and sulfur groups, which could in principle compete for alkylation. Sulfur was the most nucleophilic center and therefore lead to the formation of sulfonium salt, while no reaction with nitrogen was observed. This was concluded as N-methyl formation was not detected.[29] Therefore C-S bond cleavage by reaction with methyl iodide appear to proceed without any interference from presence of basic nitrogen species in molecule.

Additional information on the reaction chemistry corresponding to S-Alkylation is discussed in Chapter 3.

2.7. Selection of solvent for S-alkylation reaction

As mentioned in section 2.6.2, the S-alkylation reaction requires a polar reaction medium to progress. Table 2.7 lists widely used polar solvents in organic chemistry.[31] The dipole moment for each solvent is also noted in this table.

Table 2.7 Polar solvents and their dipole moments[31]

Solvent	Structure	Dipole moment (D, Debye)
Acetone		2.88
N, N- Dimethylformamide (DMF)		3.82
Acetonitrile		3.92
Dimethyl Sulfoxide		3.96
Tetrahydrofuran		1.75
Ethyl Acetate		1.78
Dichloromethane		1.60

Dimethyl sulfoxide has the highest dipole moment and therefore it could be the best solvent for the reaction with methyl iodide. This solvent contains one sulfur atom and the present work deals with the reaction between sulfur and methyl iodide. It was suspected that sulfur in dimethyl sulfoxide may interfere with our intended reaction. N,N-dimethylformamide (DMF) and acetonitrile are similar in terms of dipole moment. Finally DMF was finally selected as polar solvent as reaction media for this study, which will be reported in Chapters 3 and 4.
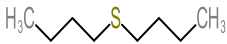
2.8. Selection of organosulfur model compounds
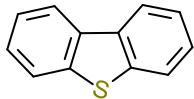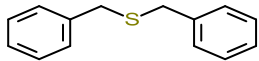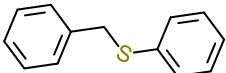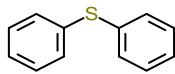
As detailed in section 2.2, asphaltenes molecules are complex macromolecules. Therefore ascertaining the reaction pathways is challenging. Methyl iodide being a reactive compound may react with asphaltene in many ways in addition to cleavage of C-S bonds. Herbert[32] has demonstrated that reaction between aromatics and methyl iodide proceed as methylation reaction. Asphaltenes contain aromatic molecules that may react with methyl iodide.

Model compounds are thus used to better understand possible reactions and thus help to navigate through complex reaction pathways with asphaltenes.

The work presented in Chapter 4 deals with reactions focused around the C-S bond in asphaltenes. Therefore model organosulfur compounds were selected for study in Chapter 3. Multiple model compounds were selected to represent different chemical environments for the C-S bonds that could be present in asphaltenes.

Following compound were selected for representing some of the chemical bonds in asphaltenes.

1. Di-*n*-butyl sulfide ( ): -This compound represents the chemical bond between carbon and sulfur in asphaltene. Along with bond between carbon and sulfur, di-*n*-butyl sulfide represent the alkyl chain present in asphaltenes. Results obtained by Hofmann[16] indicated the presence of sulfide linked alkyl chains. This molecule represent the acyclic aliphatic C-S bonds present in asphaltenes.

2. Tetrahydrothiophene ( ): - Payzant et. al.[12] has reported the presence of cyclic sulfides in asphaltenes. Tetrahydrothiophene represents cyclic sulfides present in asphaltenes.

3. Dibenzothiophene ( ): - As reported in table 2.4, thiophenic sulfur constitutes nearly 70 wt% of the total sulfur content in asphaltenes. This molecule also represent the aromatics ring present in asphaltenes alongside thiophenic sulfur.

4. Dibenzyl sulfide ( ): - This compound falls into the category of aliphatic sulfur. The difference between di-*n*-butyl sulfide and this compound is presence of two aromatic rings in place of alkyl chains on both sides of the sulfur, making both carbons of the C-S bonds benzylic. Simultaneous presence of sulfide and aromatic nature in this compound mimics asphaltenes structure as presented in section 2.2.

5. Benzyl Phenyl sulfide ( ): - Asphaltene structure are reported to be highly aromatic in nature, therefore aliphatic sulfur are speculated to be attached directly to aromatic ring too. Benzyl phenyl sulfide represent such chemical bonds along with benzyl type of carbon and sulfur linkages.

6. Diphenyl Sulfide ( ): - This compound represent bivalent sulfur attached directly to the aromatic carbon on both sides. The carbon atoms in the C-S bonds are part of the aromatic.

Given the complexity of asphaltene structure, studying the possibility of side reaction is highly relevant for the reaction between asphaltenes and methyl iodide. Reaction conditions was taken from the previous work on the reaction between asphaltenes and methyl iodide by Shaw.[22]

2.9. References

1. Crick, F. What Mad Pursuit: A Personal View of Scientific Discovery; Alfred P. Sloan Foundation series. Basic Books: New York, **1988**; pp 150.

2. Gray, M. R. Upgrading Oilsands Bitumen and Heavy Oil, 1st Edition; The University of Alberta Press: Edmonton, Alberta, **2015**.

3. ASTM 6560-12; Standard Test Method for Determination of Asphaltenes (Heptane Insolubles) in Crude Petroleum and Petroleum Products. May **2012**.

4. Mullins, O. C.; Sheu, E. Y. Fine Particle Society; American Chemical Society, Structures and Dynamics of Asphaltenes; Plenum Press: New York, **1998**.

5. Wiehe, I. A. Process Chemistry of Petroleum Macromolecules; CRC Press: Boca Raton, **2008**.

6. Siskin M.; Kelemen, S. R.; Eppig, C. P.; Brown, L. D.; Afeworki, M. Asphaltene Molecular Structure and Chemical Influences on the Morphology of Coke Produced in Delayed Coking. *Energy Fuels* **2006**, 20, 1227-1234.

7. Moschopedis, S. E.; Fryer, J. F.; Speight J. G. Investigation of Asphaltene Molecular Weights. *Fuel* **1976**, 55, 227-232.

8. Zajac, G. W.; Sethi, N. K.; Joseph, J. T. Maya Petroleum Asphaltene Imaging by Scanning Tunneling Microscopy: Verification of Structure from 13C and Proton Nuclear Magnetic Resonance. *Am. Chem. Soc., Div. Fuel Chem.* **1997**, 42, 423-426.

9. Speight, J. G. Evidence for the type of Polynuclear Aromatic in Nonvolatile Fractions. In Polynuclear aromatic compounds; Ebert, L. B. Ed.; Advances in Chemistry Series; American Chemical Society: Washington, DC, **1987**.

10. Sheu, E. Y.; Mullins, O. C. Fine Particle Society Asphaltenes: Fundamentals and Applications; Plenum Press: New York, **1995**.

11. Schuler, B.; Meyer, G.; Peña, D.; Mullins, O.C.; Gross, L. Unraveling the Molecular Structure of Asphaltenes by Atomic Force Microscopy. *J. Am. Chem. Soc.* **2015**, 137, 9870−9876.

12. Payzant, J. D.; Mojelsky, T. W.; Strausz, O. P. Improved Methods for the Selective Isolation of Sulfide and Thiophenic Classes of Compounds from Petroleum. *Energy Fuels* **1989**, 3, 449-454.

13. Zhao, A., Sparks, B. D., Kotlyar, L. S., and Chung, K. H. Reactivity of Sulphur Species in Bitumen Pitch and Residua during Fluid Coking and Hydrocracking. *Petrol. Sci. Technol.* **2002**, 20, 9-10, 1071-1085.

14. Pomerantz, A. E., Seifert, S. J., Bake, K. D., Graddock, P. R., Mullins, O. C., Kodalen, B. G., Kirtley, S. M., and Bolin, T. B. Sulfur Chemistry of Asphaltenes from a Highly Compositionally Graded Oil Column. *Energy Fuels* **2013**, 27, 4604-4608.

15. Kemp-Jones, A. V., and O. P. Strausz. Investigation of Possible Routes to Asphaltene in Nature. *Am. Chem. Soc. Div. Fuel Chem. Preprints* **1977**, 22 (3), 132-139.

16. Hofmann, I. C.; Hutchison, J.; Robson, J. N.; Chicarelli, M. I.; Maxwell, J. R. Evidence for Sulfide Links in a Crude Oil Asphaltene and Kerogens from Reductive Cleavage by Lithium in Ethylamine. *Org. Geochem.* **1992**, 19 (4-6), 371-387.

17. Waldo, G. S.; Mullins, O. C.; Penner-Hahn, J. E.; Cramer, S. P. Determination of the Chemical Environment of Sulfur in Petroleum Asphaltene by X-ray Absorption, *Fuel* **1992**, 71, 53-56.

18. Peng, P.; Morales-Izquierdo, A.; Hogg, A.; Strausz, O. P. Molecular Structure of Athabasca Asphaltene: Sulfide, Ether, and Ester Linkages. *Energy Fuels* **1997**, 11, 1171-1187.

19. Asaoka, S.; Nakata, S.; Shiroto, Y.; Takeuchi, C. Asphaltene Cracking in Catalytic Hydrotreating of Heavy Oils 2. Study of Changes in Asphaltene Structure during Catalytic Hydroprocessing. *Ind. Eng. Chem. Pro. Des. Dev.* **1983**, 22, 242-248.

20. Papayannakos, N. Kinetics of Catalytic Hydrodesulfurization of a Deasphalted Oil and of the Asphaltenic and Non-Asphaltenic Fractions of a Petroleum Residue. *Appl. Catal* **1986**, 24, 99-107.

21. Takeuchi, C.; Fukui, Y.; Nakamura, M.; Shiroto, Y. Asphaltene Cracking in Catalytic Hydrotreating of Heavy Oils 1. Processing of Heavy Oils by Catalytic Hydroprocessing and Solvent Deasphalting. *Ind. Eng. Chem. Proc. Des. Dev.* **1983**, 22, 236-242.

22. Shaw, J. E. Molecular Weight Reduction of Petroleum Asphaltenes by Reaction with Methyl Iodide-Sodium Iodide. *Fuel* **1989**, 68, 1218-1220.

23. Mao, X. Alkylation of Asphaltenes. MSc Thesis, University of Alberta, Edmonton, AB, Canada, **2015**.

24. Lengyel, A.; Magyar, S.; Kalio, D.; Hancsók, J.; Catalytic Coprocessing of Delayed Coker Light Naphtha with Light Straight-Run Naphtha/FCC Gasoline. *Petrol. Sci. Technol.* **2010**, 28, 946-954.

25. Melpolder, F. W.; Brown, R. A.; Young, W. S.; Headington, C. E.; Composition of Naphtha from Fluid Catalytic Cracking. *Ind. Eng. Chem.* **1952**, 44 (5), 1142-1146.

26. Cady, W. E.; Marschner, R. F.; Cropper, W. P. Composition of Virgin, Thermal, and Catalytic Naphthas from Mid-Continent Petroleum. *Ind. Eng. Chem.* **1952**, 44, 1859-1864.

27. Ali, M. A.; Tatsumi, T.; Masuda, T. Development of Heavy Oil Hydrocracking Catalysts using Amorphous Silica-Alumina and Zeolites as Catalyst Supports. *Appl. Catal., A: General* **2002**, 233, 77-90.

28. Hensen, E. J. M.; Poduval, D. G.; Magusin, P. C. M. M.; Coumans, A. E.; Van-Veen, J. A. R. Formation of Acid Sites in Amorphous Silica-Alumina. *J. Catal.* **2010**, 269, 201-218.

29. Shigeru, O. Organic Chemistry of Sulfur. Plenum Press: New York, **1977**.

30. Reid, E. E. Organic Chemistry of Bivalent Sulfur. Vol. 2. Chemical Publishing Company, **1958**.

31. Speight, J. G. Lange's Handbook of Chemistry. McGraw-Hill. 16th Edition, **2005**, Table - 2.49, 2.470 - 2.494.

32. Brown, H. C.; Jungk, H. The Reaction of Benzene and Toluene with Methyl Bromide and Iodide in presence of Aluminium Bromide; Evidence for a Displacement Mechanism in the Methylation of Aromatic Compounds. *J. Am. Chem. Soc.* **1955**, 77, 5584-5589.

3. Reaction of organosulfur model compounds with methyl iodide

Abstract

The present work investigates the reaction between organosulfur compounds and methyl iodide focused on C-S bond scission. Interference from solvent during reaction was also studied in this chapter. The reaction was observed to proceed via sulfonium species intermediate, with trimethyl sulfonium iodide being identified in the reaction products of some reactions.
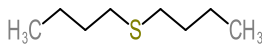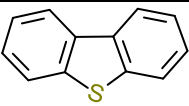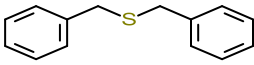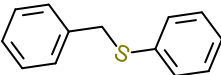
Key words: - Organosulfur compounds, C-S bond scission, Methyl iodide, Sulfonium

3.1. Introduction

Sulfur is the most abundant heteroatom in asphaltenes. The prevalence of carbon-sulfur bonds in asphaltenes and the reaction of methyl iodide degradation of vulcanized rubber[1] have inspired this present work on exploring asphaltenes conversion by reaction with methyl iodide.

This chapter deals with reaction of methyl iodide with organosulfur compounds. Model compounds used in this work represent different chemical environments for aliphatic sulfur both in cyclic and acyclic form and includes thiophenic sulfur as control. Compounds selected for this work (table 3.1) have been justified in section 2.8.

Table 3.1 Model organosulfur compounds used for reaction with methyl iodide

	Organosulfur compound	Chemical Structure
1	Di-*n*-Butyl Sulfide (DnBS)	
2	Tetrahydrothiophene (THT)	
3	Dibenzothiophene (DBT)	
4	Dibenzyl sulfide (DBS)	
5	Benzyl Phenyl sulfide (BPS)	

Reaction conditions employed for this study were taken from the previous study on the reaction between asphaltenes and methyl iodide by Shaw.[2] No comment has been provided by Shaw on the possibility of solvent interference and any side reactions during reaction between asphaltenes and methyl iodide. The choice of solvent is extremely important aspect of chemical reactions.[3] The present chapter explores the possibility of THF (tetrahydrofuran) and DMF (N,N-dimethylformamide) as solvents for the reaction with methyl iodide and side reactions other than reactions with C-S bond of the model compounds. An attempt is also made to ascertain whether both THF and DMF solvents are required for facilitating the reaction between C-S bonds and methyl iodide.

The objective of this work is to confirm the chemistry of reaction resulting in scission of C-S bond by reaction of organosulfur compounds with methyl iodide.

3.2. Experimental

3.2.1. Materials

Di-*n*-butyl sulfide (DnBS) with 98% purity was purchased from Alfa Aesar. The compound is used as it was supplied. Tetrahydrothiophene was purchased from Alfa Aesar. The supplied material was used without further purification. The purity of supplied material was 98%. Dibenzothiophene (DBT) was procured from Sigma Aldrich. The supplied material was used without further processing. Purity of dibenzothiophene supplied was 98%. Dibenzyl sulfide was purchased from Fisher Alfa Aesar with a purity of 99%. The supplied material was used as received. Benzyl Phenyl sulfide with 98% purity was also purchased from Alfa Aesar. This was used without any further purification. Tetrahydrofuran (THF) was used for dissolving asphaltenes. This was procured from Fisher Scientific with a purity of 99+%. No further purification was done. Butylated hydroxytoluene was added to THF by supplier. N,N-dimethylformamide (DMF) was procured from Fisher Scientific with a purity of 99.5%. DMF was used as polar solvent for facilitating the reaction. This chemical was used as received. Methyl iodide (CH_3I) was procured from Alfa Aesar with a purity of 99% and it was stabilized with copper by the supplier. This was used as obtained. Ultra-high purity (UHP 5.0) helium with purity of 99.999% was procured from Praxair supplied in cylinders. High purity (HP 4.8) nitrogen with purity of 99.998% was procured from Praxair supplied in cylinders.

This work deals with handling flammable and carcinogenic hydrocarbons. Therefore safety precautions were extremely important for safe handling of chemicals. Lab coat, safety goggles and gloves were used all the time during work in lab. Reaction ingredients were added to the reactor inside the fume hood to minimize the exposure. Gas products were collected inside the fume hood.

Special care was taken for handling of CH_3I. It was placed always in refrigerator and taken out only when required for adding to the reaction mixture. CH_3I was always handled inside the fume hood.

3.2.2. Equipment

Balances purchased from Mettler Toledo (model number MS6001S and ML3002E) were used for all weight measurements during this study. The Mettler Toledo MS6001S has a weighing capacity of 6200 g with readability of 0.1 g, whereas the Mettler Toledo ML3002E has a weighing capacity of 3200 g with readability of 0.01g.

The reactions were conducted in a closed batch reactor made of steel, fitted with a pressure gauge and needle valve. This reactor, once filled with the reaction mixture, was placed inside a constant temperature sand bath. The constant temperature sand bath was purchased from Techne (model SBS – 4) and Omega (model FSB – 3). The sand inside the bath was fluidized using air connected below sand bath. A temperature measurement with type K thermocouple and Omron made control system is installed with this sand bath. The setup is shown in figure 3.1.
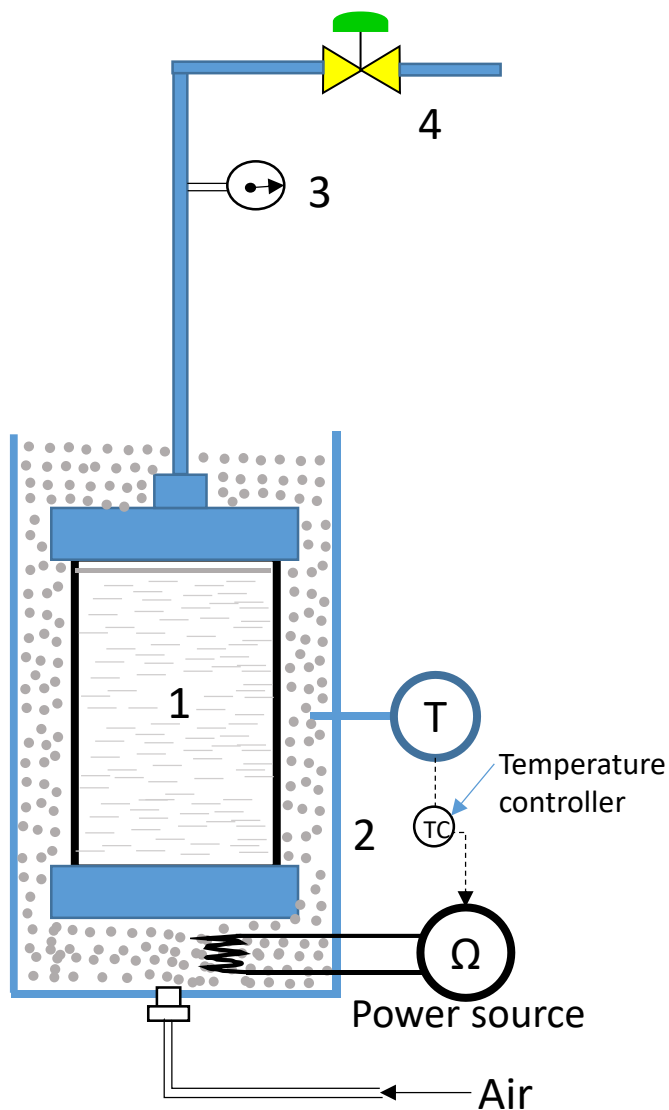
Figure 3.1 Schematic diagram of reactor as placed inside fluidized sand bath. 1) Reactor with reaction ingredient, 2) Sand bath with fluidizing sand fitted with temperature measurement, controller and power source, 3) Pressure gauge, 4) Needle valve

3.2.3. Procedure

The original study by Shaw[2] was conducted using THF and DMF, both solvents were used in this investigation. The interference from solvents during reaction was not reported in past studies. Therefore this study of reaction between model compounds and methyl iodide conducted first in a way to determine any interference from the solvent. Therefore solvent and methyl

iodide were placed inside a reactor at reaction conditions to evaluate if there was any interaction between solvent and methyl iodide.

3.2.3.1. Procedure for reactions conducted for exploring solvent interference

In order to study the possibility of solvent interference with reaction, five sets of reactions were conducted and reaction products were analyzed. One sulfide compound was needed to conduct these reactions. Di-*n*-butyl sulfide was selected as sulfur compound in each of these reactions when needed. Table 3.2 provides the composition of reaction mixture of five sets of reactions.

Table 3.2 Reaction setup for five sets of reactions.

	Set – 1	Set – 2	Set – 3	Set – 4	Set – 5
THF	Yes	No	No	Yes	No
DMF	No	Yes	Yes	No	No
DnBS	No	No	Yes	Yes	Yes
CH_3I	Yes	Yes	Yes	Yes	Yes

Writing "Yes" in the cell indicate that reaction ingredient is present in corresponding set of reactions and contrarily writing "No" means that ingredient is not present in that set of reactions.

Reaction ingredients were weighed and placed inside the reactor (item 1, figure 3.1) as per table 3.2 indicating ingredient's presence in that set of reactions. The exact weight of reaction ingredients has been provided in table 3.4. Nitrogen was used for pressurizing, up to 0.7 MPa, for leak testing. After a successful leak test, reactors were depressurized, measured at pressure gauge (item 3, figure 3.1), to ambient pressure the needle valve (item 4, figure 3.1) was closed.

In addition to facilitating leak test, the pressurization with nitrogen also help in removing atmospheric oxygen from the reactor. The residual oxygen in the reactor remained equal to about 3 vol%.

The closed reactors were then placed inside the constant temperature sand bath that was maintained at constant temperature equal to 75 °C measured by a thermocouple installed in sand bath (item 2, figure 3.1). Reaction time selected was 24 hours. This reaction time was chosen based on earlier studies.[2] All reactors were taken out of the sand bath and allowed to cool to ambient temperature. The weight of the reactor was measured and recorded. Then gas product was collected from the reactor and reactor was weighed again. The difference in weight of reactor before and after gas product collection is used as the weight of gas product. Since this is a low temperature process, negligible increase in the pressure of reactor was observed after the reaction time was over, i.e. low gas make.

Reactors were opened and liquid product was collected. This study was used to identify main reaction products and therefore only the liquid product was analyzed. The liquid product was analyzed using gas chromatography for separation and a mass selective detector was used for identification.

3.2.3.2. Procedure for reactions conducted in DMF solvent

Based on the results obtained after studying the result of the solvent effect on reaction, another procedure was followed for conducting the study on the reaction between organosulfur compounds and methyl iodide. One set of reactions was conducted for each sulfur model compound presented in table 3.1. Each reaction was conducted in presence of DMF solvent only. Reaction ingredients in this procedure were organosulfur compound, DMF, and CH_3I. Table 3.3

summarizes the organosulfur compound for each set of reaction along with set number. All reaction ingredients were placed inside the reactor. Each ingredient was weighed. The same procedure as mentioned in section 3.2.3.1 was followed for this set of reactions. Only liquid product was analyzed.

Table 3.3 Organosulfur compound for each set of reaction

	Set – 6	Set – 7	Set – 8	Set – 9	Set – 10
Organosulfur Compound	Di-*n*-butyl sulfide	Tetrahydrothiophene	Dibenzothiophene	Dibenzyl sulfide	Benzyl phenyl sulfide

3.2.3.3. Procedure for reaction of dibenzothiophene with methyl iodide at elevated pressure

The boiling point of methyl iodide at ambient pressure (0.1 MPa) is 42.4 °C. Stull[4] has provided the vapor pressure of methyl iodide at different temperatures; it was reported to be 0.2 MPa at 65.5 °C and 0.5 MPa at 101.8 °C. NIST[5] has calculated the Antoine equation coefficients from the data given by Stull. Using these Antoine coefficients, the vapor pressure of methyl iodide was calculated at 75 °C. The vapor pressure of methyl iodide at 75 °C is 0.26 MPa.

The maximum pressure observed during reaction was below the minimum readable pressure on the pressure gauge installed on the reactor (item 3, figure 3.1), which indicated that at 75 °C the reaction proceeded mainly in the liquid phase. Although the actual vapor pressure of methyl iodide in the reaction environment will be different than in its pure form, the reaction was conducted at 4.4 MPa to ensure that almost all methyl iodide remained in liquid phase. Only one

37

set of reactions was conducted with this procedure. This set was numbered as set-11. In addition to the steps followed in section 3.2.3.1, the reactor was pressured to 4.83 MPa and a leak test was done. Then reactor pressure was lowered to 4.4MPa gauge after successful leak test. Then the reactor was placed inside the sand bath and section 3.2.3.1 procedure was followed thereafter.

3.2.4. Analysis

Gas chromatography coupled with mass spectrometer was used for identification of product molecules. Agilent 7820A GC coupled with Agilent 5977E series MSD (Gas chromatograph coupled with mass selective detector) system was used for analyzing the liquid sample in this study. GC-MSD consisted of two functions combined in one box. Gas chromatography is used for separating the sample based on difference in elution time for different compounds. Compounds eluted from gas chromatography enters the MSD section. Molecules entering MSD are then identified and their abundance is measured. Relative abundance against elution time along with molecule identification is presented as result.

The gas chromatography section of the GC-MSD used an HP-5MS (5% phenyl methyl siloxane) column from Agilent. This column has dimension of 30 m long, 250 μm internal diameter, and 0.25 μm film thickness. The sample is injected with split injection system with 100:1 split ratio. The sample was separated using the oven temperature program starting at 35 °C held for 5 minutes and then raising oven temperature by 5 °C per minute to 320 °C. This temperature was held for one minute. Eluting compounds are transferred to MSD system via MSD transfer line maintained at constant temperature equal to 325 °C. A timed event was created in the detector to avoid saturation with solvent. The detector was switched off at the elution time corresponding to the solvents THF and DMF.

MSD system employed in this study consisted of three sections namely ionization, mass analyzer and detector. Mass spectrometer used in this study is fitted with electron impact ionization system. Electrons are generated from heated filament and accelerated by an anode. Accelerated electrons collide with the gas molecules that have entered mass spectrometer after eluting from gas chromatography. Collision with electron ionizes the gas molecule, which enters the mass analyzer zone of spectrometer and the mass to charge ratio is measured. The mass analyzer in this system employs four hyperbolic quadrupoles rods with hyperbolic cross-section placed perfectly parallel to each other making a channel between four rods. Alternating electric field is applied across the hyperbolic quadrupoles. Gas ions pass though the channel surrounded by hyperbolic quadrupoles. In order to ensure that gas ions are only impacted by electric fields, a vacuum environment is maintained in mass spectrometer system. A vacuum pump is utilized for maintaining 10^{-6} MPa vacuum. Abundance of each gas ion after mass analyzer is measured using a detector. The detector system involves measuring current as gas ions lose their charge to the detector. An electron multiplier is used as detector system in the GC-MSD used in this study. Electron multiplier detector utilize multiple dynodes for accelerating gas ions and facilitating generation of several secondary charged particles by colliding very high velocity gas ions with dynodes. A series of multiple dynode systems are installed for achieving sufficient number of charged particles for measuring current. The higher the number of charged particles, the higher is the detection and measurement accuracy. Current after the last dynode is measured. Measured current is presented as abundance of the gas ion entering the detector system.

Mass selective detector result is presented as spectrum. The mass to charge ratio (m/z) from the mass analyzer is plotted on the X-axis and abundance as measured from detector on Y- axis. The

step size for m/z measurement used is 0.1 unit. Range of 10 to 600 m/z has been scanned in this study. Scan frequency of 2.5 scans per second has been used.

GC-MSD ChemStation software provided by Agilent was used for identifying molecules in the sample. Mass spectra in NIST library were used by this software for identifying the molecules based on their electron impact mass spectrum.

3.3. Results

3.3.1. Study of interference of solvent

As detailed in section 3.2.3.1, five reactions were conducted, numbered set – 1 to set – 5. The weight of each reaction ingredient and product are presented in the table 3.4 below.

Table 3.4 Weight of reaction ingredients for solvent interference study

	Set – 1	Set – 2	Set – 3	Set – 4	Set – 5
	THF-CH_3I	DMF + CH_3I	DMF + DnBS +CH_3I	THF + DnBS +CH_3I	DnBS + CH_3I
DMF (g)	0	12.12	12.10	0	0
THF (g)	3.03	0	0	3.00	0
DnBS (g)	0	0	0.28	0.27	0.51
CH_3I (g)	4.08	3.99	7.08	7.02	7.12
Total weight of reactor before reaction (g)	380.02	406.58	392.21	402.46	381.49
Total weight of reactor after reaction before gas sample collection (g)	379.95	406.67	392.14	402.37	381.63
Weight of gas sample (g)	0.05	0.01	0.11	0	0

The comparison between weight of total reactor with reaction ingredients before and after reaction indicate that there is negligible loss of material during the reaction. Therefore the analytical results will be representative of the reaction studied under this work.
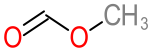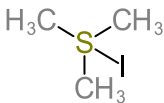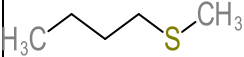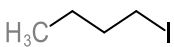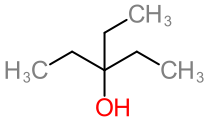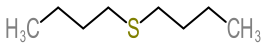
Liquid reaction product was analyzed using GC-MSD. The result with identified molecules is presented in figure 3.2.
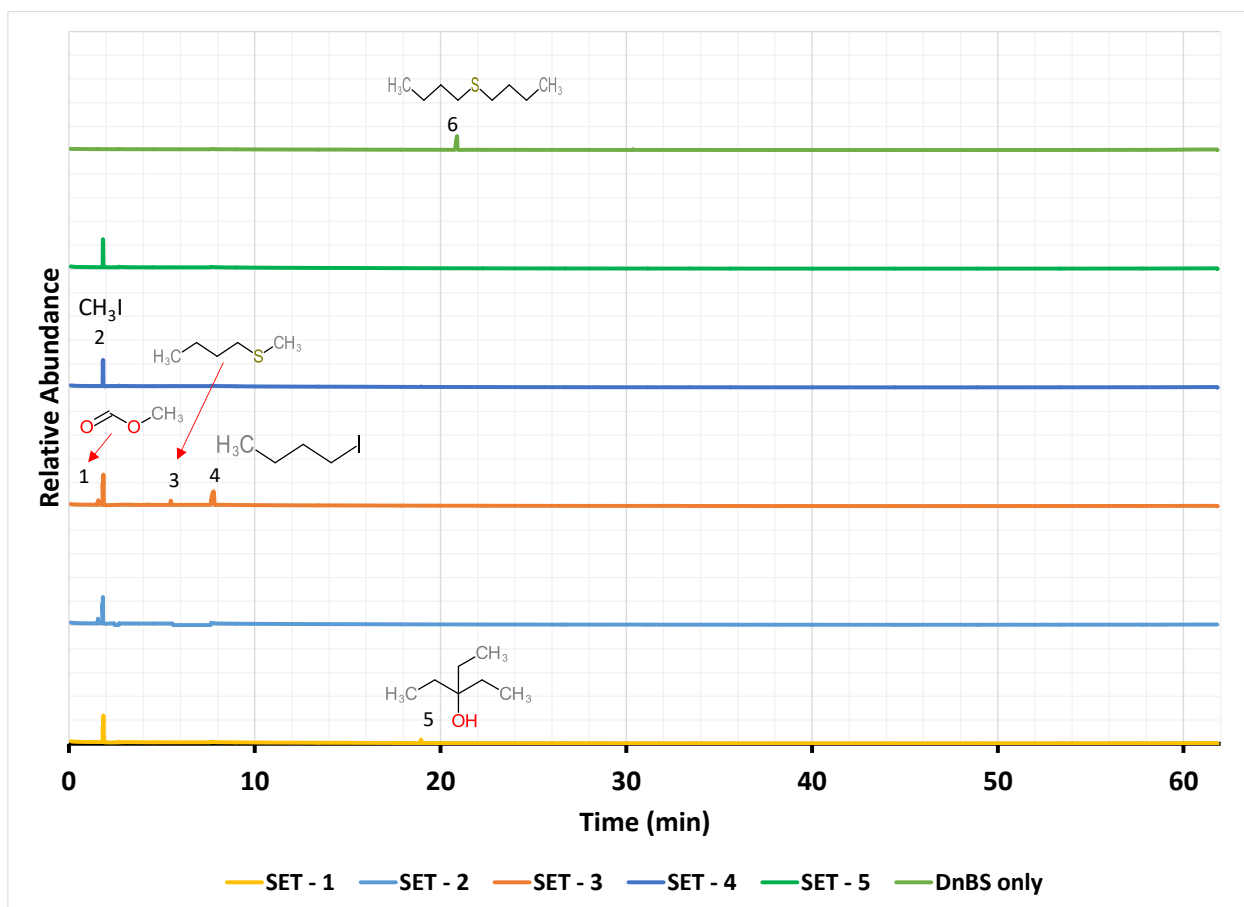
Figure 3.2 Identified molecules and its relative abundance obtained from analysis of liquid product using GC-MSD

The list of identified molecules and their retention time are presented in the table 3.5 along with their structure.

Table 3.5 List of molecules identified and their retention time in the liquid product after reaction for solvent interference study.

Peak serial number	Structure	Name	Retention time (min)
1		Methylformate	1.57
2a		Methyl iodide	1.80
2b		Trimethylsulfonium iodide	1.85
3		Methyl-*n*-butyl sulfide	5.36
4		*n*-butyl iodide	7.72
5		3-ethyl-3-pentanol	18.93
6		Di-*n*-butyl sulfide	20.88

White colored precipitate was found in set – 4 reaction. This white precipitate is shown in figure 3.3 (a). THF was added to the product but whole product was not dissolved. The dissolved fraction of product was analyzed using GC-MSD. The solid product was not analyzed.

When DnBS was placed with CH_3I in reactor in set – 5 without any solvent then a red colored solid material was found left inside the reactor. Only a solid product was observed. THF was added to solid product for analyzing any dissolved fraction using GC-MSD, but only methyl iodide appeared to have dissolved in the THF. The main reaction product was therefore not

soluble in THF. Figure 3.3 (b) shows the red color solid material left after reaction time is passed. Remaining solid residue was not analyzed further.

(a) White color solid material after reaction time with DnBS, CH$_3$I and THF in the reactor (Set – 4)

(b) Red color solid material after reaction time with DnBS and CH$_3$I inside the reactor without any solvent (Set – 5)

Figure 3.3 Solid material obtained after 24 hours for di – n – butyl sulfide and CH$_3$I inside the reactor with and without THF solvent.

The peak observed at retention time equals to 1.57 minutes in figure 3.2 corresponds to methyl formate. This is an impurity present in solvent DMF.

3.3.2. Reaction between organosulfur compound and CH$_3$I in DMF solvent

Based on the results presented in section 3.3.1, DMF was selected as solvent for the study of reaction between model organosulfur compounds and CH$_3$I. Individual reaction between CH$_3$I and each organosulfur model compound in the presence of DMF were conducted. The weight of each reaction ingredient is presented in table 3.6.

Table 3.6 Weight of reaction ingredients for each set of reaction of organosulfur compound with methyl iodide

	Set – 6	Set – 7	Set – 8	Set – 9	Set – 10
Sulfur Compound	Di-*n*-butyl sulfide	Tetrhydrothiophene	Dibenzothiophene	Dibenzyl sulfide	Benzyl phenyl sulfide
DMF (g)	17.16	13.28	13.16	14.81	13.10
Organosulfur compound (g)	0.27	0.32	0.27	0.26	0.26
CH_3I (g)	7.37	12.12	5.86	5.07	5.39
Total weight of reactor before reaction (g)	397.46	416.24	391.94	412.34	393.19
Total weight of reactor after reaction and before gas product collected (g)	397.46	416.18	392.06	412.32	393.15
Weight of gas sample (g)	0.1	0.0	0.1	0	0

The weight of CH_3I used in each reaction is different. This difference is due to different weight percent sulfur content in each of the organosulfur compound. Constant molar ratio of methyl iodide to sulfur is maintained for each reaction. This molar ratio was equal to 30. This ratio was

selected arbitrarily, but it was ensured that the organosulfur compound is the limiting reagent in each reaction.

There was negligible loss of material during reaction time. Thus results obtained from this study will be representative of reaction product.

The liquid product from each reaction was analyzed using GC-MSD as detailed in section 3.2.4. The chromatogram and molecules identified for each peak are presented for the liquid reaction products after reaction of each organosulfur compound listed in table 3.1 with methyl iodide.
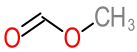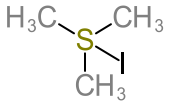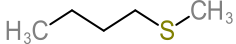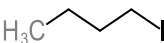
3.3.2.1.   Reaction of di-*n*-butyl sulfide (Set – 6)

Di-*n*-butyl sulfide reacts with CH_3I at the reaction conditions employed in this study, i.e. 75 °C temperature and self generated pressure. Di-*n*-butyl sulfide is not detected in the product mixture. This indicated that conversion of di-*n*-butyl sulfide is 100% during the reaction time of 24 hours. Table 3.7 presents the list of molecules identified, their structure and retention time.
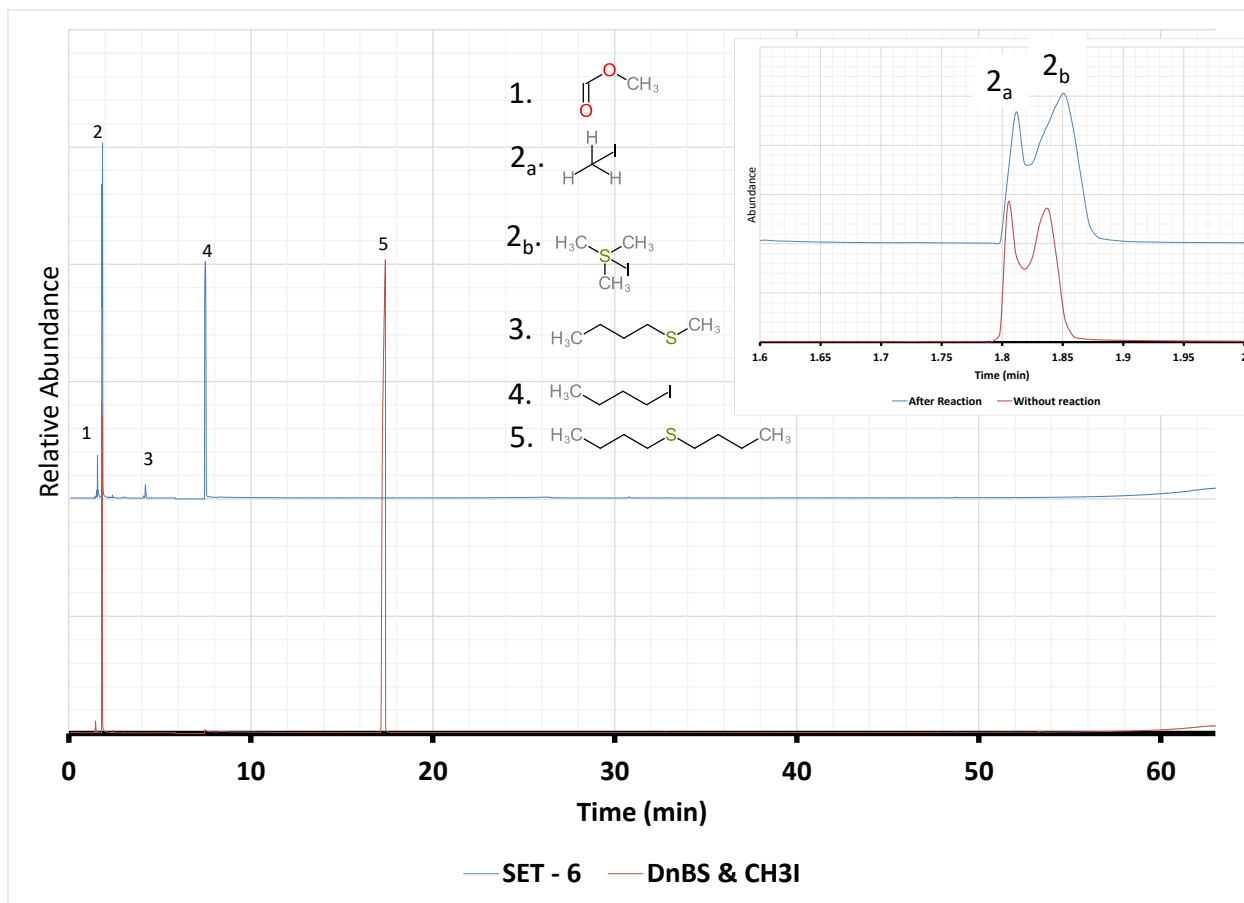
Figure 3.4 Chromatogram and identified molecules in the reaction product of reaction of di-*n*-butyl sulfide with CH_3I.

Table 3.7 List of molecules identified and their retention time in the liquid product after reaction of di-*n*-butyl sulfide with methyl iodide

Peak Serial number	Structure	Name	Retention time (min)
1		Methyl formate	1.57
2a		Methyl iodide	1.80
2b		Trimethyl sulfonium iodide	1.85
3		Methyl-*n*-butyl sulfide	5.36
4		*n*-butyl iodide	7.72
5		Di-*n*-butyl sulfide	20.88
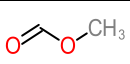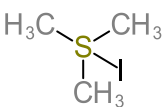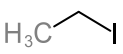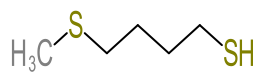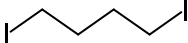
3.3.2.2. Reaction of tetrahydrothiophene (Set – 7)

Reaction product analysis indicate that tetrahydrothiophene reacts with CH_3I with 100% conversion of tetrahydrothiophene to products (figure 3.5). Tetrahydrothiophene is not detected in the product mixture. 1,4-di-iodobutane is detected after reaction between CH_3I and tetrahydrothiophene. This indicates the cleaving of both bonds between carbon and sulfur atoms. The chromatogram and identified molecule peaks are presented in figure 3.5. The list of molecules in product mixture and their retention time is presented in table 3.8.

Figure 3.5 Chromatogram and identified molecules in the reaction product of reaction of tetrahydrothiophene with CH_3I.

Table 3.8 List of molecules identified and their retention time in the liquid product after reaction of tetrahydrothiophene with methyl iodide

Peak Serial number	Structure	Name	Retention time (min)
1		Methyl formate	1.57
2$_a$		Methyl iodide	1.80
2$_b$		Trimethyl sulfonium iodide	1.85
3		Ethyl iodide	2.40
4		Tetrahydrothiophene	6.86
5		Methyl-*n*-butantiol sulfide	22.319
6		Butyl-1,4-diiodide	22.86
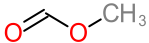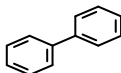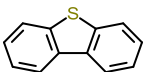
3.3.2.3.   Reaction of dibenzothiophene (Set – 8)

Dibenzothiophene and CH$_3$I were reacted in presence of DMF for 24 hours. The chromatogram and identified peaks are presented in figure 3.6. There was no change observed in the composition after the reaction time is over. All the molecules identified in the reaction product are exactly same as the molecules at the start of reaction time. It can be therefore concluded that dibenzothiophene does not react with CH$_3$I at the reaction conditions employed in this study. A list of molecules in product mixture and their retention time are provided in the table 3.9.
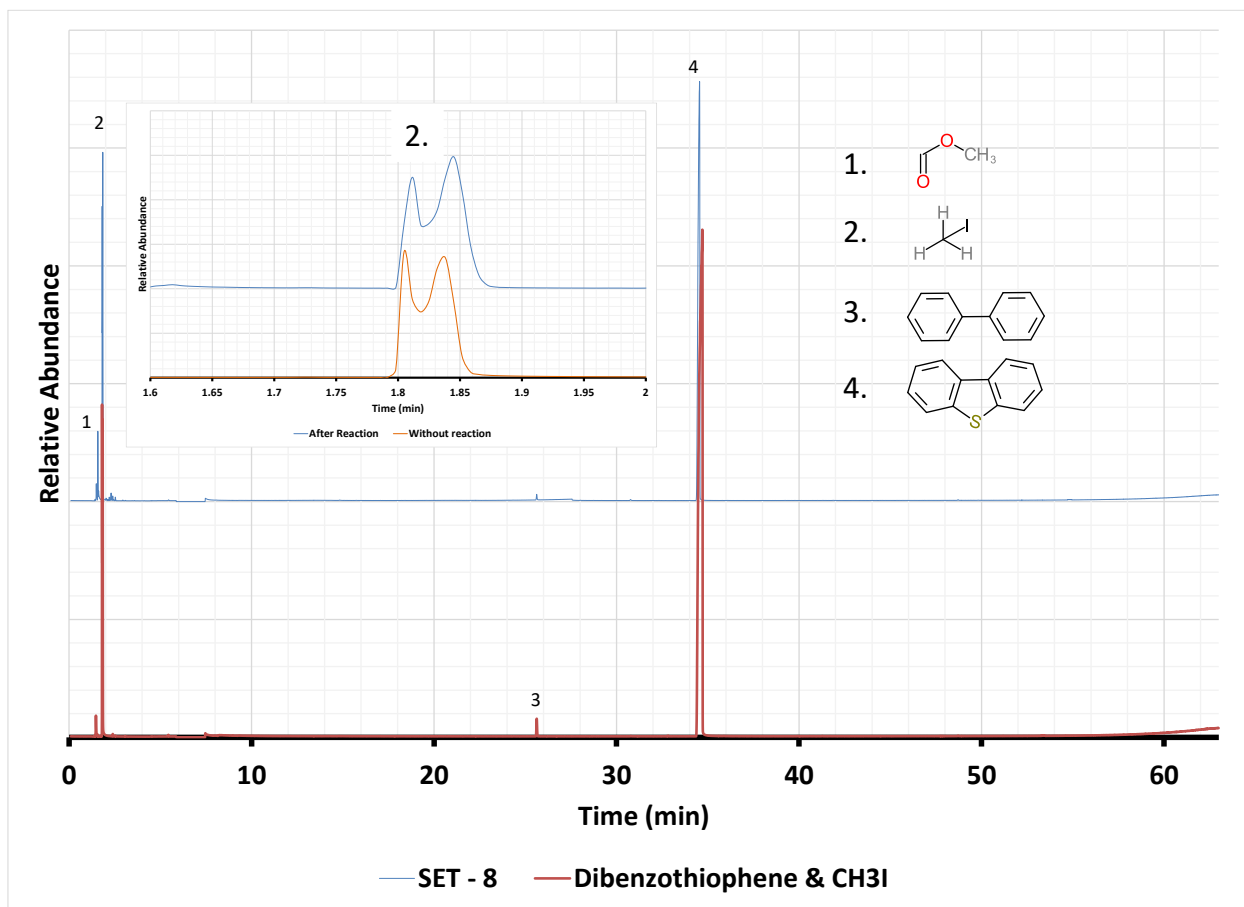
Figure 3.6 Chromatogram and identified molecules in the reaction product of reaction of dibenzothiophene with CH$_3$I.

Table 3.9 List of molecules identified and their retention time in the liquid product after reaction of dibenzothiophene with methyl iodide

Peak Serial number	Structure	Name	Retention time (min)
1		Methyl formate	1.57
2		Methyl iodide	1.80
3		Diphenyl	25.64
4		dibenzothiophene	34.49

3.3.2.4. Reaction of dibenzyl sulfide (Set – 9)

The chromatogram for the reaction product of reaction between dibenzyl sulfide and CH_3I in the presence of DMF solvent is shown in figure 3.7. Peaks in the chromatogram are associated with compounds. Dibenzyl sulfide is not detected in the product mixture. This indicate 100% conversion of dibenzyl sulfide. Reaction product formed after cleaving both chemical bonds between carbon and sulfur. Both carbon sulfur bonds are replaced with two separate carbon and iodine bonds, e.g. peak number 6. Other molecules are also detected as indicate by peak number 3, 4, 5, 7 and 8. Table 3.10 lists the molecules identified and their retention time.
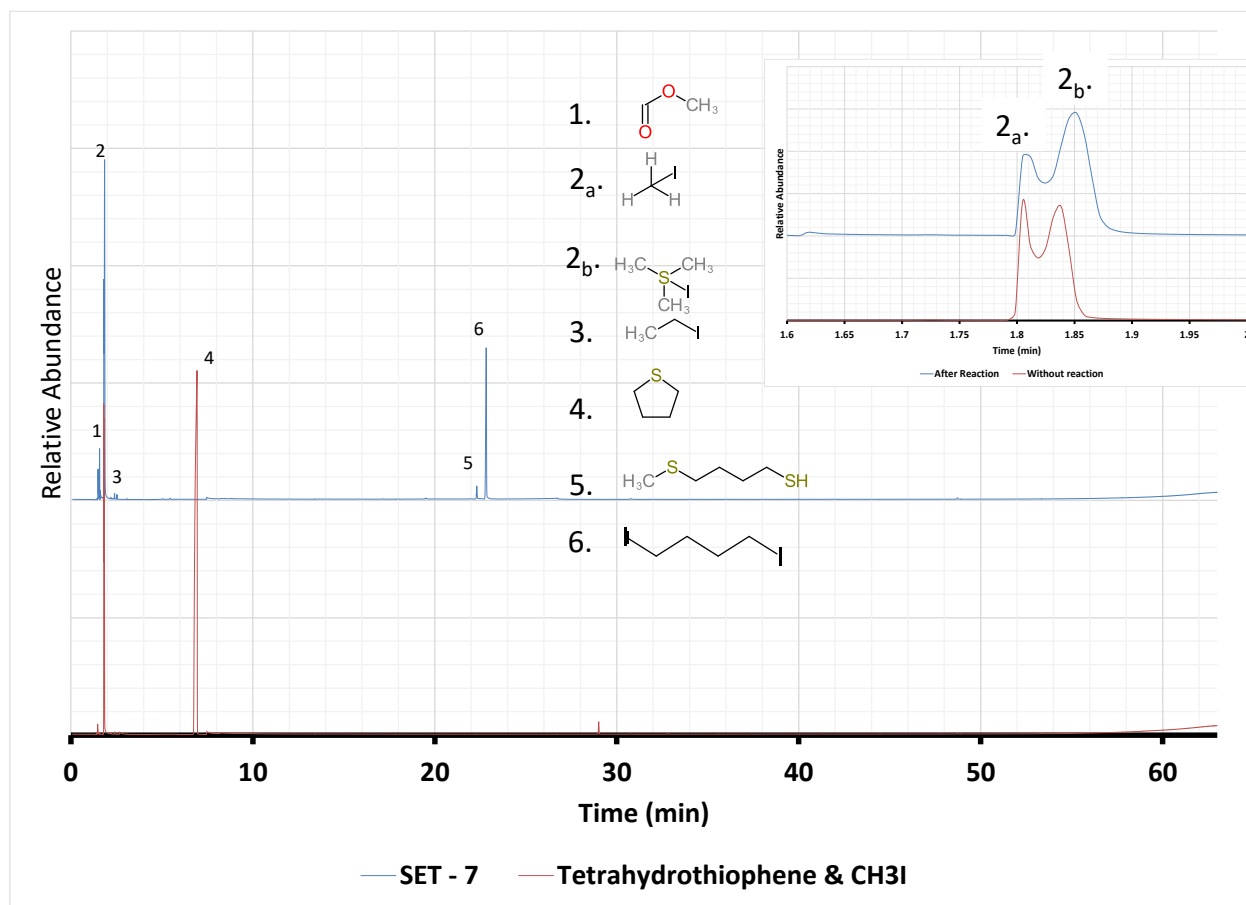
Figure 3.7 Chromatogram and identified molecules in the reaction product of reaction of dibenzyl sulfide with CH₃I.

Table 3.10 List of molecules identified and their retention time in the liquid product after reaction of dibenzyl sulfide with methyl iodide

Peak serial number	Structure	Name	Retention time (min)
1		Methyl Formate	1.57
2a		Methyl iodide	1.80
2b		Trimethyl sulfonium iodide	1.57
3		Methyl benzyl ether	13.87
4		Benzyl alcohol	15.44
5		Methyl benzyl sulfide	16.89
6		Benzyl iodide	20.42
7		Dibenzyl	29.21
8		Diphenyl sulfide	30.79
9		Dibenzyl sulfide	36.02

3.3.2.5.   Reaction of benzyl phenyl sulfide (Set -10)
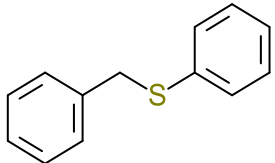
Benzyl phenyl sulfide was reacted with methyl iodide in presence of DMF as reaction medium. The reaction product was analyzed using GC-MSD. The chromatogram and compounds identified for peaks are presented in figure 3.8. Molecules identified in the product mixture and their retention time are listed in table 3.11. Benzyl phenyl sulfide is not detected in the reaction product. Therefore 100% conversion of benzyl phenyl sulfide is concluded. Formation of benzyl iodide (peak 7) and methyl phenyl sulfide (peak 6) indicate the cleavage of carbon and sulfur bond on the benzyl side of benzyl phenyl sulfide. The bond between sulfur and aromatic ring is not cleaved because of this reaction between benzyl phenyl sulfide and CH_3I at reaction conditions employed in this study.

Figure 3.8 Chromatogram and identified molecules in the reaction product of reaction of benzyl phenyl sulfide with CH₃I.

Table 3.11 List of molecules identified and their retention time in the liquid product for reaction of benzyl phenyl sulfide with methyl iodide

Peak serial number	Structure	Name	Retention time (min)
1		Methyl formate	1.57
2$_a$		Methyl iodide	1.80
2$_b$		Trimethyl sulfonium iodide	1.57
3		Methyl benzyl ether	13.87
4		Benzyl alcohol	15.44
6		Methyl phenyl sulfide	17.01
7		Benzyl iodide	20.42
8		Dibenzyl	29.21
9		Diphenyl	30.79

| 10 | | Benzyl phenyl sulfide | 33.27 |

3.3.3. Reaction between dibenzothiophene and CH₃I at elevated pressure (Set – 11)

To confirm that the absence of reaction between dibenzothiophene and CH_3I was not due to poor mass transport that would limit contact between dibenzothiophene and CH_3I, one reaction was performed at higher pressure. The procedure is detailed in section 3.2.3.3. Reaction ingredients were weighed as presented in table 3.12.

Table 3.12 Weight of reaction ingredients for reaction of Dibenzothiophene with methyl iodide at elevated pressure under nitrogen environment.
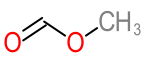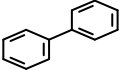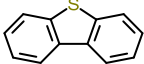
Sulfur Compound	Dibenzothiophene
DMF (g)	13.36
Dibenzothiophene (g)	0.31
CH_3I (g)	7.96
Total weight of reactor before pressurizing (g)	396.04
Weight of nitrogen added for pressurizing (g)	1.6
Total weight of reactor after reaction without nitrogen (g)	396.08
Weight of gas sample (g)	1.4

Liquid product from reaction was analyzed using GC-MSD for identification of compounds formed during the reaction. Gas product was not analyzed. The chromatogram and peaks identified from analysis of liquid product using GC-MSD are presented in figure 3.9. The list of molecules identified and their retention time are listed in table 3.13. The chromatogram for reaction product doesn't show formation of new molecules because of reaction. Therefore it can be concluded that elevating pressure doesn't help in favoring the reaction between dibenzothiophene and CH_3I at 75 °C.
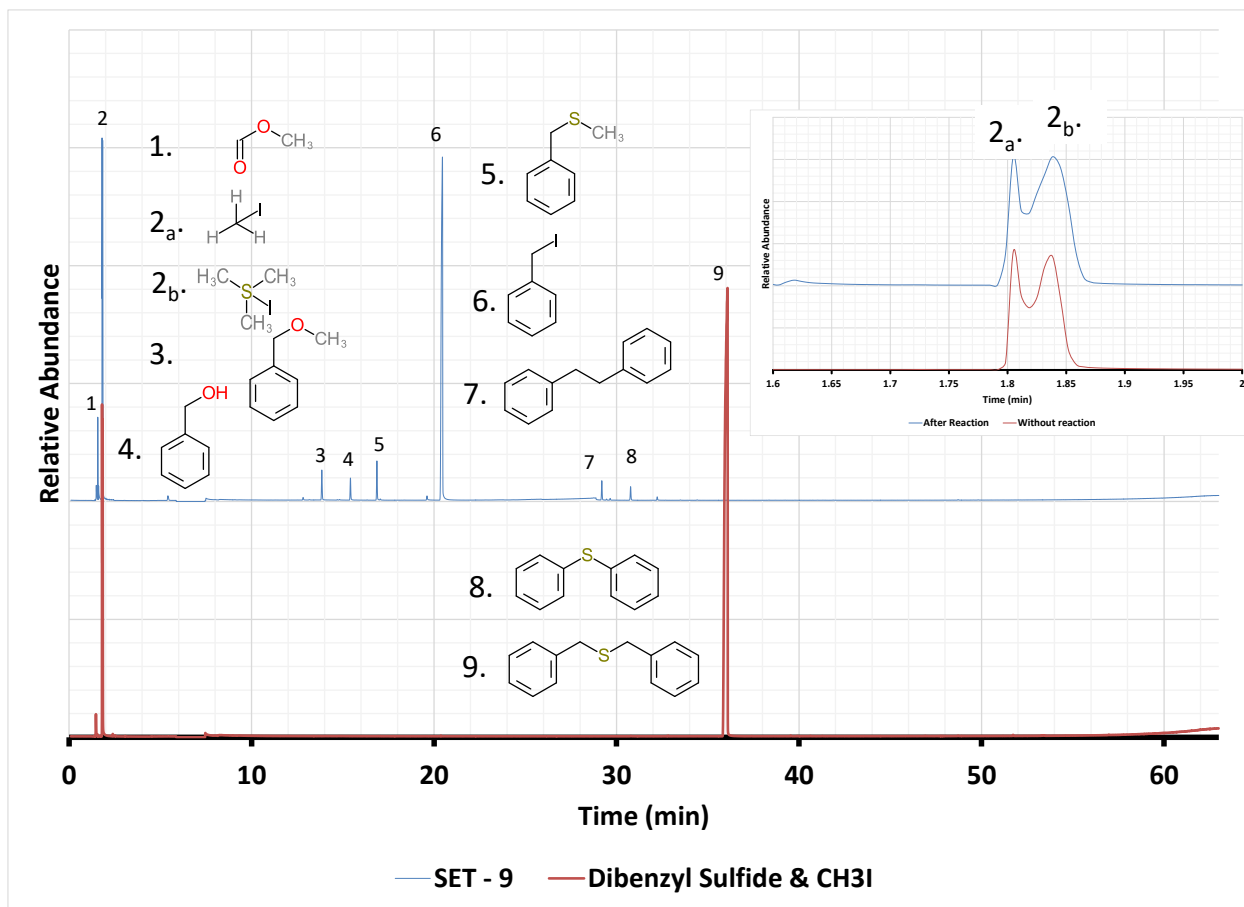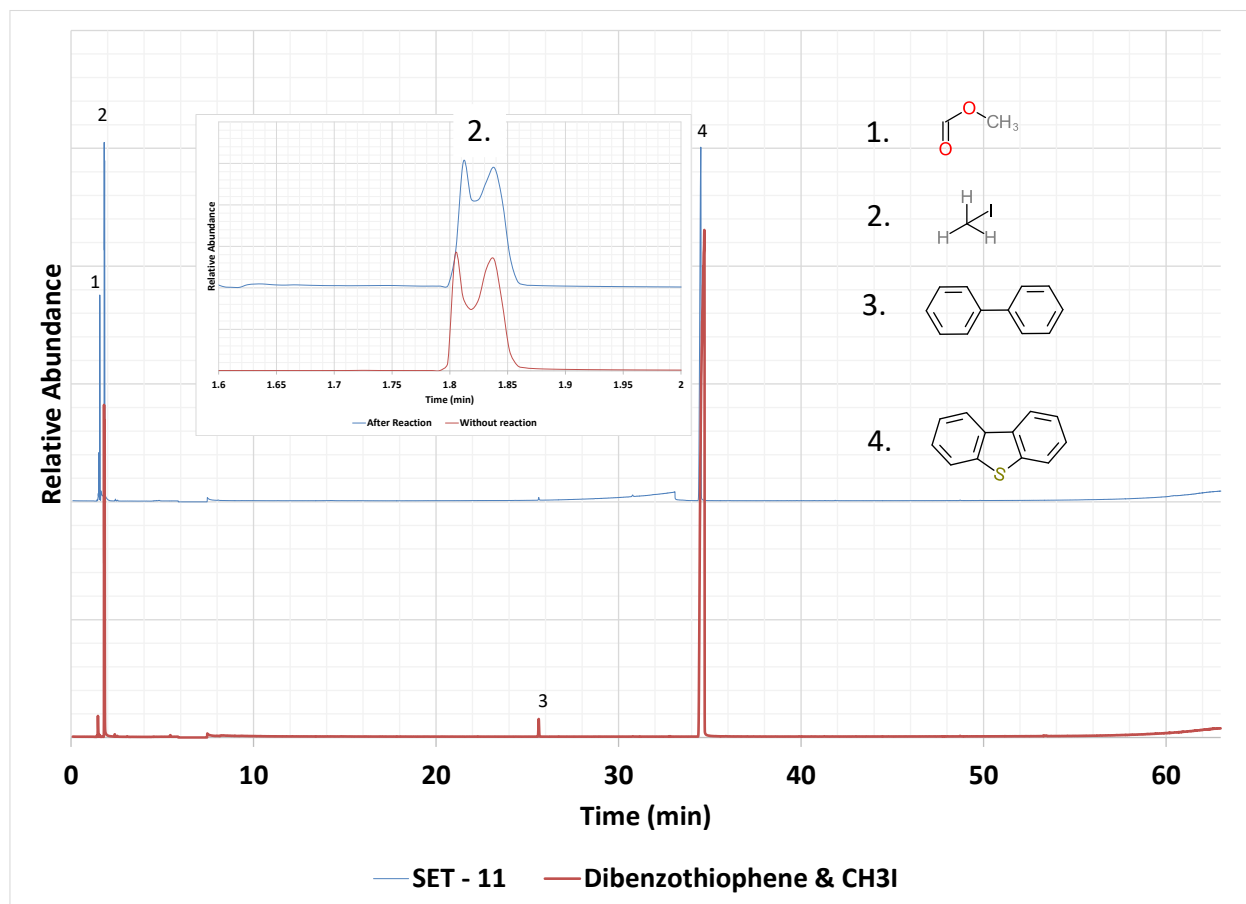

Figure 3.9 Chromatogram and identified molecules in the reaction product of reaction of and dibenzothiophene with CH_3I at elevated pressure
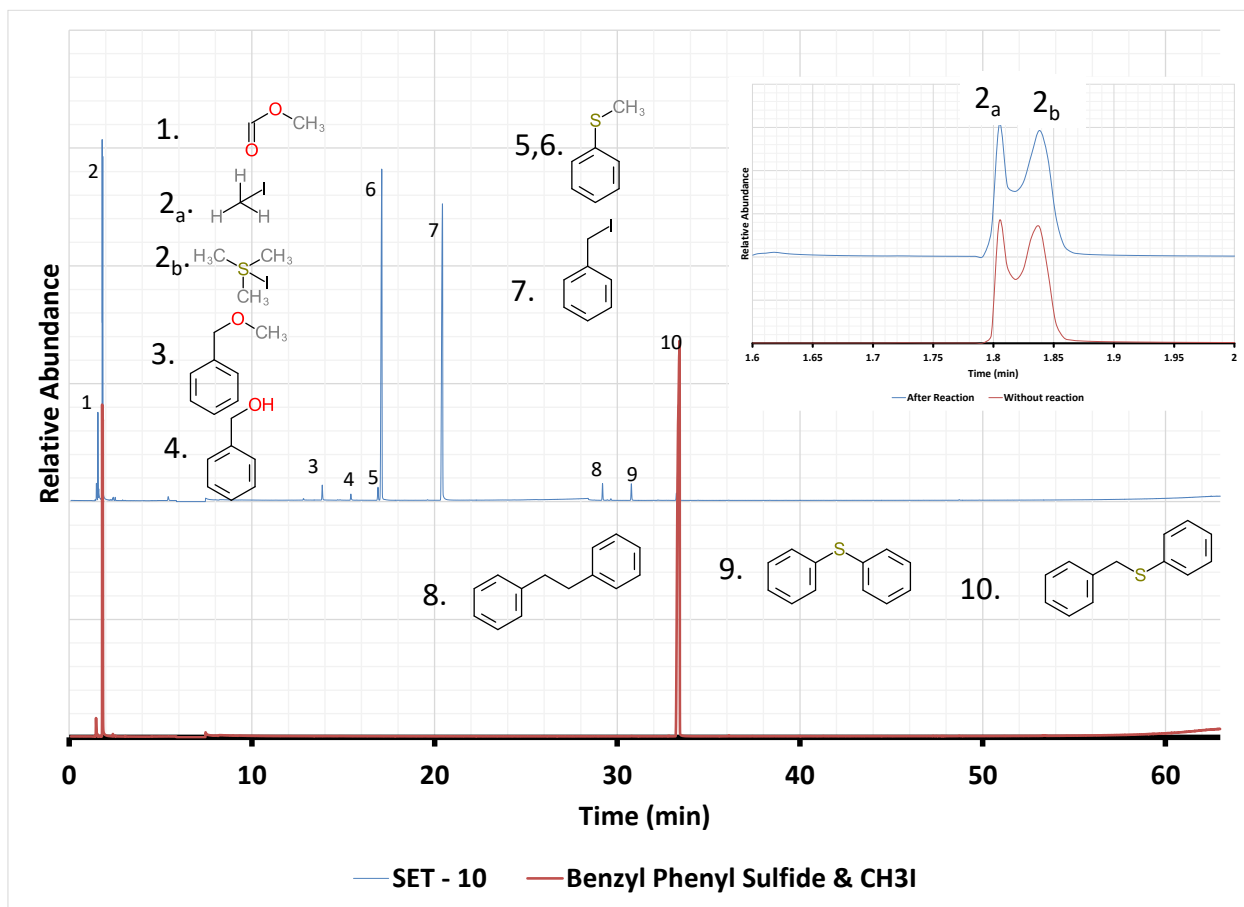
Table 3.13 List of molecules identified and their retention time in the liquid product after reaction of dibenzothiophene with methyl iodide at elevated pressure under nitrogen environment

Peak serial number	Structure	Name	Retention time (min)
1		Methyl formate	1.57
2		Methyl iodide	1.80
3		Diphenyl	25.64
4		Dibenzothiophene	34.49

3.4. Discussion

3.4.1. Interference of solvent

As mentioned before, while analyzing liquid product, the mass spectrometer's detector is turned off at the elution time when solvent enters the spectrometer. This is done for avoiding saturation of the detector. Therefore no peak is observed for DMF and THF in the chromatogram presented in figure 3.2. The chromatogram in figure 3.2 indicated that set – 1 reaction product contained only 3-ethyl-3-pentanol. Formation of this molecule appears to be due to reaction between THF and CH_3I. The chromatogram in figure 3.2 corresponding to set – 2 reaction indicated that no product is formed because of reaction between CH_3I and DMF.

3.4.2. Reaction of organosulfur compounds with methyl iodide in DMF solvent

Results presented in section 3.3, demonstrate the cleavage of C-S bonds in organosulfur compounds where at least one C-S bond is aliphatic. The only organosulfur compound that was not converted was dibenzothiophene.

The reaction product analysis demonstrates that reaction between CH_3I and organosulfur compounds targeted the chemical bond between carbon and sulfur. Aromatic and alkyl carbon remain unaffected at the reaction conditions employed in this work. The unbalanced reaction pathways for each organosulfur compound are presented in figure 3.10.
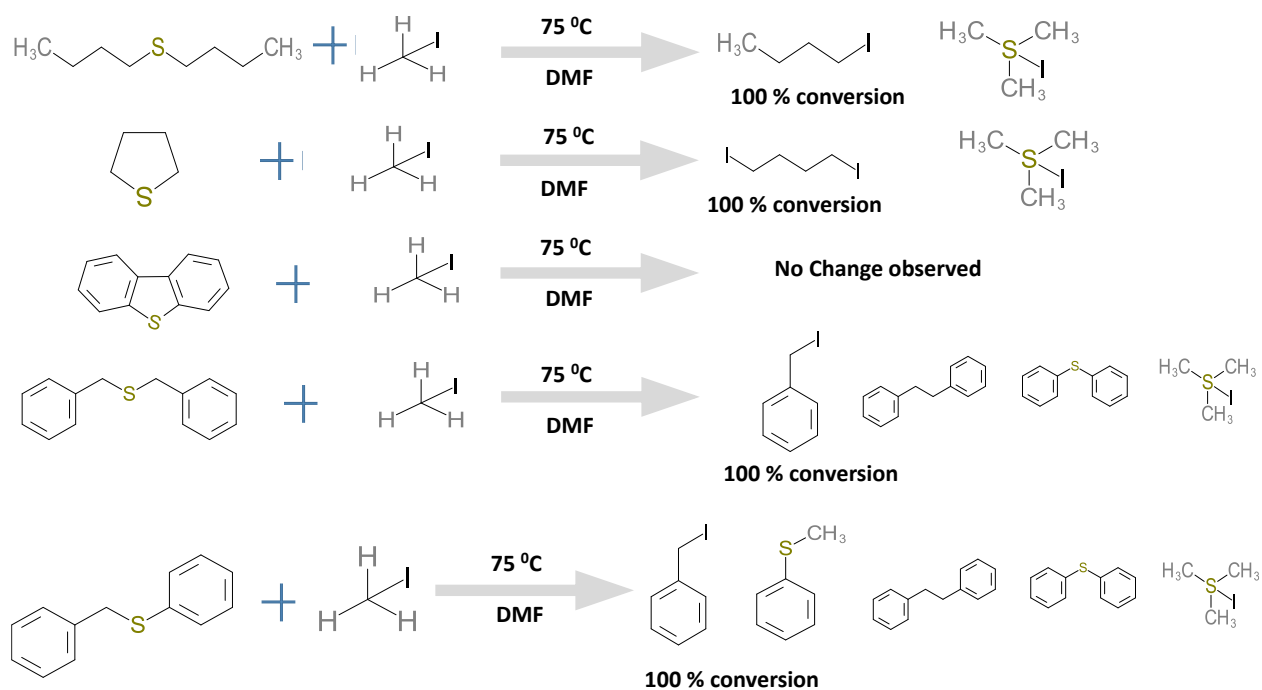
Figure 3.10 Suggested reaction pathways for reaction between organosulfur compounds and CH_3I.

The reactions indicated in figure 3.10 indicate that sulfur from organosulfur compound is removed as trimethyl sulfonium iodide. However, cleavage of carbon sulfur bond directly attached to the aromatic ring, either as aliphatic sulfur, or as thiophenic sulfur, was not achieved by reaction with CH_3I.

Oxygenates were also detected in the liquid products. The formation of oxygenates during reaction can be attributed to the residual oxygen left inside the reactor.

Asphaltene structure is highly complex and therefore definitive conclusion about presence of a particular type of C-S chemical bonds cannot be conclusively made. However a directional speculation can be made regarding the reaction of carbon sulfur bonds in asphaltene with methyl iodide at 75 °C temperature in DMF solvent. The results indicate that reaction between asphaltenes and CH_3I would be possible and scission of some aliphatic carbon sulfur bonds in asphaltenes is anticipated. The conversion of asphaltenes with CH_3I is described in Chapter 4.

3.5. Conclusion

- DMF used as solvent in this work does not react with CH_3I on its own. However, transfer of oxygen was observed in some reaction products after reaction in the presence of organosulfur compounds.

- Aliphatic sulfur reacts readily with CH_3I in presence of DMF. The conversion of aliphatic sulfur compounds is 100% at 30:1 excess of CH_3I at 75 °C after 24 hours.

- Methyl iodide does not cleave carbon sulfur bond directly attached to aromatic rings as in thiophenic and phenylic sulfur.

- Increasing pressure in the reactor does not help in facilitating reaction of thiophenic sulfur with CH_3I.

3.6. References

1. Selker M. L. Kemp A. R. Reaction of Methyl Iodide with Sulfur Compounds. *Ind. Eng. Chem.* **1944**, 36 (January), 16-20.

2. Shaw, J. E. Molecular Weight Reduction of Petroleum Asphaltenes by Reaction with Methyl Iodide-Sodium Iodide. *Fuel* **1989**, Vol 68 September, 1218-1220.

3. Murray, P. M., Bellany, F., Benhamou, L., Bucar, D. K., Tabor, A. B., Sheppard, T. D. The Application of Design of Experiments (DoE) Reaction Optimization and Solvent Selection in the Development of New Synthetic Chemistry. *Org. Biomol. Chem.* **2016**, 14, 2373 – 2384.

4. Stull, D. R. Vapor pressure of Pure Substances Organic Compounds. *Ind. Eng. Chem.* **1947**, 39, 4, 517-540.

5. NIST Chemistry WebBook, SRD 69. http://webbook.nist.gov/ (accessed on Nov 06, **2017**), Properties of methyl iodide.

4. Reaction of asphaltenes with methyl iodide via S-alkylation reaction

Abstract

The present work investigates sulfur alkylation enabled scission of C-S bonds in asphaltenes using methyl iodide under nitrogen environment. No measurable benefit was found as a result of reaction between asphaltenes and methyl iodide. This was concluded using results from thermogravimetric analysis and elemental composition of reaction products and was contrary to what was anticipated based on the work reported in chapter 3.

Keywords: - Asphaltenes, C-S bond scission, Methyl iodide, Oilsands bitumen upgrading

4.1 Introduction

Results presented in chapter 3 indicate that methyl iodide reacts with aliphatic sulfur in both acyclic and cyclic forms. However, thiophenic and phenylic sulfur do not react with methyl iodide. Asphaltenes is known to contain nearly 30% of its total sulfur in aliphatic form.[1] The role of sulfur in asphaltenes and effect of its removal has also been explained in section 2.2 and 2.3 of chapter 2. Therefore it was hypothesized that carbon sulfur bond scission enabled by reaction between asphaltenes and methyl iodide will result in beneficial changes in asphaltenes.

The present chapter presents the results obtained after reaction conducted between methyl iodide and asphaltenes at reaction conditions adopted from Shaw's work.[2] Reactions were also conducted under modified conditions.

The objective of this work was to evaluate the reaction of asphaltenes with CH_3I for asphaltenes conversion to lighter hydrocarbon molecules.

4.2 Experimental

4.2.1   Materials

Feed material for this study was raw asphaltenes sourced from the Nexen Energy ULC Long Lake upgrader.   The asphaltenes were industrially precipitated using *n*-pentane and will be referred to as C_5-asphaltenes. Characterization data of the asphaltenes are presented in table 4.1.

Table 4.1. C_5-Asphaltene feed characterization[3]

Property	Value
Aliphatic/aromatic hydrogen ratio	7.17 ± 0.18
Micro carbon residue (MCR), wt%	36
Chemical analysis, wt%	
Carbon	82.09 ± 0.12
Hydrogen	8.06 ± 0.07
Nitrogen	1.15 ± 0.01
Sulfur[#]	7.82 ± 0.11
Density at room temperature $\sim 23\ {}^0C$ (g/ml)	1.087 ± 0.076

 # Sulfur content of asphaltenes used in this study was measured separately during study using X-Ray Fluorescence spectroscopy and result was 8.7 wt%. This value was used for calculation.

Tetrahydrofuran (THF) was used for dissolving asphaltenes. This was procured from Sigma Aldrich with a purity of 99+%. No further purification was done. N,N-dimethylformamide (DMF) was procured from Fisher Scientific with a purity of 99.5%. DMF was used as polar solvent for facilitating the reaction. This chemical was used as received. Sodium iodide dihydrate $(NaI.2H_2O)$ was purchased from Acros Organic with a purity of 99+% and no further processing was done on the chemical received. Methyl iodide (CH_3I) was procured from Alfa Aesar with a

purity of 99% and was stabilized by copper by the supplier. (Copper provides stabilization of methyl iodide during its storage and significantly reduces the decomposition of methyl iodide under light). This was used as obtained. HPLC grade Chloroform with purity of nearly 99.25% was procured from Fisher Scientific. Approximately 0.75% ethanol was added by the supplier as preservative in chloroform. Carbon disulfide (CS_2) with purity of 99.9% was procured from Fisher Scientific. This was used as received. Distilled water was produced in laboratory using Millipore MilliQ equipment available in the lab.

The gas cylinders were all procured from Praxair: Ultra-high purity (UHP 5.0) helium with purity of 99.999%, high purity (HP 4.8) nitrogen with purity of 99.998%, hydrogen with purity of 99.95 %, and compressed air with a composition in the range 19.5-23.5 % oxygen and 76.5-80.5 % nitrogen.

In addition to safety precautions mentioned in section 3.2.1 additional precautions were required for work in this chapter owing to the use of chloroform. Chloroform is carcinogenic and poisonous if inhaled. Therefore coworkers were informed of chloroform in use. Chloroform was always handled inside the fume hood for minimizing the exposure.

4.2.2   Equipment

A Heidolph rotary evaporator was used for solvent evaporation from the product mixture. Solvent evaporation was conducted under reduced pressure using a vacuum pump from Heidolph that was attached to this rotary evaporator. This rotary evaporator is fitted with temperature controlled water bath. Schematic diagram of evaporator is given in figure 4.3.

All other equipment and the balances used for measurements were the same as described in chapter 3. Glassware will be described in section 4.2.3.1.

4.2.3 Procedure

Industrially precipitated asphaltenes was ground using a mortar and pestle to fine powder for reaction. The reaction between asphaltenes and methyl iodide was conducted in four groups of experiments. Each group consisted of two sets of reactions. One reaction was conducted with CH_3I and the second reaction followed same procedure but without CH_3I. Comparison of results from these two reactions helped with interpretation. It made it possible to differentiate between changes taking place due to the reaction conditions and changes that could be attributed to the reaction between asphaltenes and CH_3I.

Table 4.2 presents a description of the eight sets of reactions. The numbering follows on that of chapter 3.

Table 4.2 Detail about reactions involving C_5 asphaltenes with and without CH_3I

Reaction set	Detail about reaction
Set – 12	Reaction between C_5 asphaltenes and CH_3I in glassware with procedure by Shaw[2]
Set – 13	C_5 asphaltenes processed with same procedure as set – 12 without adding CH_3I
Set – 14	Reaction between C_5 asphaltenes and CH_3I in closed reactor
Set – 15	C_5 asphaltenes processed with same procedure as set – 14 without adding CH_3I
Set – 16	Reaction between C_5 asphaltenes and CH_3I in closed reactor without sodium iodide
Set – 17	C_5 asphaltenes processed with same procedure as set – 16 without adding CH_3I
Set – 18	Reaction between C_5 asphaltenes and CH_3I in closed reactor without sodium iodide at elevated nitrogen pressure
Set – 19	C_5 asphaltenes processed with same procedure as set – 18 without adding CH_3I

4.2.3.1 Reaction between asphaltenes and methyl iodide in flask (Set - 12 and Set - 13)

The reaction procedure in this study was adapted from the procedure followed by Shaw.[2] Powdered asphaltenes was placed in a conical flask (item 8, figure 4.1) and DMF along with THF was added to the flask. Methyl iodide and $NaI.2H_2O$ were added to reaction mixture thereafter. THF was used for dissolving asphaltenes. As concluded in chapter 3, THF is not required for facilitating the expected reaction between C-S bond and CH_3I. Two sets of reaction was performed, one with CH_3I (Set – 12) and second without adding CH_3I (Set – 13). A magnetic stirrer was placed in both reaction mixtures. The weight was recorded at each stage using a Mettler Toledo balance. The weights are presented in table 4.4. The flask was kept on a hot plate (item 7, figure 4.1) maintained at 75 °C with condenser (item 4, figure 4.1) fitted over it. Condenser temperature was maintained at 2 °C. A nitrogen connection was fitted over the condenser to maintain the nitrogen environment inside the reaction flask. Constant nitrogen flow of nearly 20 % of the scale was established. The nitrogen flow rate was maintained by adjusting the needle valve on the rotameter (item 3, figure 4.1). The rotameter was not calibrated. This is because the constant flow of nitrogen was maintained only for ensuring nitrogen environment over the reaction mixture. Nitrogen pressure at the cylinder outlet was controlled equal to 1.48 MPa using pressure regulator (item 2, figure 4.1). Flow rate and cylinder outlet pressure was maintained to ensure that constant nitrogen flow was established through reaction system. A chiller (item 6, figure 4.1) was used for supplying coolant to the condenser. A further precaution to eliminate ingress of air and maintain a nitrogen environment was to submerging the outlet tube end of the gas line in a water filled in a volumetric cylinder (item 5, figure 4.1). The height of water above tube end was 270 mm, effectively providing some positive pressure in the system.
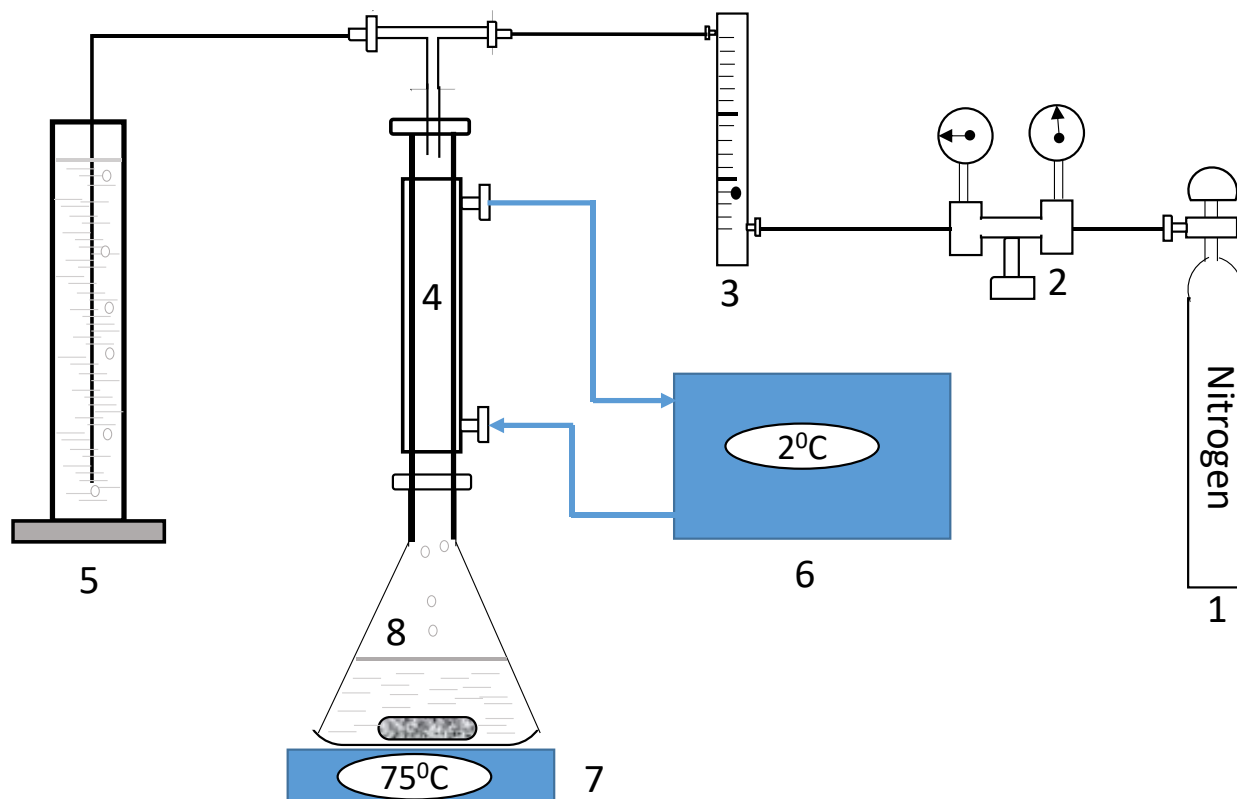
Figure 4.1. Reaction setup for reaction between asphaltene and methyl iodide in conical flask reactor. 1) Nitrogen cylinder 2) Pressure Regulator 3) Rotameter 4) Condenser 5) Water filled volumetric cylinder 6) Chiller 7) Hot plate 8) conical flask with reaction mixture and magnetic stirrer

For safety reason the whole setup (excluding nitrogen cylinder and Chiller) shown in figure 4.1 was placed inside the fume hood.

The reaction mixture was kept under reflux conditions at 75 °C for 24 hours under nitrogen flow. Then the reaction mixture was allowed to cool to ambient temperature and 200 ml distilled water was added and then 400 ml chloroform was added to the flask. The resulting solution was transferred into separating funnel. The separating funnel was shaken with stopper in place followed by allowing it to rest for settling. Two separate phases were observed as shown in figure 4.2.
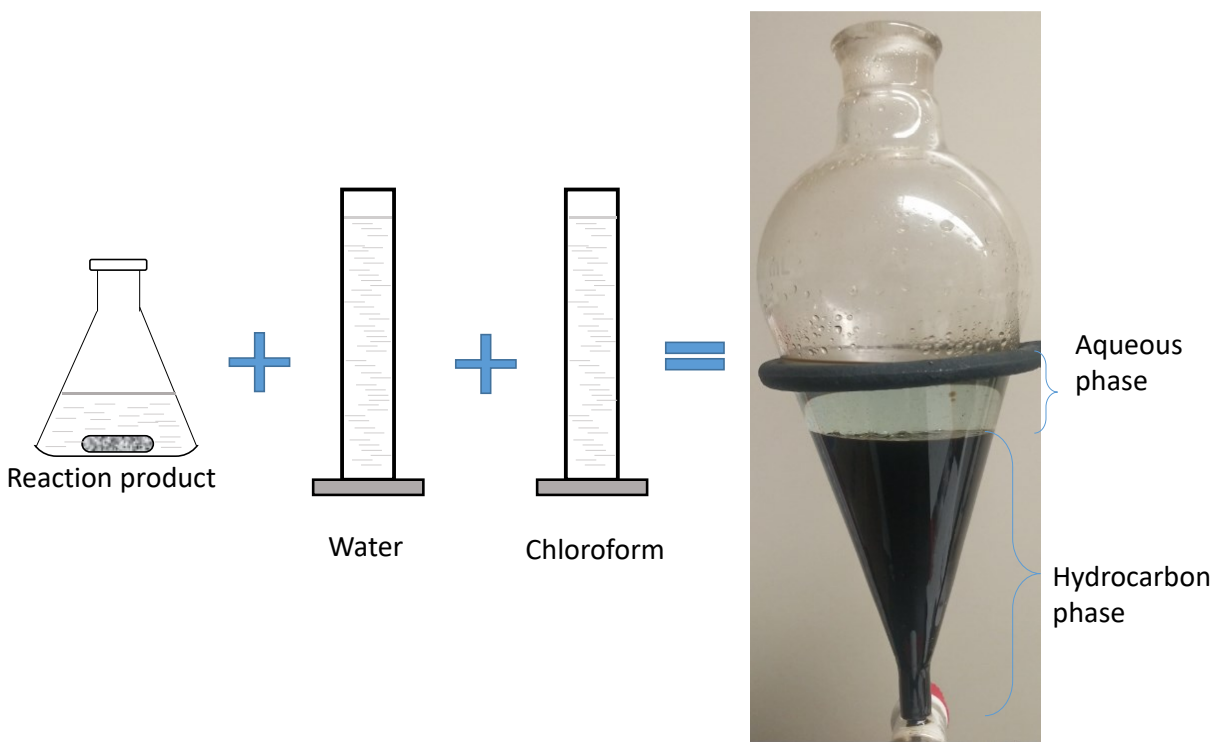
Figure 4.2. Product extraction using chloroform and water washing

The hydrocarbon phase was denser than the aqueous phase. The reaction product was washed four times with distilled water for removal of water soluble compounds such as NaI, THF and DMF. The number of water washing steps was selected so that the weight of water removed becomes equal to the weight of water added. A total of four washing steps were performed. 100 ml distilled water was used for each water wash. The water washed product mixture in chloroform was evaporated in a Heidolph rotary evaporator fitted with vacuum pump. Schematic diagram of the rotary evaporator is presented in figure 4.3.
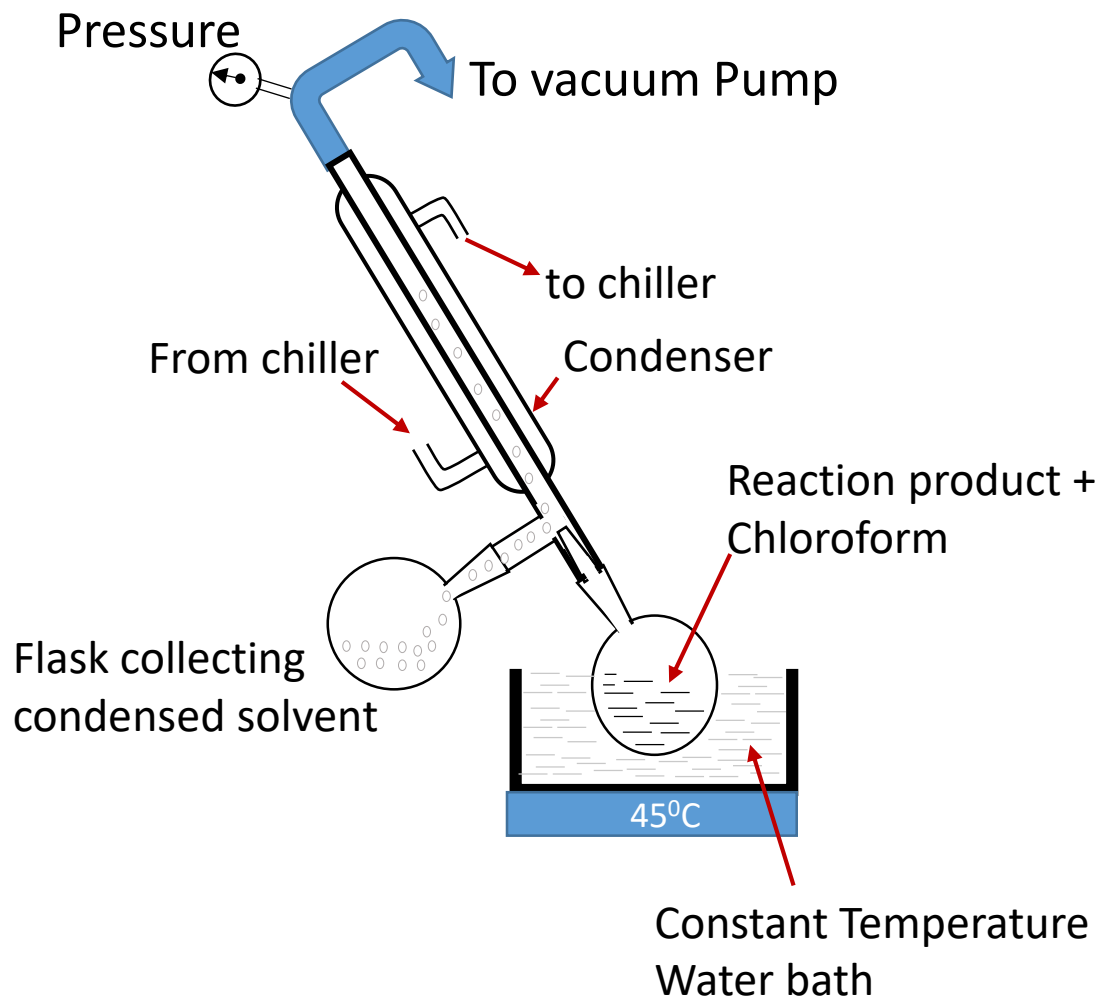
Figure 4.3 – Schematic diagram of rotary evaporator

The evaporation was performed at different pressures. Firstly 0.05 MPa pressure was maintained in the evaporating flask for removing chloroform and then subsequently pressure was reduced to 0.04, 0.007 and 0.001 MPa for removal of remaining traces of THF, water and DMF respectively. The temperature of rotavap water bath was maintained at 45 °C. Duration of evaporation at the lowest pressure of 0.001 MPa was 120 min. This duration was selected because no further loss in weight of product was observed. Residue weight was calculated from

difference between clean evaporating flask and weight of evaporating flask after evaporation. Residue weight was compared with the weight of the asphaltenes used as feed material.

During water washing of the reaction product, an emulsion was observed at the interface. However, the separation was attained to satisfactory level after leaving the mixture for nearly 2 hours.

This reaction was conducted in flask with continuous flow of nitrogen though the system. Therefore the overall material balance during the reaction was not considered. The residue product collected from evaporating flask was analyzed. No other product was analyzed.

4.2.3.2   Reaction between asphaltenes and methyl iodide in closed batch reactor (Set -14 and Set -15)

Another set of reactions was conducted in closed batch reactor under nitrogen environment at self-generated pressure. The closed reactor system employed for this study was exactly same as detailed in the section 3.2.3 and figure 3.1.

Powdered asphaltenes was added to the empty reactor. THF and DMF solvents were added to the reactor. THF was used as solvent for dissolving asphaltene. $NaI.2H_2O$ was added to the reactor followed by addition of CH_3I. The weight of each reaction ingredient is noted in table 4.7. Two sets of reactions were performed, one with CH_3I and second without adding CH_3I. Both reactors were closed and checked for leaks by pressurizing with nitrogen up to 0.7 MPa pressure as measured on the pressure gauge (item 3, figure 3.1). After no leak was found, the reactors were slowly depressurized completely and the valve (item 4, figure 3.1) was closed. The reactor was placed inside the constant temperature bath (item 2, figure 3.1) fitted with temperature measurement and automatic temperature control based on measured temperature and its set point.

The reactor was kept in the constant temperature (75 °C) for 24 hours. The reactor was removed from the fluidized sand bath and allowed to cool to ambient temperature. Gas sample bags were filled with nitrogen and evacuated three times while waiting for the reactor to cool. This was done to clean the gas bag of any residual impurity. Gas product was collected in the gas sample bag. Weight of gas sample was calculated by taking difference of reactor weight before and after taking gas sample out. The liquid product mixture was transferred to a separating funnel. Then the reactor was washed with water followed by washing with chloroform. The washed out liquid was added to the separating funnel containing the product mixture. In total, 100 ml water and 200 ml of chloroform were used in this step. The separating funnel was then shaken with stopper in place and allowed to rest for settling (for example, figure 4.4). Water washing and evaporation of solvents was performed in the same way as explained in the procedure 4.2.3.1 above.

Product residue (solid) from the evaporating flask was collected after solvent removal. The weight of product was calculated from difference between weight of clean evaporating flask and weight of evaporating flask after solvent evaporation. The residue solid product, and gas product were analyzed. No other product was analyzed.

4.2.3.3 Reaction between asphaltenes and methyl iodide in closed batch reactor without adding sodium iodide (Set -16 and Set -17)

During the water washing for product separation as described in section 4.2.3.1, formation of a "sludge" was observed. The separation between hydrocarbon and aqueous phases were attained after resting for few hours. However the separation was not complete and part of hydrocarbon phase was taken out with the aqueous phase. The following series of pictures indicate the phase separation with respect to time.
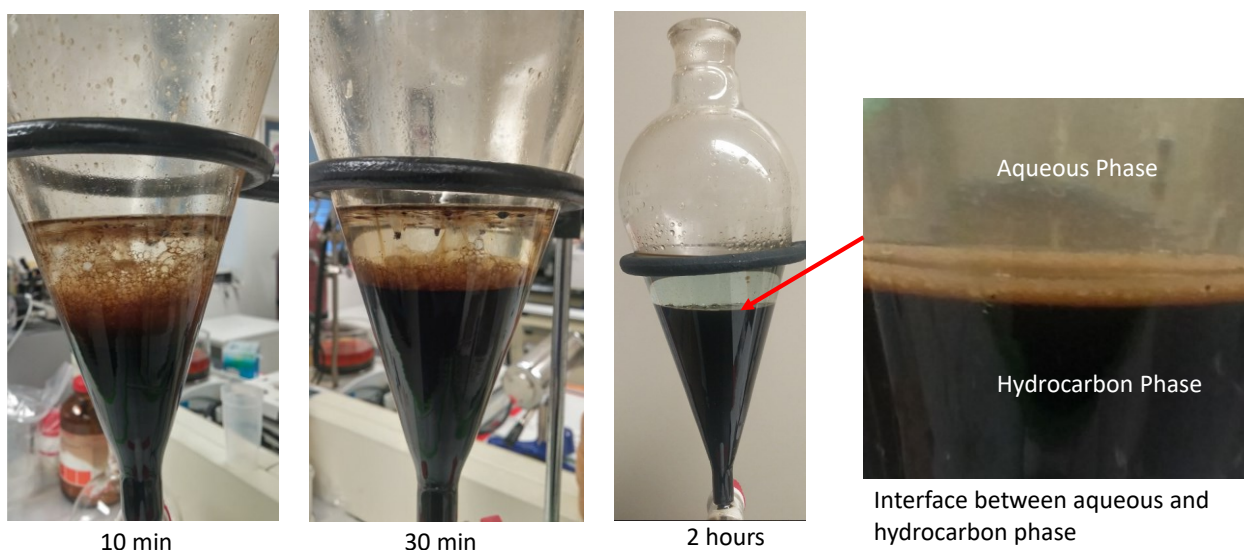
Figure 4.4. Formation of mixed phase at the interface between aqueous and hydrocarbon phase and separation progress with time.

This indicates that there was loss of hydrocarbon product with the aqueous phase. It was not possible to recover the entrained hydrocarbon from the aqueous phase. Addition of sodium iodide mandated the water wash procedure in section 4.2.3.2. Therefore another set of reactions was performed without adding sodium iodide. Moreover the results in chapter 3 indicated that presence of sodium iodide is not necessary for cleavage of C-S bonds with methyl iodide.

A measured quantity of powdered asphaltenes was placed inside the reactor followed by adding a weighed quantity of THF, DMF and CH_3I to the reactor. Two sets of reactions were performed, one with CH_3I (Set – 16) and second without adding CH_3I (Set – 17). The same procedure for reaction was used as described in section 4.2.3.2.

After reaction the reactor was opened and the product mixture was transferred to a weighed and labelled evaporating flask. A rinse of 100 ml chloroform was used to ensure all products were transferred to the evaporating flask. Water was not used in this procedure. Rotary evaporator

fitted with a vacuum pump was used for evaporating the solvents from the product mixture in the same way as described in section 4.2.3.1.

The details about mass of each reaction ingredient and relevant mass balance is presented in the results section.

4.2.3.4 Reaction between asphaltenes and methyl iodide in closed batch reactor at high pressure without adding sodium iodide (Set -18 and Set -19)

In order to test the effect of pressure on this reaction, reactions were performed at 75 °C at 4.83 MPa under nitrogen atmosphere. The procedure as described in section 4.2.3.3 was followed for conducting this reaction. The only difference was with respect to pressure inside the reactor.

The product was collected as explained in section 4.2.3.3. The product residue and the gas product were analyzed.

4.2.4 Analysis

Reaction products from this work were analyzed. Table 4.3 provides the list of analyzes employed in this study.

Table 4.3. Analysis methods and equipments used

Analysis	Equipment	Analysis goal	Supplier
Thermal Decomposition	Thermal gravimetric analysis (TGA)	Thermal behavior	Mettler Toledo
Elemental composition	X-Ray Fluorescence spectrometry (XRF)	Sulfur, iodine	Bruker S2
Gas chromatography	Gas chromatography (GC)	Gas composition	Agilent
Scanning Electron microscopy	Zeiss Sigma 300 VP-FESEM	Iodine content	Zeiss

Thermal behavior of the reaction product after solvent evaporation was investigated using Mettler Toledo TGA/DSC1 Star$_e$ system. This TGA system consisted of microbalance with weighing range up to 5 g with resolution of 0.1 μg. The maximum furnace temperature was 1100 °C. Alumina crucibles of 70 μL capacity were used for analysis. The samples were placed in the alumina crucibles that were transferred to the heating chamber by a sample robot. No lid was used on the crucible. Nitrogen cylinder was used for supplying nitrogen to the heating chamber. The weight of each crucible was measured by placing inside the heating chamber before putting sample in it. Continuous measurement of sample weight and chamber temperature is done automatically. Following program was used for performing TGA on reaction products.

1. Maintain temperature of 30 °C for 10 minutes under nitrogen flow of 50 ml/min

2. Raise the temperature from 30 °C to 600 °C at the rate of 10 °C/min under constant flow of nitrogen equal to 50 ml/min.

3. Maintain temperature at 600 °C for 60 minutes while keeping the nitrogen flow constant at 50 ml/min.

The sample weight was plotted against temperature. The onset and occurrence of loss in mass of sample during the analysis period was interpreted. Above mentioned program was inspired by the standard method (ASTM D4530) for measuring microcarbon residue (MCR) content of heavy oils. The weight of residue left after analysis was interpreted as equivalent to the MCR and it indicated the change in coking tendency of the product with respect to starting asphaltenes.

A Bruker S2 RANGER XRF was used for quantifying the sulfur and iodine content of reaction products. X-Rays generated from a 50 watt X-ray tube were used for excitation of the sample placed in disposable cup with lid and transparent bottom. SpectorMembrane™ prolene 3.0 μm thick thin film was used to create the transparent bottom in the sample holding disposable cup. Silicon Drift Detector was used for detecting fluorescence radiation from sample. Helium gas from a cylinder was used for maintaining inert atmosphere inside the sample chamber during measurement. The Bruker S2 RANGER XRF was calibrated before measuring sulfur and iodine content. Copper disc calibration was performed followed by quality check with vendor supplied BAXS S2 glass standard. Measurement of sulfur and iodine in the sample was incumbent upon the successful calibration and quality check. Since the product recovered after reaction was in solid form, the product was dissolved in THF before placing inside the disposable cup in liquid form. Complete coverage of transparent bottom of disposable cup was ensured during each measurement by placing sufficient amount of liquid sample in the cup. There was no existing

method for iodine content measurement. Therefore a new method was created for measuring iodine content in liquid sample. Sodium iodide dihydrate ($NaI.2H_2O$) was used as compound with known iodine content for creating the new method. Sodium iodide dihydrate was dissolved in THF for creating solutions with iodine contents ranging from 0.01 wt% to 6 wt%. In order to measure iodine in the samples from reaction, THF was used as solvent. The weight of sample and THF solvent was noted and used for calculating the actual content of sulfur and iodine in the sample. The matrix for calibration and measurement was THF.

Gas chromatography was used to determine the composition of the gas product generated during reaction. The analysis was performed using an Agilent gas chromatograph (model number 7890A) fitted with metal packed column and 45/60 Molecular sieve 13X support matrix. The FID (flame ionization detector) response was used for quantification. The temperature program for the gas chromatograph used was as follows:

1. Once the temperature reached 70^0C, the GC is ready to receive the sample. Hold for 7 minutes.
2. Raise the temperature at 10 °C/min to 250 °C and hold for 2 minutes.
3. Reduce the temperature of the oven from 250 °C to 70 °C at a rate of 30 °C/min.
4. Hold the oven temperature at 70 °C for 8 minutes.

Field Emission Scanning electron microscope (FE-SEM) was used for measuring the iodine content in the residue left after TGA analysis. TGA instrument used for this study mandated the use of less than 10 milligram of sample and a small mass of residue was left after heating to 600 °C. The weight of residue left was less than 5 milligram. Therefore it was not possible to use XRF available in lab and FE-SEM facility in earth science department was used for measuring

the iodine content. Zeiss Sigma 300 VP-FESEM was used for iodine content measurement, also using XRF. It has resolution of nearly 10 nm. Schottky thermal field emitter is used as electron source. This equipment is fitted with secondary and backscattered electron detectors, an in-lens electron detector, and a cathodoluminescence detector. A Bruker energy dispersive X-Ray fluorescence system with dual silicon drift detector each with an area of 60 mm^2 and a resolution of 123 eV has also been fitted in this instrument. The sample quantity requirement for FE-SEM has no lower limit. Therefore this facility was used for iodine content measurement. A metal stub with flat surface was used as sample holder. One side of double sided sticking carbon tape was placed over the flat surface of the stub and other sticky surface of carbon tape is used for fixing the sample to hold it in place. The stub with sample was then transferred to the microscope chamber and the analysis was performed. Iodine content was reported in weight percent.

4.2.5 Calculation

Material balance calculation was performed for each set of reaction conducted in the closed batch reactor. In case of procedure followed in section 4.2.3.1 to 4.2.3.4 material balance calculation was performed. Weight recovery for each reaction was calculated by Eq.1 using the following components:

1. Total weight of reactor with reaction ingredient before closing the reactor (A) measured in grams: - Weight of reactor after closing the reactor was not used for reason mentioned below in point 3.

2. Weight of gas sample (B) measured in grams: - Weight of gas sample was calculated from difference between weights of reactor after reaction is over and after gas product is taken out.

3. Total weight of reactor with liquid product mixture (C) measured in grams: - This is weight of reactor containing product mixture after it is opened. The weight of reactor before opening was not used, because weight of sand and changes, due to heat, in silver glue used for closing reactor.

$$Weight\ Recovery\ (wt\%) = \frac{A\ (g) + B\ (g)}{C\ (g)} \times 100 \qquad \text{Eq. 1}$$

Note that this method of calculation includes the reactor mass and is therefore less sensitive to material losses.

The sulfur and iodine content in starting asphaltenes and reaction product was not directly measured but measured in diluted solution. The following measurements were used for calculating the sulfur content of the sample in wt% using Eq.2 and the iodine content of the sample in wt% using Eq.3:

1. Total weight of solution in vial (T) measured in grams: - This was calculated by adding the weight of sample added to the vial and weight of solvent, THF in this case.

2. Sulfur content measured in the solution (S) measured in wt%: - The solution was placed in disposable cup with transparent bottom and sulfur content of the solution is measured.

3. Iodine content measured in the solution (I) measured in wt%: - Iodine content of the solution placed in disposable cup was measured.

4. Weight of sample in vial (W) measured in grams

Sulfur content of solvent, THF in this case, is zero. Therefore sulfur content in the sample is calculated as below

$$Sulfur\ content\ in\ sample\ (wt\%) = \frac{T\ (g)\ \times S\ (wt\%)}{W\ (g)} \times 100 \qquad \text{Eq. 2}$$

In the similar way the iodine content of the sample was calculated as follows. Iodine content of the solution as measured using XRF is given as I in wt%.

$$Iodine\ content\ in\ sample\ (wt\%) = \frac{T\ (g)\ \times I\ (wt\%)}{W\ (g)} \times 100 \qquad \text{Eq. 3}$$

It was observed that the total weight of residue product obtained after solvent evaporation is higher than the weight of starting asphaltenes. Therefore sulfur and iodine content of product in wt% cannot be used as a parameter to evaluate the efficacy of the reaction. Absolute amount of sulfur and iodine in the sample in grams is used for interpreting the reaction results. Absolute amount of sulfur and iodine is calculated by multiplying the content of the sample in wt% and the total weight of reaction product or the starting asphaltenes as the case may be.

It was speculated that the higher total weight of product obtained after product separation than the weight of starting asphaltenes was due to residual solvent, new C-I bond formation or incomplete reagent removal. Weight of residue considering the loss of iodine and solvent during TGA analysis is a key is a key parameter to evaluate the reaction product. This calculation will be using following values.

1. Weight of reaction product (P) as measured in grams

2. Weight percent of solvent entrapped in reaction product (So) measured in weight percent

3. Weight percent of TGA residue (TR) measured in weight percent

4. Iodine content of reaction product (I) measured in weight percent using XRF method

5. Iodine content of TGA residue (TRI) measured in weight percent using SEM method.

6. Total weight of iodine (WI) removed during TGA calculated in grams.

7. Weight of product (PT) excluding solvent and iodine which are lost during TGA calculated in grams.

8. TGA Residue (R) in weight percent, considering that solvent and iodine are removed during TGA.

$$WI \ (g) = (P \times I - P \times (TR/100) \times TRI)/100$$

$$PT \ (g) = P - WI - P \times \frac{So}{100}$$

$$R \ (wt\%) = \frac{TR}{(PT/P)} \qquad \text{Eq. 4}$$

4.3 Results

Results are presented by section for reactions conducted as per procedures detailed in sections from 4.2.3.1 to 4.2.3.4.

4.3.1 Reaction between asphaltenes and methyl iodide in flask under nitrogen environment (Set – 12 and set – 13)

Two sets of reactions were conducted, one with methyl iodide and second one without methyl iodide added following the procedure as detailed in section 4.2.3.1. Block flow diagram for conducting this reaction is shown in figure 4.5. Table 4.4 provides the weight of each reaction ingredient in the reaction mixture.
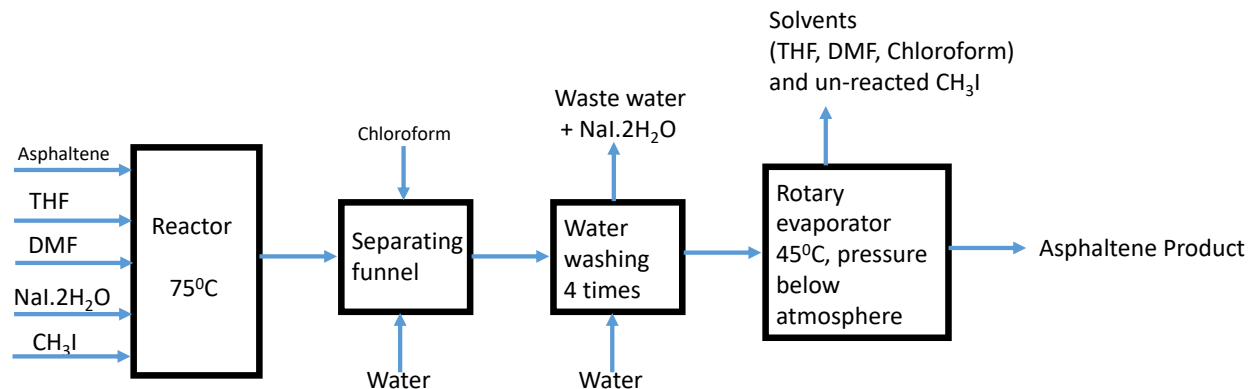
Figure 4.5 Block flow diagram for conducting the reaction between asphaltene and methyl iodide in conical flask reactor

Table 4.4. Weight of reaction ingredients for reaction between asphaltene and methyl iodide in conical flask reactor

Reaction Mixture Constituents	Set – 12	Set – 13
C_5 Asphaltenes (g)	2.10	2.05
NaI.$2H_2O$ (g)	4.55	4.20
THF (g)	24.35	23.39
DMF (g)	76.82	73.28
CH_3I (g)	57.64	0.0

The product weight after separation is measured after ensuring solvents are evaporated as much as possible. Product weight percent is calculated with respect to the initial asphaltenes weight taken for the reaction. Since this reaction was conducted in open reactor system. Therefore the material balance for overall reaction system could not be considered for closure.

Table 4.5. Weight of starting asphaltene and reaction product

	n-C$_5$ Asphaltenes Weight (g)	Product Weight (g)	Product wt%
Set – 12	2.10	3.01	143
Set – 13	2.05	2.06	100

The elemental analysis with respect to sulfur and iodine was performed using XRF. The analysis results are presented in table 4.6.

Table 4.6. Elemental composition and absolute amount of sulfur and iodine in reaction product

Element	Set – 12	Set – 13
Sulfur (wt %)	4.41	9.06
Iodine (wt %)	11.9	0
Sulfur Initially (g)	0.182	0.178
Sulfur in product(g)	0.132	0.185
Iodine in product (g)	0.358	0

From these analyses it is clear that iodine remained in the reaction product after washing. It was unlikely that the iodine remaining in set – 12 sample was due to NaI, because the NaI could be completely removed from set – 13, which had no iodine remaining in the product after washing. The analyses in table 4.6 also indicated that the amount of sulfur remaining in the set – 12

product was about 27 % less, which is close to amount of aliphatic sulfur fraction reported in literature (see Chapter 2).

Thermal analysis is the most basic method for analyzing the change in behavior of the asphaltenes. The TGA method as detailed in section 4.2.4 was used for thermal analysis of reaction product. The resulting TGA mass loss versus temperature curves for set – 12 and set – 13 are shown in figure 4.6 and compared against that of the C$_5$ asphaltenes feed material.
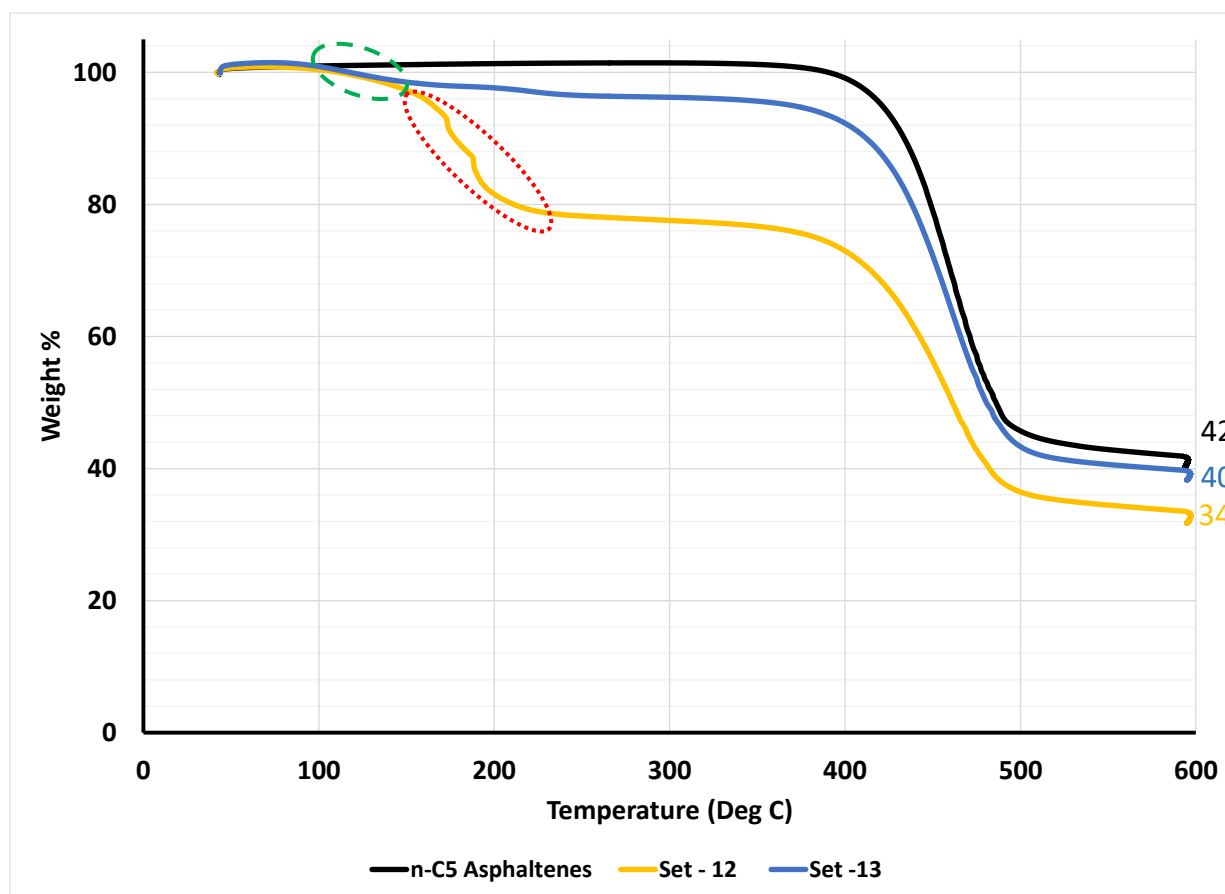
Figure 4.6. Thermogravimetric analysis curve for the reaction product of reaction of asphaltenes with methyl iodide in a conical flask reactor

The reduction in the sample weight starts at 100 °C for set – 12 and 13. The loss in mass as highlighted by the dashed green oval in figure 4.6 is attributed to residual solvent that remained after product separation and work-up. The significant loss in sample weight for the set – 12 sample started at a temperature of 150 °C, as highlighted in dashed red oval in figure 4.6. Mass loss in this temperature region was not observed for the C_5 asphaltenes feed and was minor for set – 13. This loss in mass of the set – 12 sample cannot be attributed to solvent only. This is because both sets of reaction with and without CH_3I have undergone exactly same process and the mass loss indicated by the red oval occurred to a more significant extent when CH_3I was present. All of the materials analyzed exhibited most mass loss in the 400–500 °C temperature range.

The MCR (microcarbon residue) of the C_5 asphaltenes feed was 42 wt%. After correcting for the residual solvent in the set – 13 sample, the MCR on an asphaltenes basis was also 42 wt% (40/96×100). When the same is done for set – 12, taking the mass remaining at 300 °C as indicative of the asphaltenes mass in the product, the MCR on an asphaltenes basis was 44 wt% (34/78×100). There was no meaningful change in the MCR of the asphaltenes that remained after conversion with CH_3I. This was somewhat surprising considering the reduction in sulfur reported in table 4.6. The mass loss below 400 °C also did not explain all of the extra mass noted in table 4.5.

In order to evaluate the effectiveness of this reaction on asphaltenes, similar reactions were conducted in a closed reactor so that material balance for the reaction could be calculated.

4.3.2 Reaction between asphaltenes and methyl iodide in closed batch reactor under nitrogen environment (Set – 14 and set – 15)

Two sets of reactions were conducted in a closed batch reactor. The experimental procedure was detailed in section 4.2.3.2 and was followed for both reactions. A block flow diagram to illustrate the procedure was shown in figure 4.5.

The weight recovery after reaction is calculated by dividing the sum of total weight of the reactor after reaction and the gas product weight by the total weight of reactor before starting the reaction according to Eq.1. The weights were recorded and reported in table 4.7.

Table 4.7. Weight of reaction ingredients for reaction between asphaltene and methyl iodide in a closed batch reactor

Reaction Mixture Constituents	Set – 14	Set – 15
n-C$_5$ Asphaltenes (g)	1.02	1.00
NaI.2H$_2$O (g)	2.00	2.02
THF (g)	5.14	8.81
DMF (g)	12.57	10.00
CH$_3$I (g)	13.36	0
Empty reactor (g)	373.84	412.49
Total Weight before reaction (g)	409.14	435.59
Total weight after reaction is over (g)	404.97	433.10
Gas Product weight (g)	0.14	0.05
Weight recovery in reaction (wt %)	99.02	99.43

The weight of the solid reaction product after both reactions were compared with weight of starting C$_5$ asphaltenes feed material used in each reaction (table 4.8).

Table 4.8. Weight of starting asphaltene and reaction product

Reaction set	n-C$_5$ Asphaltenes Weight (g)	Product Weight (g)	Product wt% w.r.t feed
Set – 14	1.02	1.31	130
Set – 15	1.00	1.01	100

The elemental analysis with respect to sulfur and iodine is performed using XRF. This analysis was also used for calculating the absolute amount of sulfur and iodine in reaction product using Eq.2 and Eq.3 detailed in section 4.2.5. Table 4.9 provides the analysis results and the calculation results.

Table 4.9. Sulfur and iodine weight percent and absolute content in reaction product measured by XRF

Element	Set – 14	Set – 15
Sulfur (wt %)	4.88	10.13
Iodine (wt %)	17.59	0
Starting Weight (g)	1.02	1.00
Product Weight (g)	1.31	1.01
Sulfur Initially(g)	0.088	0.087
Sulfur in product(g)	0.064	0.101
Iodine in product (g)	0.23	0

Similar observations as for the set – 12 and set – 13 experiments reported in table 4.6 could be made for set – 14 and set – 15. Iodine could be removed by washing from set – 15, but not set – 14. The total amount of sulfur remaining in the solid product after reaction with CH_3I (set – 14) was about 27 % less than that of the feed asphaltenes. However, an observation that was disconcerting was that the sulfur in the product from set – 15 was more than that of the feed, which is impossible (no sulfur containing reagents were added) and indicated that there was an analytical problem.

The gaseous product obtained in the closed reactor system was analyzed by GC. The composition of the gas phase is given in the table 4.10. The GC results indicate that no H_2S was detected in the product gases. This was not surprising, because the anticipated sulfur elimination product following from Chapter 3 would be the $(CH_3)_3S^+I^-$ salt. The hydrocarbon products were not anticipated. However, the industrial asphaltenes were produced by solvent deasphalting and one possible explanation could be that residual solvent remained in the asphaltenes.

Table 4.10. Gas composition for the gas product collected after reaction on N_2 free basis

Component	Set – 14 (mol%)	Set – 15 (mol%)
Methane	0	0
Propane	5.0	0
n-pentane	0	0.7
iso-hexenes	15.9	89.3
n-hexane	78.8	0
CO_2	0.2	9.9

Thermogravimetric analysis (TGA) was performed on the reaction products. The results are presented in the figure 4.7. The mass loss regions previously identified and described for figure 4.6 (see section 4.3.1) were also encountered in figure 4.7. There was solvent related mass loss starting around 100 °C (green oval in figure 4.7) and additional mass loss more specific to the reaction with CH_3I starting around 180 °C (red oval in figure 4.7). The set – 15 product appeared to be solvent free.
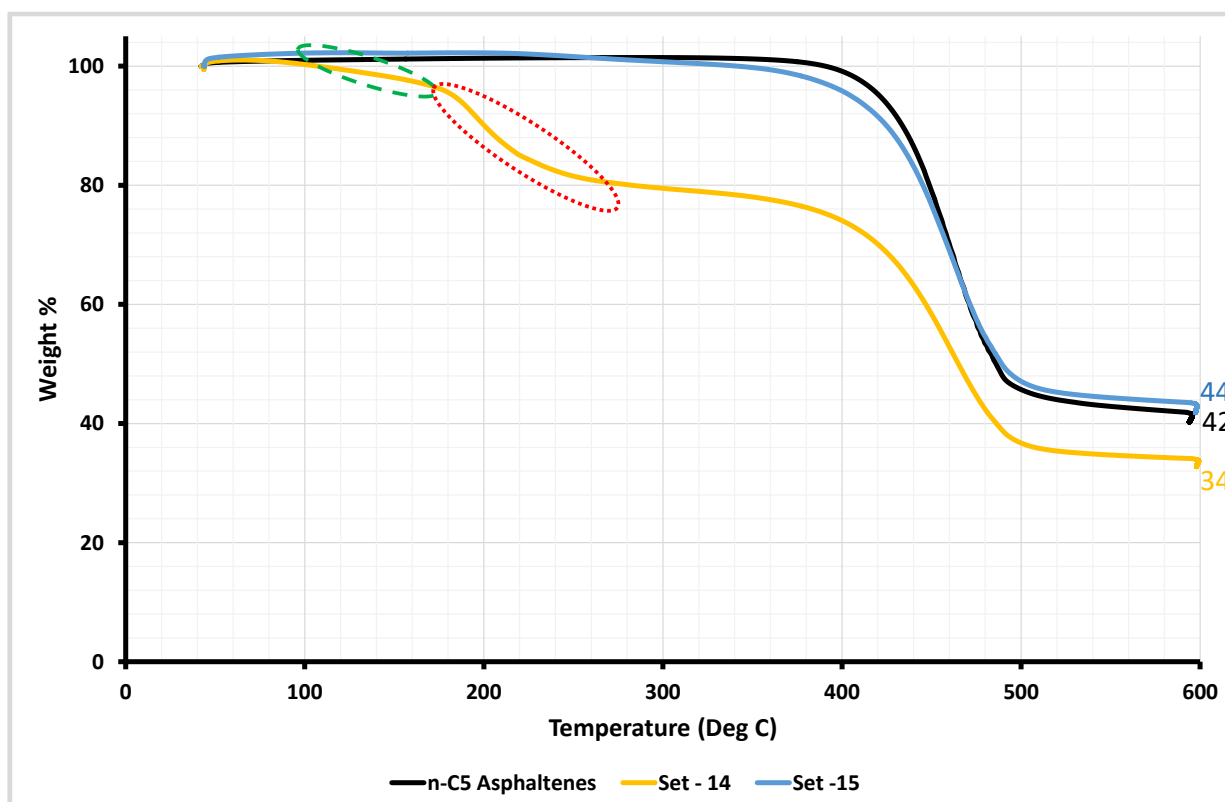
Figure 4.7. Thermogravimetric analysis curve for the reaction between asphaltenes and methyl iodide in closed batch reactor

The MCR of the set – 14 product, assuming the asphaltenes portion was the material remaining at 300 °C, was 43 wt% ($34/79\times100$). Using this assumption the calculated MCR was close to the 42 wt% MCR of the asphaltenes feed and the 44 wt% MCR of the set – 15 control experiment. However, this did not fully account for the excess mass in table 4.8.

Residue obtained after heating the reaction product with CH_3I (set – 14) to 600 °C in the TGA, was analyzed using XRF in SEM. The iodine content of TGA residue for the product of reaction with CH_3I contained 0.9 wt% by X-ray fluorescence in the SEM. Thus, the iodine content of the sample decreased from 17.6 wt% to 0.9 wt%. This indicate that most of the iodine in the solid reaction product was lost during heating, which could explain the mass loss starting around 180 °C (red oval in figure 4.7).

Based on the results present, no measurable benefit was observed following the reaction between asphaltenes and methyl iodide. The uncertainty in results of the sulfur analysis (table 4.9) and the near similar MCR values of the reaction product to that of the asphaltenes feed, were not encouraging findings.

4.3.3 Reaction between asphaltenes and methyl iodide in closed batch reactor under nitrogen environment without sodium iodide (Set – 16 and set – 17)

As mentioned in section 4.2.3.3, addition of sodium iodide to the reaction mixture mandated the use of water washing, which resulted in loss of hydrocarbon. The role of sodium iodide was not clear from the reaction mechanism. Therefore the reaction between asphaltenes and methyl iodide was conducted without adding sodium iodide. The modified block diagram for these sets of reactions are shown in figure 4.8. The material balance data is presented in table 4.11.
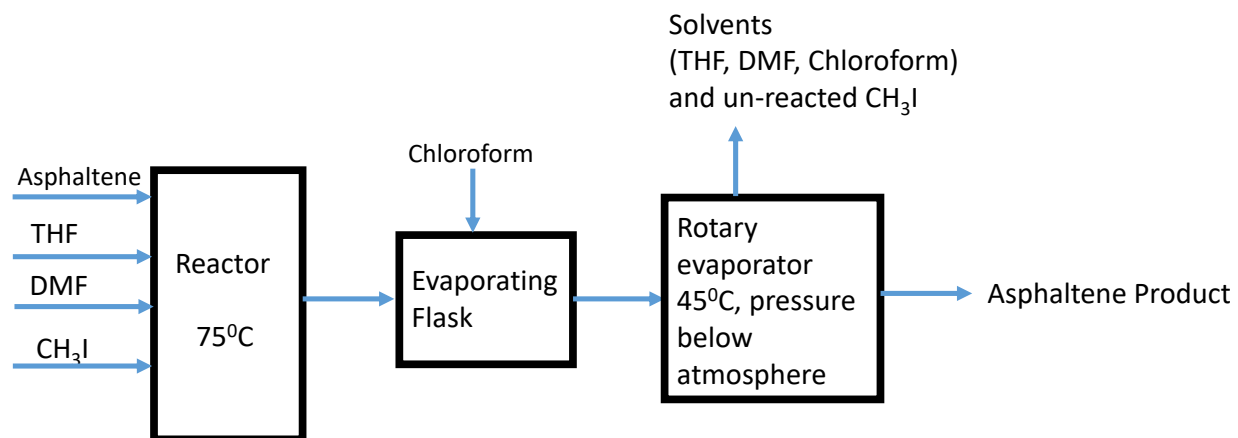
Figure 4.8. Block flow diagram for reaction between asphaltenes and methyl iodide in closed batch reactor without sodium iodide.

Table 4.11. Weight of reaction ingredient in the reactor for reaction between asphaltenes and methyl iodide without sodium iodide

Reaction Mixture Constituents	Set – 16	Set – 17
C_5 Asphaltenes (g)	0.56	0.53
$NaI.2H_2O$ (g)	0	0
THF (g)	4.55	9.85
DMF (g)	12.01	12.04
CH_3I (g)	6.61	0
Empty reactor (g)	392.17	372.91
Total Weight before reaction (g)	415.90	395.33
Total weight after reaction (g)	415.68	395.31
Gas Product weight (g)	0.10	0.10
Weight recovery in reaction (wt %)	99.98	100.02

Weight of gas is product is calculated from difference between the weights of total reactor weight before and after depressurizing the reactor for gas product collection. Since sodium iodide was not used during reaction, water washing was omitted. Chloroform was used for product extraction from the reactor. Product separation was performed for both sets of reactions as detailed in section 4.2.3.3.

The reaction product was weighed and compared with the starting asphaltenes for each set of reaction (table 4.12).

Table 4.12. Weight of reaction product of reactions conducted with and without CH_3I

Reaction sect	C_5 Asphaltenes Weight (g)	Product Weight (g)	Product wt% w.r.t feed
Set – 16	0.56	1.15	206
Set – 17	0.53	0.66	125

The product weight obtained after reaction performed without adding sodium iodide was significantly higher compared to the cases when sodium iodide was used during reaction (tables 4.5 and 4.8).

Reaction product was analyzed for sulfur and iodine content. The absolute amount of sulfur and iodine was calculated as explained in section 4.2.5 and the results are reported in table 4.13.

Table 4.13. Sulfur and iodine content in reaction product asphaltenes and absolute amount of sulfur and iodine

Element	Set – 16	Set – 17
Sulfur (wt %)	3.85	6.04
Iodine (wt %)	45.9	0
Sulfur Initially(g)	0.050	0.050
Sulfur in product(g)	0.044	0.040
Iodine content in product (g)	0.53	0

The change in absolute amount of sulfur between the starting material and reaction product after treatment asphaltenes indicated that treatment with CH_3I did not lead to an increase in desulfurization. A large amount of iodine was also detected in the product of set – 16.

The gaseous products were analyzed with GC. The results are presented in table 4.14. H_2S was not detected in the gas product.

Table 4.14. Gas product composition of the gas collected after reaction on N_2 free basis

Component	Set – 16 (mol %)	Set – 17 (mol %)
Methane	0.08	0.06
Ethane	0.04	0.09
H_2S	0	0
Propylene	0	0
Propane	1.65	0.95
i-Butane	0	0.20
n-Butane	0.37	0
cis-2-Butene	22.86	5.14
i-Pentane	12.95	18.36
n-Pentane	2.55	2.14
i-hexenes	25.28	42.70
n-Hexane	34.13	40.23
CO_2	0.09	0.11

Thermogravimetric analysis (TGA) was performed on the reaction product. There was significant reduction in sample mass that was observed for the product of reaction between asphaltenes and methyl iodide (figure 4.9).
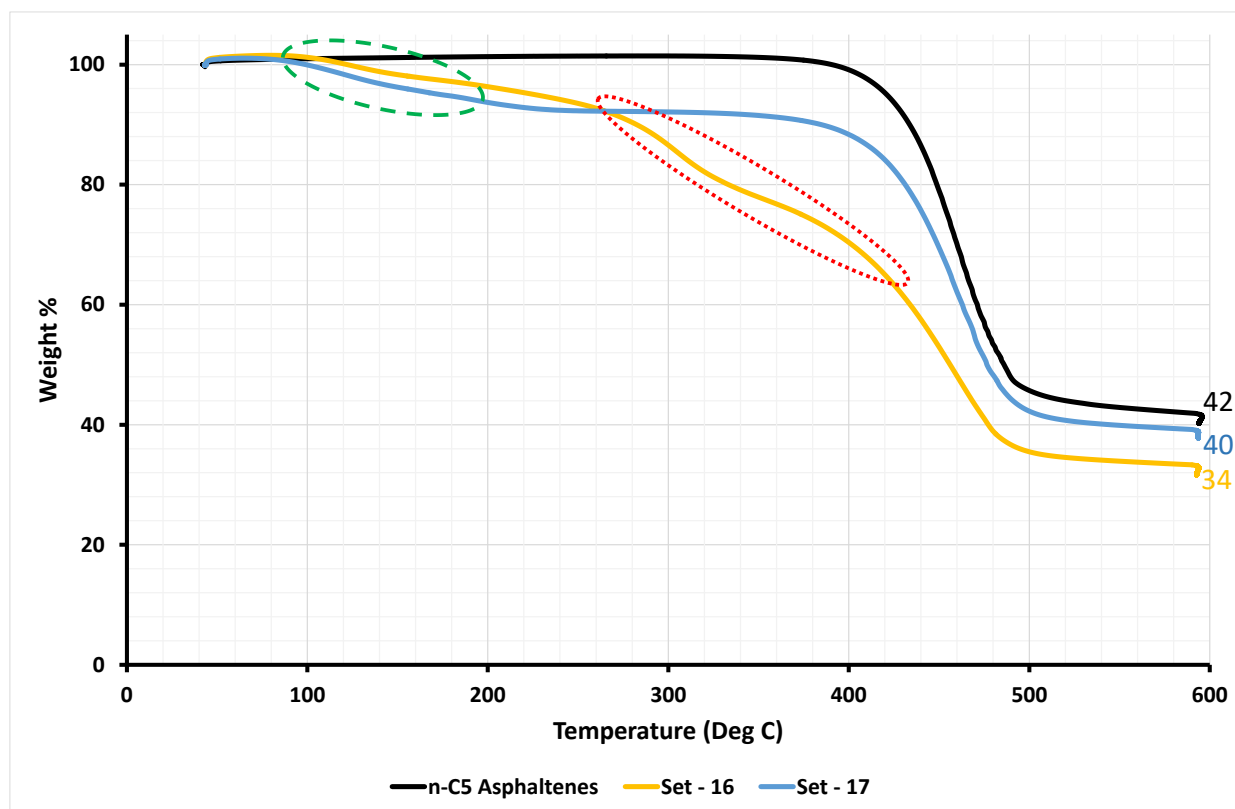
Figure 4.9. TGA analysis curve for the reaction product of reaction between asphaltenes and methyl iodide in closed batch reactor without sodium iodide

There are two distinct regions in the TGA mass loss curve, shown in dashed green and red ovals in figure 4.9, before the onset of significant cracking around 400 °C. Loss in mass highlighted in dashed green oval was attributed to the residual solvent in solid product. The solvent content of the product of reaction with CH_3I is equal to 6 wt%. The significant loss in mass has been highlighted in red oval. This loss in mass is of real interest to this work.

The residue left after 600 °C for the product of reaction with CH_3I (set – 16) was analyzed using SEM with X-ray fluorescence analysis to determine the iodine content. The iodine content in the residue was 4.3 wt%. This indicated that the iodine content of the set – 16 solid sample decreased from 45.9 wt% to 4.3 wt% during TGA. Therefore the significant loss in mass as

highlighted in red oval in figure 4.9 was attributed to reduction in iodine content in the sample during heating.

Unlike the TGA results shown in figures 4.6 and 4.7, the mass loss in the second region (red oval in figure 4.9) extended to the onset of cracking. It was not possible to use equation 4, because the weight of asphaltenes in set – 16 was not apparent from figure 4.9. The MCR content of set – 16 appeared to be high compared to that of the asphaltenes feed, and reaction without CH_3I (set – 17).

4.3.4 Reaction between asphaltenes and methyl iodide in closed batch reactor without sodium iodide at elevated pressure under nitrogen environment (Set – 18 and Set – 19)

These reactions were conducted under nitrogen at elevated pressure following the procedure as described in section 4.2.3.4 and shown in the block flow diagram in figure 4.8. Apart from the higher pressure, the set – 18 was performed in a similar way as set – 16 and set – 19 as set – 17.

The material balance data for the experiments are reported in table 4.15.

Table 4.15. Weight of reaction ingredient in the reactor

Reaction Mixture Constituents	Set – 18	Set – 19
C_5 Asphaltenes (g)	0.49	0.51
$NaI.2H_2O$ (g)	0	0
THF (g)	4.65	5.29
DMF (g)	12.39	12.1
CH_3I (g)	6.55	0.0
Empty reactor (g)	392.19	372.89
Total Weight before reaction (g)	416.28	390.77
Total weight after reaction is over (g)	415.78	390.84
Gas Product weight (g)	0.97	1.2
Weight recovery in reaction (wt %)	99.88	100.00

Product separation was performed as per the procedure provided in section 4.2.3.4. The final solid product was weighed and compared with starting asphaltenes (table 4.16).

Table 4.16. Weight of reaction product after reaction with and without CH_3I under pressure

Reaction set	Asphaltenes Weight (g)	Product Weight (g)	Product wt% w.r.t feed
Set – 18	0.49	1.07	218
Set – 19	0.51	0.64	125

The reaction product was analyzed using XRF spectroscopy for sulfur and iodine content. The sulfur and iodine content of the starting materials and products are presented in the table below (table 4.17). The absolute amount of sulfur and iodine was also calculated for better comparison.

Table 4.17. Elemental composition of reaction product after reaction with and without CH_3I after reactions performed under pressure

Element	Set – 18	Set – 19
Sulfur content (wt %)	3.79	5.96
Iodine content (wt %)	44.0	0
Sulfur Initially (g)	0.042	0.044
Sulfur in product(g)	0.040	0.038
Iodine in Product (g)	0.47	0

No significant reduction in sulfur was observed in this case, unlike that presented in section 4.3.1 and 4.3.2 (tables 4.6 and 4.9). There is similarity between the sulfur and iodine content of reaction products presented in section 4.3.3 and 4.3.4 (tables 4.13 and 4.17). This indicated that pressure has no differentiating impact on reaction between asphaltenes and methyl iodide. It also indicated that most of the sulfur remained in the product.

The gas product was analyzed using GC the composition was found as reported in table 4.18. No H_2S was detected in the gas phase product.

Table 4.18. Gas composition of gas product after reaction on N_2 free basis

Component	Set – 18 (mol %)	Set – 19 (mol %)
Methane	0	0.02
Ethane	0	0
H_2S	0	0
Propylene	0	0
Propane	0.28	0
i-Butane	0	0
n-Butane	0.11	0
cis-2-Butene	0.86	0
i-Pentane	15.54	9.36
n-Pentane	1.19	7.50
i-hexenes	53.48	47.01
n-Hexane	28.52	36.12
CO_2	0	0

The solid product was analyzed using TGA with same program as used earlier and the thermogravimetric result is shown in figure 4.10. TGA analysis of reaction products indicate the similar trend as shown in figure 4.9 and no benefit of increase in pressure was observed. The discussion in section 4.3.3 applies to this data.
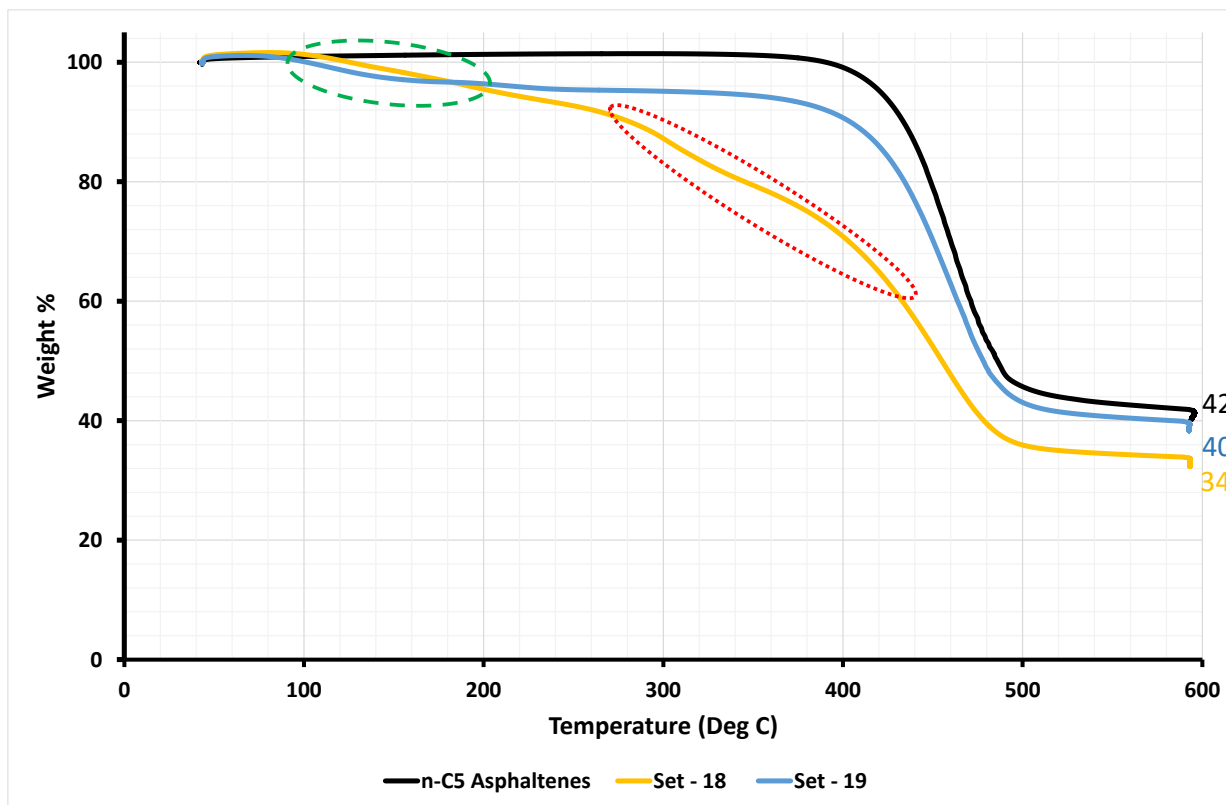
Figure 4.10. TGA analysis curve for the reaction product of reaction between asphaltene and methyl iodide in closed batch reactor without sodium iodide at elevated pressure under nitrogen environment

4.4 Discussion

Reaction between asphaltenes and methyl iodide was conducted under four different conditions in this work as given in table 4.2.

The first four experiments (set – 12 to set –15) included a water washing step and included NaI. It appeared that some sulfur was removed from the asphaltenes, presumably as water-soluble products, but the results also indicated much uncertainty as shown by the results in table 4.9. Thermogravimetric analysis of the reaction products resulted in MCR values that were close to each other.

The second four experiments (set – 16 to set –19) did not make use of NaI and did not include a water washing step. The most obvious difference was in the TGA mass loss versus temperature data. The reaction products from reaction with methyl iodide (set – 16 and set –18) displayed continuous mass loss up to 400 °C (figures 4.9 and 4.10). It was therefore not possible to distinguish between unconverted reagents and asphaltenes by TGA and a reliable MCR could not be calculated.

The gas product analysis as presented in tables 4.10, 4.14 and 4.18 indicated the detection of C_5 and C_6 hydrocarbons. This detection could be attributed to the residual solvent from deasphalting step.

In chapter 3, it was concluded that methyl iodide reacts with C-S bond under conditions employed for this work. The same reaction conditions were applied for reactions conducted in this chapter too. The results obtained in section from 4.3.1 to 4.3.4, indicated that there is possibly a reduction in sulfur content and increase in the iodine content of the product due to the reaction between asphaltene and methyl iodide. The combination of conclusions from chapter 3 and results from this chapter can be used to infer that cleavage of C-S bonds and formation of new C-I bonds in asphaltene due to reaction between asphaltene and methyl iodide took place.

No confirmed benefit of using methyl iodide as reagent for the conversion of asphaltenes was observed.

4.5 Conclusions

Based on the results and discussion presented in sections 4.3 and 4.4 respectively, following conclusions can be drawn.

1. Reaction of asphaltenes with methyl iodide is not effective for converting asphaltenes.

2. Although the use of NaI did not appear to be necessary, the water washing step that was employed in reactions with NaI removed some material that would otherwise have been volatilised in the temperature range 250–400 °C by TGA.

3. The water washed products after reaction of asphaltenes with CH_3I and NaI had a sulfur content of 27 wt% less than the feed asphaltenes. Uncertainty in the analyses precluded a strong conclusion, but it was noteworthy that the decrease in sulfur content was close to the approximately 30 wt% aliphatic sulfur content in asphaltenes reported in literature (chapter 2).

4. There was no apparent difference in the microcarbon residue (MCR) value of the asphaltenes before and after reaction with CH_3I and NaI.

5. Some iodine remained in the MCR obtained after heating the reaction products of CH_3I and asphaltenes to 600 °C.

6. Reaction between asphaltenes and CH_3I doesn't require the presence of NaI, but omission of the water washing step affected the mass loss versus temperature in such a way that continuous mass loss was observed below 400 °C, before the onset of mass loss due to thermal cracking.

7. There is no effect of increasing reaction pressure on the reaction between asphaltene and methyl iodide.

4.6 References

1. Siskin M.; Kelemen, S. R.; Eppig, C. P.; Brown, L. D.; Afeworki, M. Asphaltene Molecular Structure and Chemical Influences on the Morphology of Coke Produced in Delayed Coking. *Energy Fuels* **2006**, *20*, 1227-1234.

2. Shaw, J. E. Molecular Weight Reduction of Petroleum Asphaltenes by Reaction with Methyl Iodide-Sodium Iodide. *Fuel* **1989**, *68*, 1218-1220.

3. Mao, X. Alkylation of Asphaltenes. MSc Thesis, University of Alberta, Edmonton, AB, Canada, **2015**.

5. Alkylation reaction of model organosulfur compounds with 1-hexene over SIRAL®40 catalyst

Abstract

Acid catalyzed reaction of asphaltenes with propylene has resulted in conversion of asphaltenes to maltenes.[1] Asphaltenes conversion was attributed to C-S bond cleavage. The present work explores the reaction of organosulfur compounds with 1-hexene in presence of an amorphous silica-alumina (SIRAL®40) catalyst. Hypothetical reaction networks were proposed based on analysis of the liquid products after reaction.

Keywords: - Asphaltenes conversion, Alkylation, C-S bond cleavage, SIRAL®40

5.1. Introduction

Acid catalyzed reactions are one of the most used reactions in hydrocarbon industry. Catalysts containing acid sites are common in refining processes, such as alkylation, isomerization, reforming, and hydrocracking.

Conversion of asphaltenes to maltenes was previously found[1] and attributed to the cleavage of C-S bonds during the reaction of asphaltenes with propylene in presence of an acid catalyst. This chapter explores the reaction of the C-S bond and olefins in the presence of an acid catalyst at same reaction conditions applied previously[1] for the reaction between asphaltenes and propylene. Liquid and gas products were analyzed to ascertain what reactions involving C-S bonds lead to liquid products that could be maltenes.

Section 2.5 detailed the basis for selection of 1-hexene as the olefin species for this study. Five organosulfur compounds were selected from the list mentioned in section 2.8. These compounds and their structure are presented in table 5.1 for ease of reference.

Table 5.1 Organosulfur compounds and their structure, used for reaction with 1-hexene over SIRAL®40 catalyst

	Organosulfur compound	Structure
1	Di –n – butyl sulfide	
2	Tetrahydrothiophene	
3	Benzyl phenyl sulfide	
4	Dibenzyl sulfide	
5	Diphenyl sulfide	

Four sets of reactions with each organosulfur compound were conducted as presented in table 5.2. The reaction products from these reactions were compared to identify the reactions pertaining to C-S bonds that could be attributed to the presence of the olefin and acid catalyst. To ensure unique numbering, the numbering was continued following on the experimental numbering in chapter 4.

Table 5.2 Set of reactions for each organosulfur compound

Reaction set	Organosulfur compound	Olefin (1-Hexene)	Catalyst SIRAL®40	Remarks
20	Di-*n*-butyl Sulfide	Yes	Yes	Sulfide + Olefin + Catalyst
21	Di-*n*-butyl Sulfide	No	Yes	Sulfide + Catalyst
22	Di-*n*-butyl Sulfide	Yes	No	Sulfide + Olefin
23	Di-*n*-butyl Sulfide	No	No	Sulfide Only
24	Tetrahydrothiophene	Yes	Yes	Sulfide + Olefin + Catalyst
25	Tetrahydrothiophene	No	Yes	Sulfide + Catalyst
26	Tetrahydrothiophene	Yes	No	Sulfide + Olefin
27	Tetrahydrothiophene	No	No	Sulfide Only
28	Benzyl phenyl sulfide	Yes	Yes	Sulfide + Olefin + Catalyst
29	Benzyl phenyl sulfide	No	Yes	Sulfide + Catalyst
30	Benzyl phenyl sulfide	Yes	No	Sulfide + Olefin
31	Benzyl phenyl sulfide	No	No	Sulfide Only
32	Dibenzyl sulfide	Yes	Yes	Sulfide + Olefin + Catalyst
33	Dibenzyl sulfide	No	Yes	Sulfide + Catalyst
34	Dibenzyl sulfide	Yes	No	Sulfide + Olefin
35	Dibenzyl sulfide	No	No	Sulfide Only
36	Diphenyl sulfide	Yes	Yes	Sulfide + Olefin + Catalyst
37	Diphenyl sulfide	No	Yes	Sulfide + Catalyst
38	Diphenyl sulfide	No	No	Sulfide Only

In table 5.2 "Yes" indicates the presence of the reaction ingredient whereas "No" indicates the absence of that reaction ingredient in that reaction set. Comparison of reaction products between the first and second set for each organosulfur compound will provide data on the effect of the presence of an olefin on C-S bond conversion in the presence of the catalyst. Comparison of reaction products from first and second, with that of the third and forth set, will provide the effect of the catalyst on the reaction. Reaction products from the third and fourth set of each organosulfur compound will also be used as control experiments for observing thermal effects on C-S bonds.

The goal was to study the effects of olefin and acid catalyst on C-S bonds, therefore only gas and liquid products were analyzed. The catalyst and solid compounds that may have remained on the catalyst were not analyzed.

The objective of work in this chapter was to study the cleavage of C-S bonds and addition of alkyl chains to organosulfur compound due to the presence of 1-hexene and SIRAL®40 catalyst.

5.2.Experimental

5.2.1. Material

Di-*n*-butyl sulfide with 98% purity was purchased from Alfa Aesar. The compound was used as it was supplied. SIRAL®40 was procured from Sasol Germany GmbH. It is silica doped alumina with SiO_2 and Al_2O_3 in weight ratio of 40:60. This catalyst was supplied in powder form. Loose bulk density of SIRAL®40 is 250-450 g/l. Tetrahydrothiophene was purchased from Alfa Aesar. The supplied material was used without further purification. The purity of supplied material was 98%. Diphenyl sulfide (DPS) was procured from Alfa Aesar. The supplied material was used without further processing. Purity of diphenyl sulfide supplied was 98%. Dibenzyl sulfide was

purchased from fisher Alfa Aesar with a purity of 99%. The supplied material was used as received. Benzyl Phenyl sulfide with 98% purity was also purchased from Alfa Aesar. This was used without any further purification. Tetrahydrofuran (THF) was procured from Fisher Scientific with a purity of 99+%. No further purification was done. Butylated hydroxytoluene was added to THF by supplier.

Ultra-high purity (UHP 5.0) helium with purity of 99.999% was procured from Praxair supplied in cylinder. High purity (HP 4.8) nitrogen with purity of 99.998% was procured from Praxair supplied in cylinder.

The safety precautions stated in section 3.2.1 and 4.2.1 are applicable for the work in this chapter.

5.2.2. Equipment

The equipment employed in this study is the same as described in chapter 3.

Additionally, a Carbolite CWF furnace with, model number CWF 11/13, was used for calcination of amorphous SIRAL®40 catalyst. This electric furnace is fitted with automatic temperature controller.

5.2.3. Procedure

Amorphous SIRAL®40 catalyst was first placed in a furnace at 550 °C temperature for 6 hours under atmospheric pressure. This performed activation of the SIRAL®40 catalyst and removed residual moisture from catalyst.

The reactions were conducted in a closed batch reactor similar to figure 3.1. The only difference was that the reaction ingredients and catalyst were placed inside a glass vial and then the glass

vial was placed inside the reactor before closing the reactor, as shown in figure 5.1. The intent of using glass vial was ease of operation and to eliminate the possible contribution the metal wall of the reactor to the reaction.

The reaction time for this work was 24 hours. This reaction time was selected to be comparable with a previous study of asphaltenes conversion by alkylation over acid catalyst.[1]

The details of the procedure followed for the purpose of conducting the reaction are same as described in section 3.2.3.

Once all the reaction ingredients were placed inside the glass vial, the catalyst particles settle down at the bottom of vial owing to its higher particle density. Organosulfur compound and 1-hexene were miscible. When glass vial with all reaction ingredients was placed inside the reactor, a column of liquid was present over the layer of catalyst present at the bottom of the glass vial.
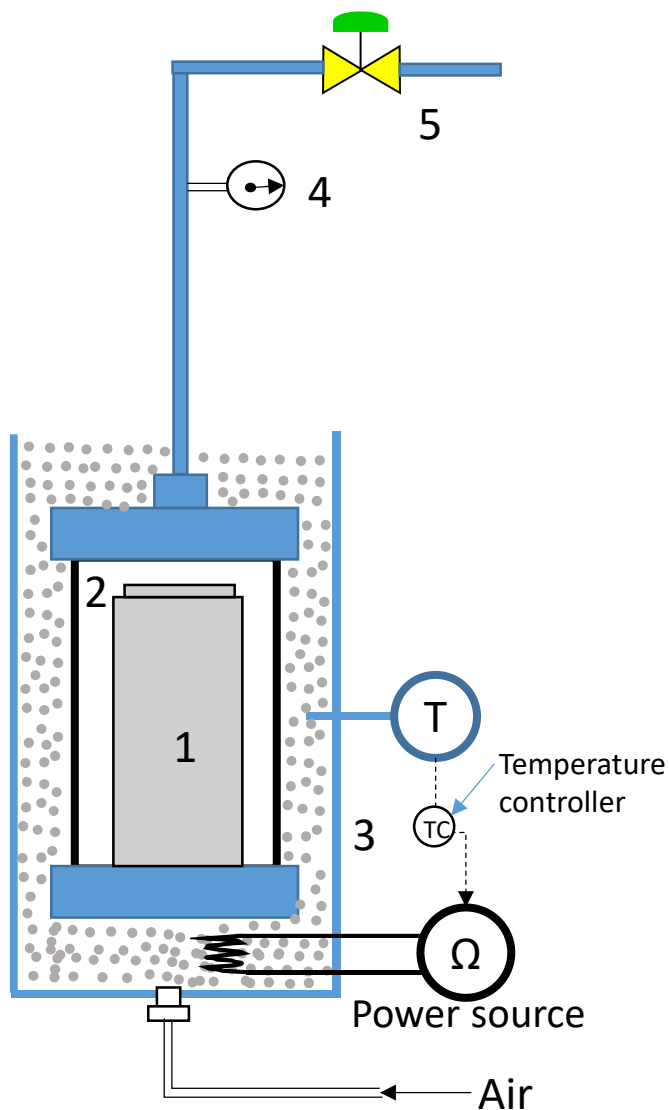
Figure 5.1 Schematic diagram of reactor as placed inside fluidized sand bath. 1) Glass vial with reaction ingredients, 2) Closed batch reactor 3) Sand bath with fluidizing sand fitted with temperature measurement, controller and power source, 4) Pressure gauge, 5) Needle valve

5.2.4. Analysis

Gas and liquid products from reactions were analyzed using gas chromatography (GC). The gas product from each reaction was analyzed using gas chromatography. Detail of GC instrument and analytical method is given in section 4.2.4. Identification of molecules in liquid reaction

products was performed using gas chromatography with mass selective detector (GC-MSD). The details of the instruments and analytical methods were given in section 3.2.4. THF solvent was used for diluting the liquid samples and the MSD was switched off at the time of elution of the diluting solvent, i.e. THF.

For analysis of liquid product sample a different temperature program than detailed in section 3.2.4 was used. The temperature program used for analyzing the liquid product sample is given below.

1. Start at 35^0C and hold for 5 minutes.

2. Raise the temperature to 60^0C at the rate 3^0C/min and hold for 1 minute.

3. Raise the temperature to 200^0C at the rate 5^0C/min and hold for 1 minute.

4. Raise the temperature to 300^0C at the rate 8^0C/min and hold for 2 minutes

5. Raise the temperature to 320^0C at the rate 10^0C/min and hold for 2 minutes.

 As mentioned in section 3.2.4, molecules in liquid product were identified using NIST database available with the GC-MSD machine used in this study.

The molecules identified in the product are presented in the result's section for each organosulfur compound reaction. The identified molecule is represented by one of the possible isomers of molecule that represent the peak at specified retention time. Presence of multiple isomers in the liquid product resulted in more than one retention time. Therefore reporting of more than one retention time indicated the presence of multiple isomers in the liquid product.

The relative concentration presented in this chapter is based on the relative area under peaks.

5.3. Results

After opening the reactors it was observed that liquid material was found outside the glass vial inside the reactor. Solid material was still contained inside the glass vial along with liquid products. In case of reactions (set – 21, set – 25, set – 29, set – 33 and set – 37) where organosulfur compound was placed with catalyst SIRAL®40 only, the liquid phase product was not easily separable from catalyst. Measured quantity of THF was added to the glass vial and the extracted liquid was analyzed as liquid product. In case of reactions (set – 23, set – 27, set – 31, set – 35 and set – 38) where only organosulfur compound was placed inside the glass vial, part of liquid product was found outside the glass vial. Measured quantity of THF solvent was added for washing reaction product from reactor and transferring it to glass vial. The collected product along with THF was analyzed as liquid product.

Di-*n*-butyl sulfide, tetrahydrothiophene and diphenyl sulfide molecules boil at temperature below 325^0C. Benzyl phenyl sulfide and dibenzyl sulfide decomposes at temperatures below 325^0C generating molecules that boils below 325^0C. Therefore at reaction conditions at least some of the hydrocarbon molecules were in the vapor phase. These vapor molecules condensed when reactor was cooled down. All the vapor molecules which were outside the glass vial condensed outside vial and therefore liquid product was found outside the glass vial in the reactor.

5.3.1. Reaction of di-*n*-butyl sulfide (Set – 20, Set – 21, Set – 22, Set – 23)

The weight of each reaction ingredient in four sets of reactions for di-*n*-butyl sulfide has been presented in table 5.3.

Table 5.3 Weight of each ingredient used in reaction for di-*n*-butyl sulfide.

Description	Set – 20	Set – 21	Set – 22	Set – 23
Empty vial (g)	7.61	7.67	7.66	7.64
Di-*n*-butyl sulfide (g)	1.03	1.27	1.03	1.53
1-Hexene (g)	4.46	0	4.57	0
SIRAL®40 (g)	0.25	0.26	0	0
Total weight of reactor with all reaction ingredients before reaction (g)	1110.4	1124.7	1112.5	1156
Total weight of reactor after reaction ended (g)	1110.2	1124.4	1112.3	1155.7
Weight recovery (wt%)	99.9	99.9	99.9	99.9
Total weight of reactor after gas product is out (g)	1110.0	1123.8	1112.3	1155.7
Weight of gas sample (g)	0.2	0.6	0	0

Gas sample collected after reaction was analyzed using GC and results are presented in table 5.4. There was no gas product formed from set – 22 and set – 23, which were the reactions performed without a catalyst and therefore no gas analyzes results are reported.

Table 5.4 Composition of gas sample for reaction of di-*n*-butyl sulfide (N_2 free basis)

Compound name	Set – 20	Set – 21	Set – 22	Set – 23
CH_4 (wt%)	3.86	0.54	-	-
CO_2 (wt%)	0.05	0.0	-	-
Ethylene (wt%)	0.32	0.25	-	-
Ethane (wt%)	1.29	1.11	-	-
H_2S (wt%)	1.48	1.44	-	-
Propylene (wt%)	1.45	2.20	-	-
Propane (wt%)	0.56	1.01	-	-
i-Butane (wt%)	0.12	6.93	-	-
n-Butane (wt%)	13.97	18.26	-	-
2-Butene (wt%)	33.37	65.91	-	-
i-Pentane (wt%)	0.28	0.94	-	-
n-Pentane (wt%)	0.28	0.17	-	-
Hexenes (wt%)	36.35	0.36	-	-
n-Hexane (wt%)	7.47	0.87	-	-
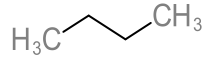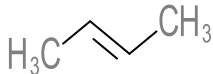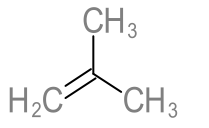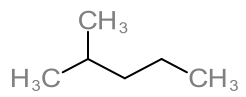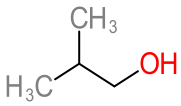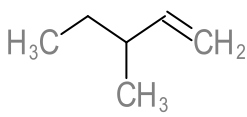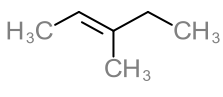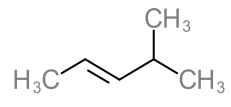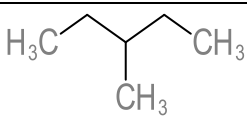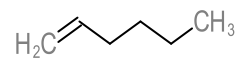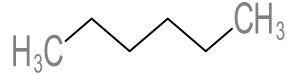
The liquid product for each set of reactions was analyzed using GC-MSD. The plots of relative abundance and their retention time is given in figure 5.2. The peaks are numbered and identified on the plot.
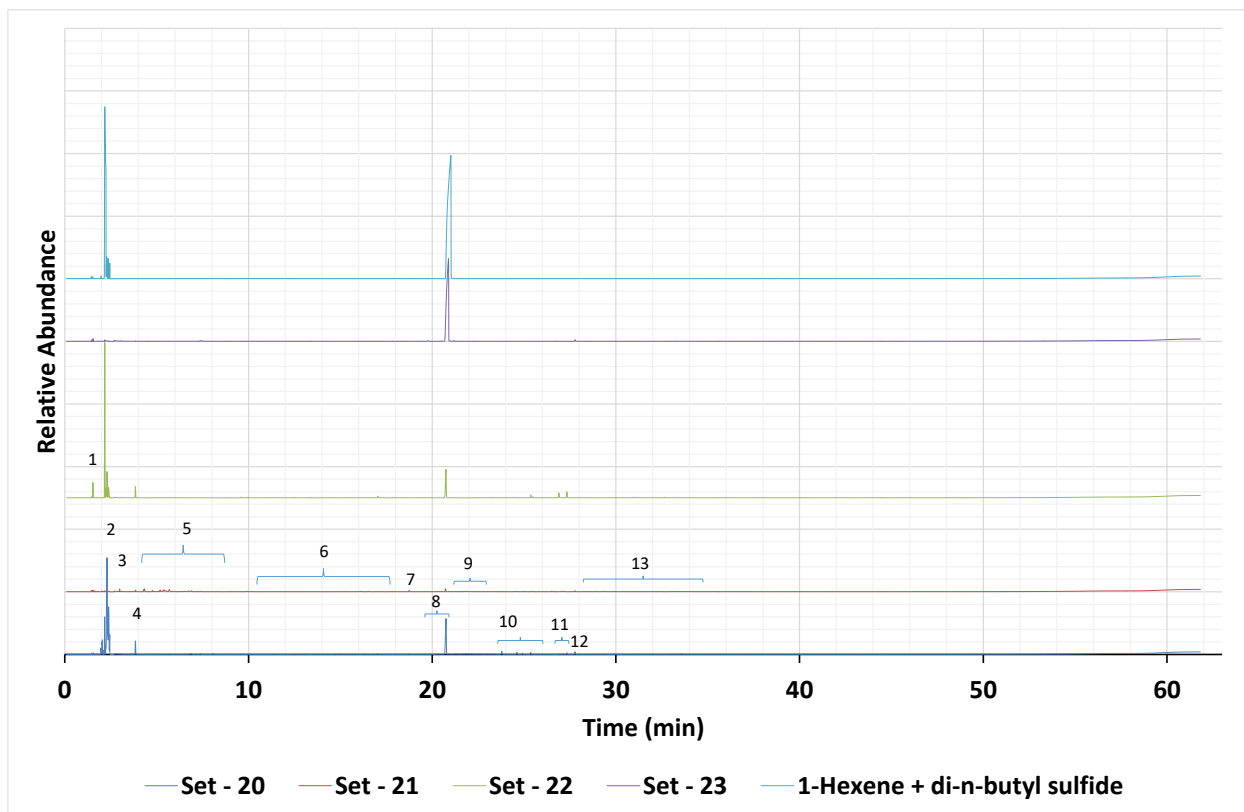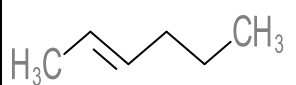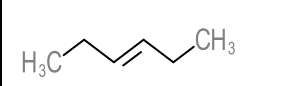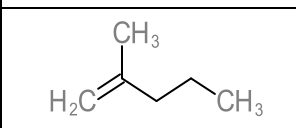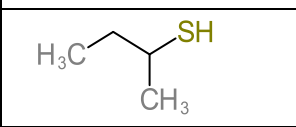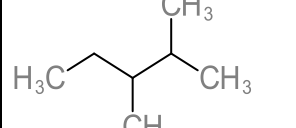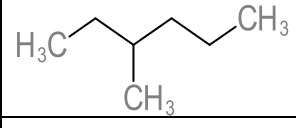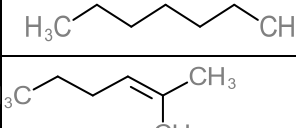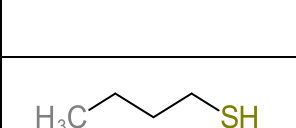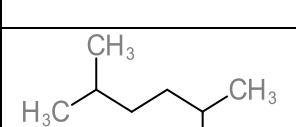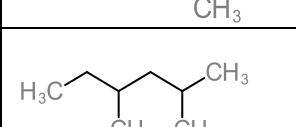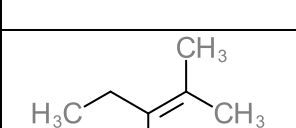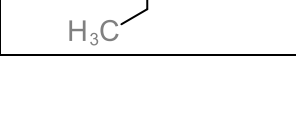
Figure 5.2 GC-MSD chromatogram for the reaction of di-*n*-butyl sulfide with 1-hexene over SIRAL® 40 catalyst
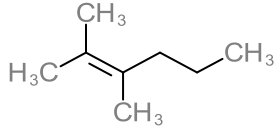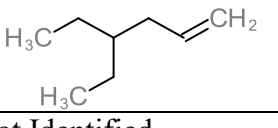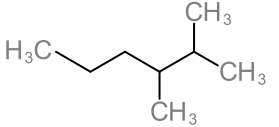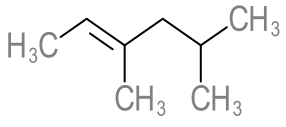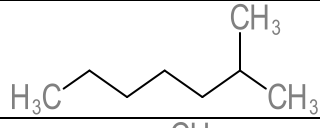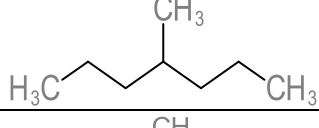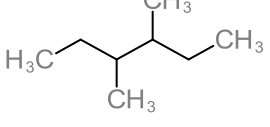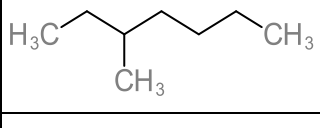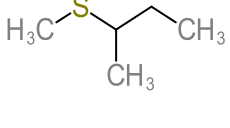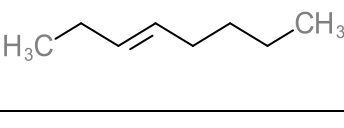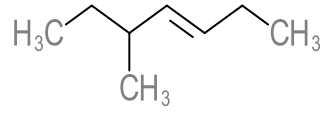
The list of molecular structures identified and retention times are given in table 5.5. The relative concentration of identified molecule is also given in table 5.5. Empty cell indicates that molecule is not present in the liquid product for that set of reaction. The molecules are identified using NIST database available in the data analysis software. The identified molecule presented in table 5.5 is given as one of the possible isomers that could represent the peak at specified retention time. Whenever more than one retention times are given, it indicates the presence of isomers of that molecule in the liquid product.
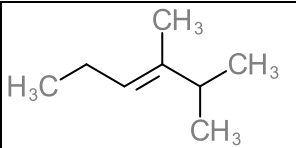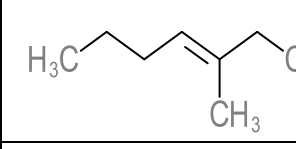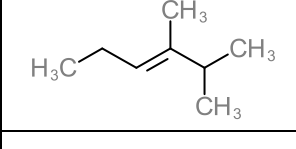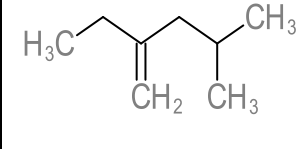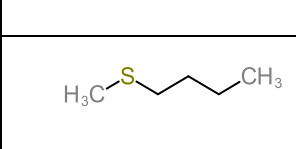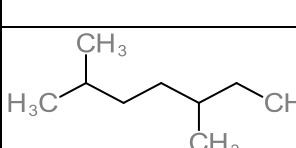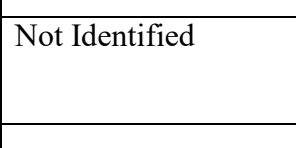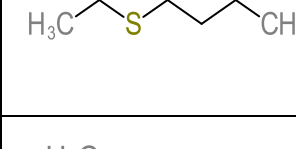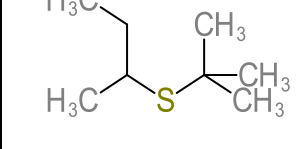
Table 5.5 List of molecules identified in the liquid product of reaction of di-*n*-butyl sulfide along with retention time and relative concentration
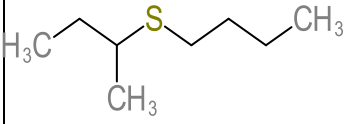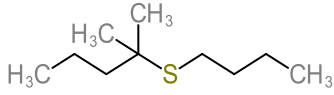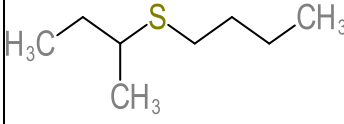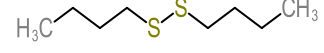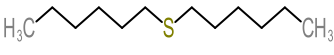
Peak Serial number	Structure	Name	Retention time (min)	Relative Concentration (wt%)			
				Set-20	Set-21	Set-22	Set-23
1		butane	1.50	-	0.13	-	-
1		2-butene	1.54	-	1.71	3.37	0.43
1		2-methyl 1-propene	1.57	0.12	0.61	-	-
1		2-methyl-pentane	1.66	-	0.48	-	-
2		2-methyl propanol	1.73	-	0.15	-	-
2		3-methyl 1-pentene	1.81	-	0.50	-	-
2		3-methyl 2-pentene	1.97	1.09	-	-	-
2		4-methyl-2-pentene	2.04	4.03	0.80	-	-
2		3-methyl pentane	2.11	0.64	0.35	-	-
2		1-Hexene	2.17	8.33	1.92	52.58	-
2		hexane	2.24	-		2.46	-
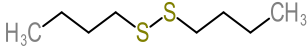
2		2-Hexene	2.30	45.03	1.42	9.75	-
2		3-Hexene	2.39	15.22	0.34	4.18	-
2		2-methyl-1-pentene	2.45	3.20	-	-	-
3		2-butanethiol	2.99	-	3.01	-	-
3		2,3 – dimethyl pentane	3.02	-	0.64	-	-
3		3-methyl hexane	3.12	-	0.76	-	-
3		heptane	3.56	-	0.26	-	-
3		2-methyl 2-hexene	3.66	-	0.32	-	-
4		butanethiol	3.84	3.20	2.14	4.03	-
5		2,5-dimethyl hexane	4.28	-	2.60	-	-
5		2,4-dimethyl hexane	4.34	-	4.07	-	-
5		2-ethyl – 2-methyl pentene	4.59	-	0.30	-	-

5		2, 3 – dimethyl 2 - hexene	4.77	-	2.04	-	-
5		4 – ethyl 1- hexene	4.83	-	0.63	-	-
5	Not Identified	NI	4.95, 5.07	-	1.26	-	-
5		2,3- dimethyl hexane	5.19	-	3.69	-	-
5		3,5- dimethyl-2- hexene	5.35	-	2.10	-	-
5		2- methy heptane	5.40	-	3.42	-	-
5		4- methyl heptane	5.46	-	1.48	-	-
5		3, 4 – dimethyl hexane	5.51	-	1.88	-	-
5		3- methyl heptane	5.69	-	4.96	-	-
5		2- (methyl sulfanyl) butane	5.83	-	0.75	-	-
5		3- octene	6.24	-	0.53	-	-
5		5- methyl 3 – heptene	6.44	-	0.37	-	-

5		2, 3 – dimeth yl 3 – hexene	6.52	-	0.83	-	-
5		3 – methyl 3 – heptene	6.76	-	1.87	-	-
5		2, 3 – dimeth yl 3 – hexene	6.90	-	2.11	-	-
5		2 – methyl – 4 – methyle ne hexane	7.20	-	0.79	-	-
5		Methyl – n – butyl sulfide	7.37	-	1.13	-	-
5		2, 5 – dimeth yl heptane	8.37	-	0.53	-	-
5	Not Identified	NI	9.93	-	0.74	-	-
6		Ethyl – n – butyl sulfide	11.37	-	0.49	-	-
6		2 – [(2-methyl 2-propan yl) sulfanyl] butane	13.20, 16.07	-	1.21	-	-
6		2 – (sec-butylsul fanyl) butane	16.14	-	0.40	-	-

No.	Structure	Compound	RT				
6	Not Identified	NI	16.53 – 17.72	-	1.65	-	-
7	H₃C–CH(CH₃)–S–CH₂CH₂CH₂–CH₃	1-(Sec–butylsulfanyl)butane	18.74	-	2.51	-	-
8	H₃C–S–CH₃ (di-n-butyl sulfide structure)	di-*n*-butyl sulfide	18.89, 20.27, 20.76	15.48	6.16	16.98	98.95
9	Not Identified	NI	20.92 – 23.00	-	2.10	-	-
10	(3,3-dimethyl-4-thiaoctane structure)	3,3-dimethyl-4-thiaoctane	23.79, 24.61, 24.95	1.77	0.68	-	-
10	Not Identified	NI	24.57, 25.05	-	0.89	-	-
10	(1-(Sec-butylsulfanyl)butane structure)	1-(Sec-butylsulfanyl)butane	25.37	0.61	-	1.33	-
10	Not Identified	NI	25.45 – 26.06	-	1.24	-	-
11	(Di–n–butyl disulfide structure)	Di – *n* – butyl disulfide	26.52	-	1.04	-	-
11	Not Identified	NI	26.92 – 27.18	-	2.06	2.45	-
11	(di-n-hexyl sulfide structure)	di-*n*-hexyl sulfide	27.33	0.49	-	2.86	-
11	Not Identified	NI	27.58	-	0.41	-	-

12	H₃C~~S–S~~CH₃	Di – n – butyl disulfide	27.78	0.80	1.69	-	0.62
13	Not Identified	NI	28.31 - onwards	-	23.85	-	-

The set – 23 results in table 5.5 indicated that little di-*n*-butyl sulfide was thermally converted, whereas acid catalysis (set – 21) revealed considerable decomposition and subsequent reaction of the olefins thus produced over the catalyst. Consequently, it was not surprising to find that thermal conversion of di-*n*-butyl sulfide and 1-hexene (set – 22) caused little reaction. Minor decomposition of the sulfide was observed, as well as double bond isomerization of the 1-hexene.

The set – 20 liquid product was surprisingly devoid of hydrocarbon isomers and very unlike the set – 21 product. In fact, the di-*n*-butyl sulfide conversion was similar to that observed in the absence of a catalyst (compare set – 20 and set – 22 di-*n*-butyl sulfide concentration in table 5.5).

5.3.2. Reaction of tetrahydrothiophene (Set – 24, Set – 25, Set – 26, Set – 27)

Four sets of reactions were conducted with tetrahydrothiophene as indicated in table 5.2 and named from set – 24 to set – 27. The weight of each ingredient is presented in table 5.6.

Table 5.6 Weight of each reaction ingredient used in reaction for tetrahydrothiophene

Description	Set – 24	Set – 25	Set – 26	Set – 27
Empty vial (g)	7.6	7.68	7.68	7.63
Tetrhydrothiophene (g)	1.13	1.37	1.34	1.76
1-Hexene (g)	4.55	0	4.5	0
SIRAL®40 (g)	0.33	0.31	0	0
Total weight of reactor before reaction (g)	1160.3	1131.2	1111.2	1125.0
Total weight of reactor after reaction ended (g)	1160.1	1131.1	1110.8	1124.7
Weight recovery (wt%)	99.9	99.9	99.9	99.9
Total weight of reactor after gas product is out (g)	1160	1130.8	1110.7	1124.6
Weight of gas sample (g)	0.1	0.3	0.1	0.1

The gas product was collected after reaction was completed and the reaction was cooled. GC analysis of gas product is presented in table 5.7 for each set of reaction.

Table 5.7 Composition of gas sample collected after reaction of tetrahydrothiophene (N_2 free basis)

Compound name	Set – 24	Set – 25	Set – 26	Set – 27
CH_4 (wt%)	3.89	1.21	1.87	0.07
CO_2 (wt%)	0.01	0.01	0.01	0.02
Ethylene (wt%)	1.92	2.07	1.44	3.96
Ethane (wt%)	4.79	2.23	0.43	0.19
H_2S (wt%)	2.44	5.4	0.30	0.30
Propylene (wt%)	4.11	6.09	0.70	0.91
Propane (wt%)	2.24	2.87	0.54	0.76
i-Butane (wt%)	2.61	5.88	0.38	0.08
n-Butane (wt%)	0	10.92	0.12	6.73
2- Butene (wt%)	4.50	39.10	1.40	3.08
i-Pentane (wt%)	0.66	1.82	4.00	2.03
n-Pentane (wt%)	4.86	0.76	0.20	1.16
Hexenes (wt%)	67.96	21.58	88.60	81.36
n-Hexane (wt%)	0.17	3.52	0.31	1.72

The GC-MSD result of the liquid products from four sets of reactions of tetrahydrothiophene is presented in figure 5.3 for relative abundance and retention time. Identifiable peaks are numbered in in the plot.
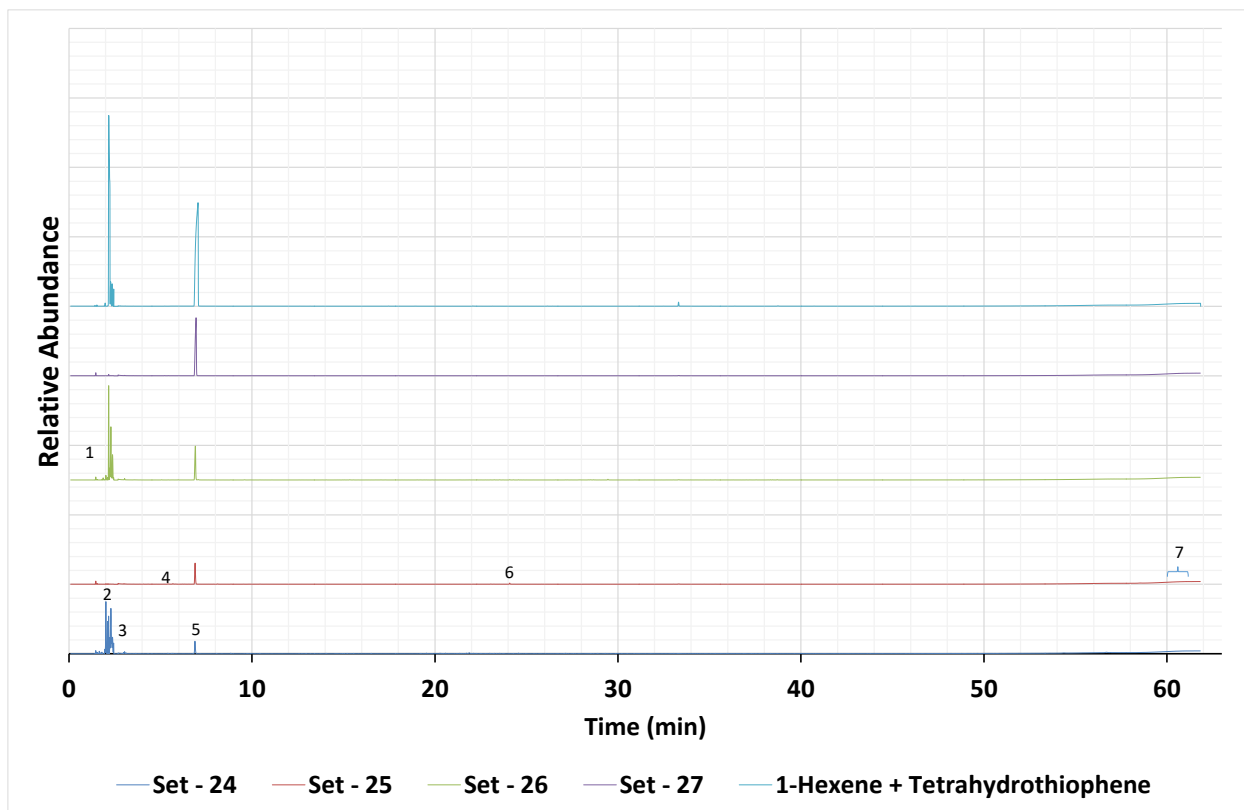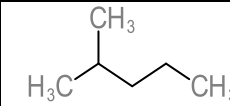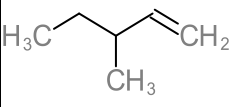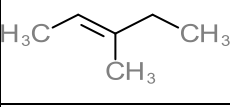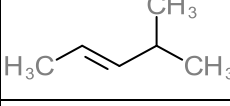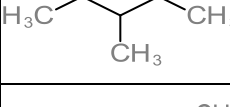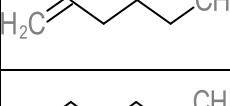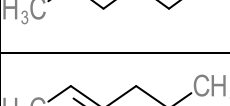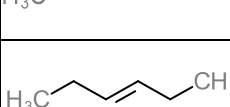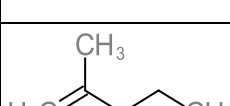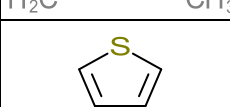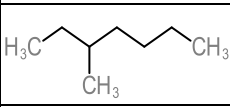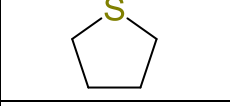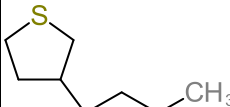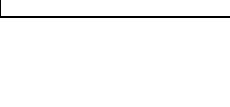
Figure 5.3 GC-MSD chromatogram for the reaction of tetrahydrothiophene with 1-hexene over SIRAL®40 catalyst.

The list of molecular structures identified and their retention time in the reaction product is given in table 5.8. The presented molecule in table 5.8 is one of the possible isomers representing the indicated peak. Therefore it is possible that multiple retention times were observed for one molecule presented in table 5.8. Relative concentration of identified molecules are also given in table 5.8.

Table 5.8 List of molecules identified in the liquid product of reaction of tetrahydrothiophene along with retention time and relative concentration

Serial number	Structure	Name	Retention time (min)	Relative Concentration (wt%)			
				Set-24	Set-25	Set-26	Set-27
1		2-methyl-pentane	1.66	0.47	-	-	-
2		3-methyl 1-pentene	1.81	0.48	-	0.70	-
2		3-methyl 2-pentene	1.97	1.22	-	-	-
2		4-methyl -2-pentene	2.04	17.94	1.20	1.44	-
2		3-methyl pentane	2.11	9.06	-	0.61	-
2		1-Hexene	2.17	12.31	-	31.00	0.68
2		Hexane	2.23	4.92	-	3.17	-
2		2-Hexene	2.30	33.34	-	27.63	-
2		3-hexene	2.39	7.90	-	10.85	-
2		2-methyl -1-pentene	2.45	3.47	-	-	-
3		Thiophene	3.04	0.73	-	-	-
4		3-methyl heptane	5.69	-	1.95	-	-
5		Tetrahydrothiophene	6.89	8.16	88.09	23.84	91.20
6		$3-n-$butyltetrahydrothiophen	24.09	-	4.04	-	-

		e					
7	Not Identified	NI	60.22 – 61.43	-	4.72	-	5.52

Some observations can be made from table 5.8. Thermally, tetrahydrothiophene appears to be fairly stable, although some heavier materials were observed at long retention times (>60 min) in the set – 27 product. The presence of H_2S in the gas product (table 5.7) indicated that at least some thermal decomposition took place.

Over the acid catalyst, some acid catalyzed ring-opening was observed, with some hydrocarbons being produced in the set – 25 product. The H_2S content in the gaseous product was more in set – 25 than in set – 27. Heavy products at long retention times (>60 min) was also observed in the set – 25 product.

The thermal conversion of tetrahydrothiophene in the presence of 1-hexene (set – 26), resulted in considerable double bond isomerization of the 1-hexene, while it appeared to suppress the formation of heavy products from tetrahydrothiophene.

In the set – 24 product, substantial skeletal isomerization of the 1-hexene was evident from the increase in various methyl pentenes. Tetrahydropthiophene was converted with ~8 wt% remaining in the product versus ~24 wt% after thermal conversion. The other sulfur-containing compounds in the liquid product, e.g. thiophene, cannot account for the loss in sulfur and the gas yield was low. It therefore appears that the conversion of tetrahydrothiophene over the acid catalyst produced sulfur-containing products that remained on the catalyst.

5.3.3. Reaction of benzyl phenyl sulfide (Set – 28, Set – 29, Set – 30, Set – 31)

Weight of each ingredient for four sets (set – 28, set – 29, set – 30, set – 31) of reaction was measured and presented in table 5.9.

**Table 5.9** Weight of each reaction ingredient used in reaction for benzyl phenyl sulfide

Description	Set – 28	Set – 29	Set – 30	Set – 31
Empty vial (g)	7.61	7.68	7.6	7.68
Benzyl phenyl sulfide (g)	0.99	1.07	1.03	1.05
1-Hexene (g)	4.23	0	4.55	0
SIRAL®40 (g)	0.29	0.27	0	0
Total weight of reactor before reaction (g)	1110.1	1124.5	1112.5	1155.5
Total weight of reactor after reaction ended (g)	1109.9	1124.3	1112.3	1155.4
Weight recovery (wt%)	99.9	99.9	99.9	99.9
Total weight of reactor after gas product is out (g)	1109.8	1124.2	1112.2	1155.3
Weight of gas sample (g)	0.1	0.1	0.1	0.1

Analysis result for gas sample collected from four sets of reaction is presented in table 5.10.

Table 5.10 Composition of gas sample collected after reaction of benzyl phenyl sulfide (N_2 free basis)

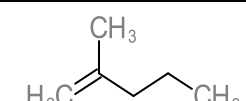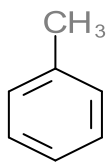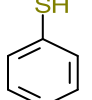| Compound name	Set – 28	Set – 29	Set – 30	Set – 31
CH_4 (wt%)	10.34	1.33	5.15	0.56
CO_2 (wt%)	0.03	1.27	0.01	0.11
Ethylene (wt%)	0.81	0.07	0.40	0.10
Ethane (wt%)	9.10	0.21	3.64	0.31
H_2S (wt%)	1.27	16.03	0.90	21.00
Propylene (wt%)	2.77	0.48	1.85	0.31
Propane (wt%)	3.36	0.54	1.79	0.51
i-Butane (wt%)	2.70	3.85	0.01	0.40
n-Butane (wt%)	0	0	0	0.02
2-Butenes (wt%)	3.67	30.40	1.32	48.65
i-Pentane (wt%)	1.22	2.02	0.31	1.49
n-Pentane (wt%)	1.31	0.99	1.09	1.13
Hexenes (wt%)	62.93	12.21	83.15	6.97
n-Hexane (wt%)	0.50	30.59	0.39	18.42
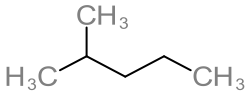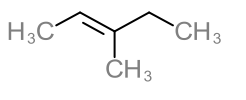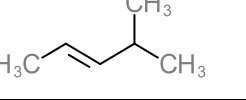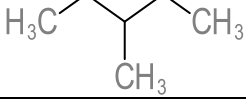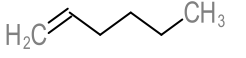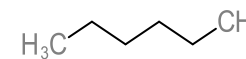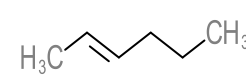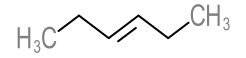
The GC – MSD result of liquid product along with the numbered peak are shown in figure 5.4.
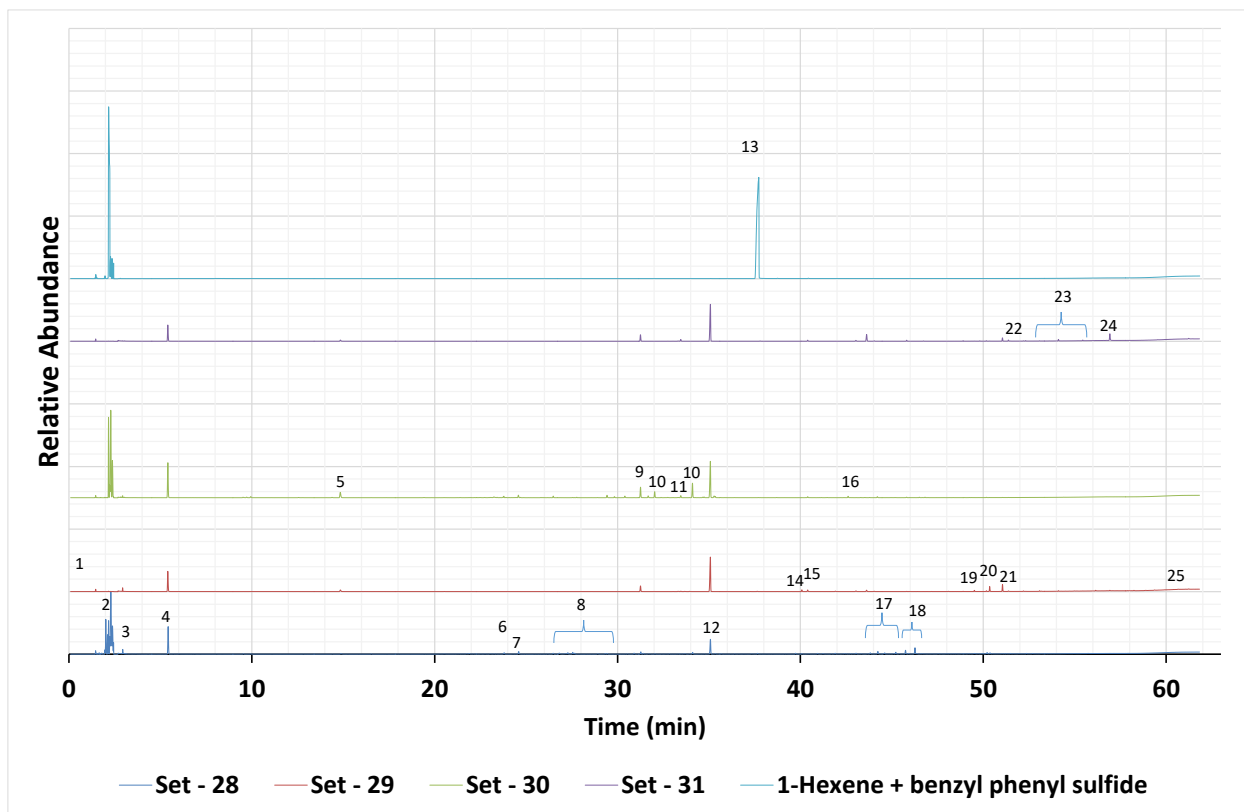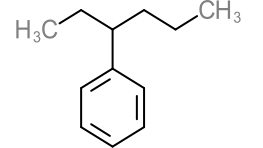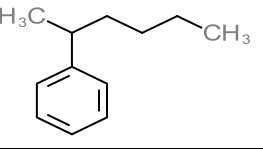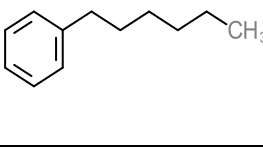
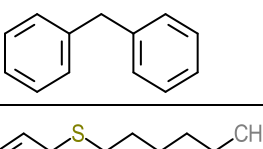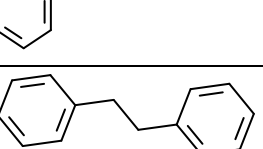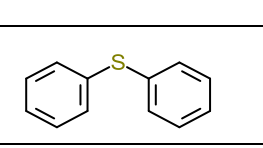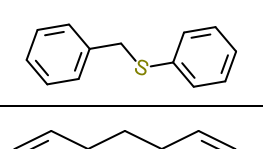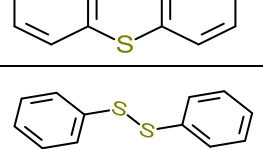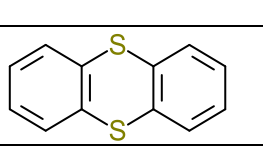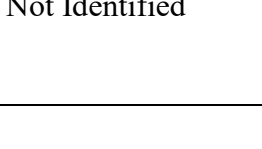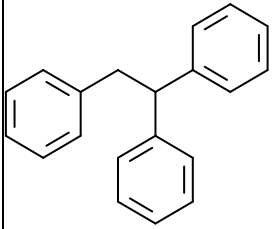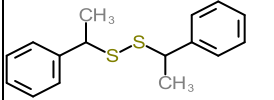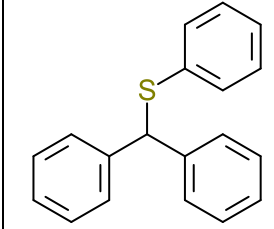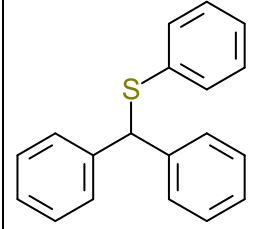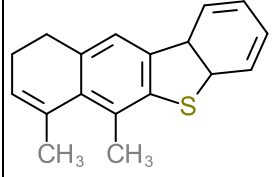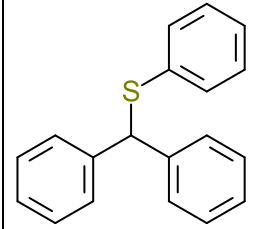**Figure 5.4** GC-MSD chromatogram for the reaction of benzyl phenyl sulfide with 1-hexene over SIRAL® 40 catalyst.

The list of molecular structures identified and their retention time in the reaction product is given in table 5.11.The presented molecular structure indicate one of the possible isomers representing the peak at specific retention time. Therefore it is possible that multiple retention times were observed for one molecule presented in table 5.11. The relative concentration of identified molecules as measured by area under peak is also presented in table 5.11.
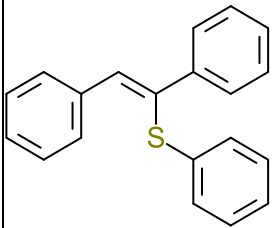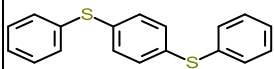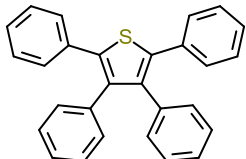
Table 5.11 List of molecules identified in the liquid product of reaction of benzyl phenyl sulfide along with their retention time and relative concentration

Serial number	Structure	Name	Retention time (min)	Relative Concentration (wt%)			
				Set-28	Set-29	Set-30	Set-31
1		2-methyl-pentane	1.66	0.23	-	-	-
2		3-methyl – 2-pentene	1.97	0.83	-	-	-
2		4-methyl-2-pentene	2.04	9.20	-	-	-
2		3-methyl pentane	2.11	3.86	-	-	-
2		1-Hexene	2.17	8.50	-	17.13	-
2		Hexane	2.24	3.83	-	2.09	-
2		2-hexene	2.30	32.00	-	29.21	-
2		3-hexene	2.39	10.45	-	10.28	-
2		2-methyl-1 -pentene	2.45	2.17	-	-	-
3		Benzene	2.95	0.93	2.43	0.33	-
4		Toluene	5.43	10.88	21.98	11.52	17.11
5		Benzenethiol	14.85	-	2.59	2.53	1.75

6		3 – hexyl-benzene	23.80	0.66	-	-	-
7		2 – hexyl benzene	24.60	1.07	-	0.81	-
8		1-hexylbenzene	27.28, 27.56, 29.43	1.21	-	0.78	-
9		Diphenyl methane	31.27	0.87	6.47	3.48	7.03
10		n – hexyl phenyl sulfide	32.03, 34.11	0.73	-	6.70	-
11		Bibenzyl	33.46	-	-	0.70	2.04
12		Diphenyl sulfide	35.08	6.28	45.45	13.85	47.21
13		Benzyl phenyl sulfide	37.95	-	-	-	-
14		Thioxanthene	40.08	-	1.97	-	-
15		Diphenyl disulfide	40.40	-	1.80	-	1.11
16			43.04	-	0.87	-	1.08
17	Not Identified	NI	43.62 – 45.22	1.90	1.82	-	8.29

18		1, 1', 1" – (1, 1, 2 – ethanetriyl) tribenzene	45.81	-	-	-	1.01
18		Bis – (phenylethyl) disulfide	46.27	2.29	-	-	-
19		1,1'-[(Phenyl sulfanyl) methylene] dibenzene	49.52	-	1.12	-	-
20		1,1'-[(Phenyl sulfanyl) methylene] dibenzene	50.18	-	0.71	-	-
20		6,7-Dimethyl-9,10-dihydrobenzo[b]naphtho[2,3-d]thiophene	50.21	0.64	-	-	-
20		1,1'-[(Phenyl sulfanyl) methylene] dibenzene	50.35	-	4.61	-	-

#	Structure	Name					
21		1,1'-[(Z)-1-(Phenylsulfanyl)-1,2-ethenediyl]dibenzene	51.05	-	6.62	-	3.05
22		Diphenyl disulfide	51.38	-	-	-	1.00
23	Not Identified	NI	53.08 – 55.44	-	1.19	-	1.99
24		Tetraphenylthiophene	56.93	-	-	-	7.33
25	Not Identified	NI	60.65	-	0.36	-	-

Benzyl phenyl sulfide was converted entirely to products as no benzyl phenyl sulfide was detected in the liquid product of all four sets (Set – 28, 29, 30 and 31).

Presence of peak 7, 8, and 10 in set – 28 and 30 indicate that presence of catalyst is not necessarily required for alkylation of the olefin with the aromatic after the scission of C-S bond in presence of 1-hexene.

Very high concentration of diphenyl sulfide in liquid products of set – 29 and set – 31 reactions indicates that benzyl phenyl sulfide is preferentially converted to diphenyl sulfide in the absence of 1–hexene.

5.3.4. Reaction of dibenzyl sulfide (Set – 32, Set – 33, Set – 34, Set – 35)

Reactions of dibenzyl sulfide was conducted in four sets. The weight of each ingredient is presented in table 5.12.

Table 5.12 Weight of each reaction ingredient used in reaction of dibenzyl sulfide.

Description	Set – 32	Set – 33	Set – 34	Set – 35
Empty vial (g)	7.71	7.64	7.64	7.61
Dibenzyl sulfide (g)	1.07	1.06	1.05	1.18
1-Hexene (g)	4.63	0	4.53	0
SIRAL®40 (g)	0.3	0.35	0	0
Total weight of reactor before reaction (g)	1135.5	1106.6	1128.8	1108.1
Total weight of reactor after reaction ended (g)	1135.3	1106.4	1128.6	1108.0
Weight recovery (wt%)	99.9	99.9	99.9	99.9
Total weight of reactor after gas product is out (g)	1135.2	1106.1	1128.5	1107.9
Weight of gas sample (g)	0.1	0.3	0.1	0.1

Gas sample collected after reaction completion was analyzed using GC method. The results are presented in table 5.13.

Table 5.13 Composition of gas sample collected after reaction of dibenzyl sulfide (N_2 free basis)

Compound name	Set – 32	Set – 33	Set – 34	Set – 35
CH_4 (wt%)	4.43	6.84	1.74	0.22
CO_2 (wt%)	0.49	0.16	0.02	0.03
Ethylene (wt%)	0.76	0.37	0.43	0.10
Ethane (wt%)	3.98	2.31	1.37	0.26
H_2S (wt%)	2.22	16.04	2.17	17.30
Propylene (wt%)	2.16	0.11	1.23	0.20
Propane (wt%)	1.80	7.73	0.97	0.19
i-Butane (wt%)	3.01	2.18	0.20	0.10
n-Butane (wt%)	0	2.44	0.03	0
2-Butenes (wt%)	7.63	1.22	1.23	0.69
i-Pentane (wt%)	0.17	47.59	0.84	2.75
n-Pentane (wt%)	1.05	0.88	0.47	1.11
Hexenes (wt%)	72.72	7.45	89.29	77.20
n-Hexane (wt%)	0.14	68.20	0.58	15.41
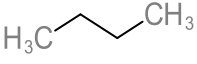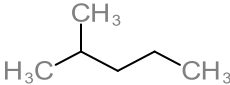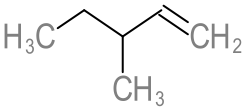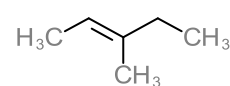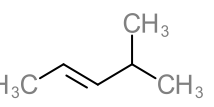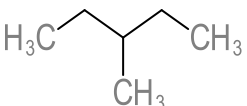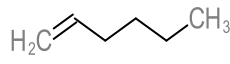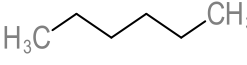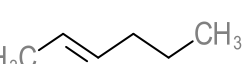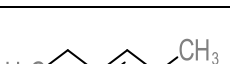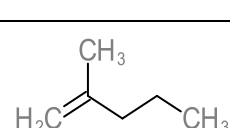
Liquid product from each set of reaction was analyzed using GC-MSD. The plot of relative abundance versus retention time along with numbered peaks are presented in figure 5.5.
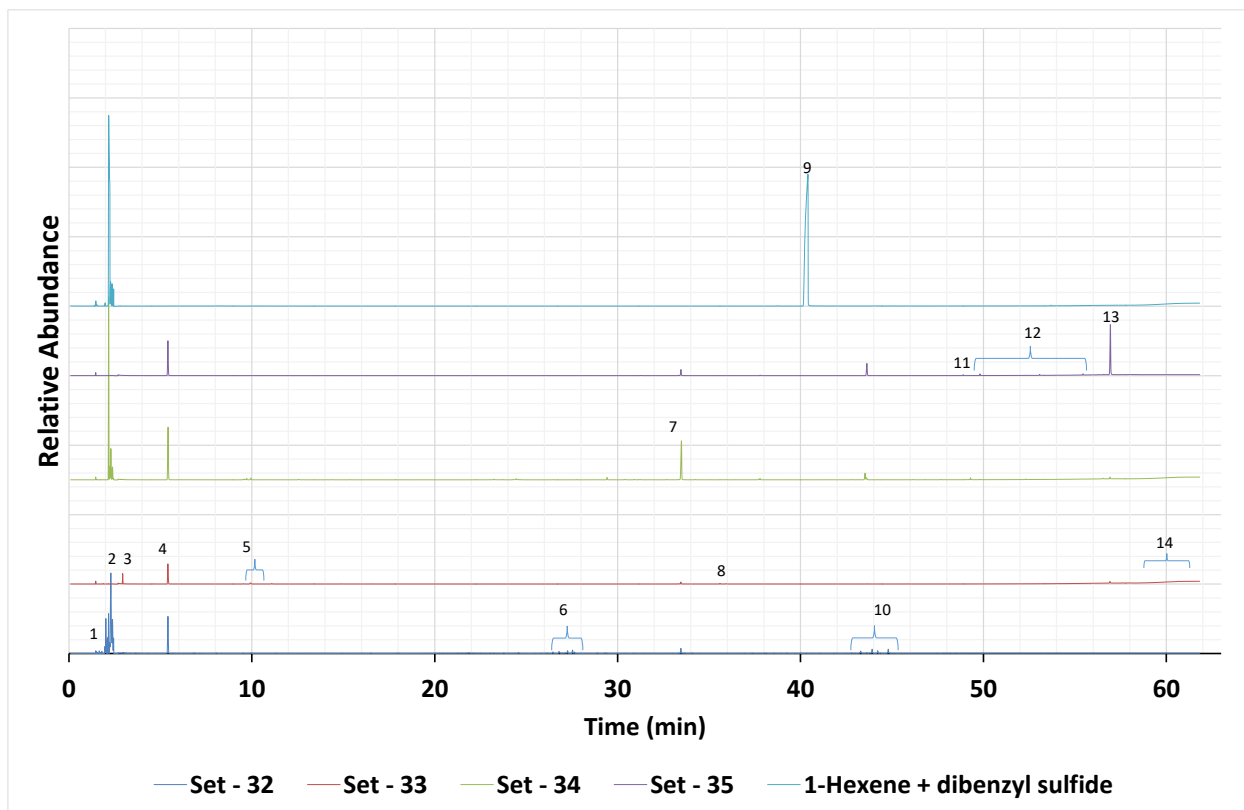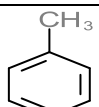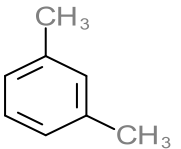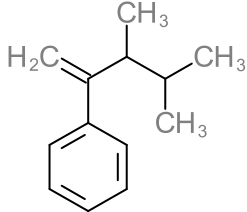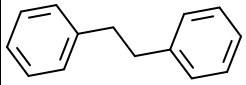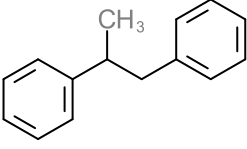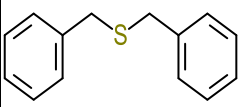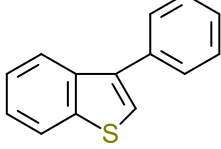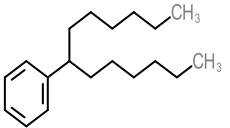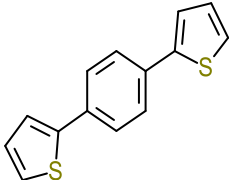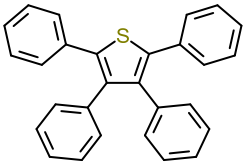
Figure 5.5 GC-MSD chromatogram for the reaction of dibenzyl sulfide with 1-hexene over SIRAL® 40 catalyst.

The list of molecular structures identified and their retention time along with relative concentration in the reaction product is given in table 5.14. The chemical structure provided in table 5.14 corresponds to one of the possible isomers present in liquid product. Therefore it is possible that multiple retention times were observed for one molecule presented in table 5.14.

Table 5.14 List of molecules identified in the liquid product after reaction of dibenzyl sulfide along with retention time and relative concentration

Peak number	Structure	Name	Retention time (min)	Relative Concentration (wt%)			
				Set-32	Set-33	Set-34	Set-35
1		butane	1.50	0.16	-	-	-
1		2-methyl pentane	1.66	0.32	-	-	-
2		3-methyl 1-pentene	1.81	0.33	-	-	-
2		3-methyl 2-pentene	1.97	1.23	-	-	-
2		4-methyl-2-pentene	2.04	8.80	-	-	-
2		3-methyl pentane	2.11	2.88	-	-	-
2		1-Hexene	2.17	8.55	-	44.52	-
2		Hexane	2.24	2.00	-	2.54	-
2		2-hexene	2.30	36.89	-	8.26	-
2		3-hexene	2.39	10.47	-	3.67	-
2		2-methyle-2-pentene	2.45	3.16	-	-	-

#	Structure	Name					
3		Benzene	2.94	-	17.50	-	-
4		Toluene	5.41	13.56	58.89	21.09	27.22
5		m-xyelene	9.92	-	5.39	-	-
6		2 – phenyl – 3, 4 – dimethyl – 1 - pentene	26.46, 26.80, 27.27, 27.54	3.74	-	-	-
7		Bibenzyl	33.46	1.90	6.21	17.43	4.95
8		1, 1' – (1, 2 – propane diyl)dibenzene	35.60	-	1.54	-	-
9		Dibenzyl sulfide	40.02	-	-	-	-
10		3 – phenyl – 1- benzothiophene	43.64	-	-	-	11.17
10		7- Phenyltridecane	43.29, 43.52, 43.92, 44.22, 44.80	5.37	-	2.49	-
11		2,2 – (p- phenylene) dithiop	48.89	-	-	-	0.55

			hene				
12	Not Identified	NI	49.82-55.44	0.65	-	-	4.45
13		Tetraphenylthiophene	56.92	-	5.15	-	41.30
14	Not Identified	NI	59.02 – 61.24	-	5.33	-	10.35

Dibenzyl sulfide is converted entirely to products in all four sets (set – 32, 33, 34, and 35) of reactions. Detection of molecules at peak 4 and 7 (in figure 5.5) in liquid product of all four sets of reaction indicate that temperature of 325 °C is sufficient for C-S bond scission in dibenzyl sulfide.

In set – 33, detection of peak 3, 4, 5, 7, and 8 (in figure 5.5) constitute 89.53 wt% of the liquid products and do not contain any sulfur. This indicate that in the presence of the catalyst at 325 °C, it promotes C-S bond scission preferably and removing sulfur as H_2S. Whereas heating dibenzyl sulfide alone to temperature of 325 °C results into mainly formation of tetraphenylthiophene (peak 13 in figure 5.5) as evident in set – 35. This indicate that aromatic rings are concentrated around sulfur containing thiophenes when dibenzyl sulfide is heated alone.

Presence of peak 6 and 10 (in figure 5.5) in set – 32 reaction liquid product indicate the scission of C-S bond and at the same time addition of straight chain.

5.3.5. Reaction of diphenyl sulfide (Set – 36, Set – 37, Set – 38)

In case of di-phenyl sulfide only 3 sets of reactions were conducted. The weight of each reaction ingredient is presented in table 5.15.

Table 5.15 Weight of each reaction ingredient used in reaction of diphenyl sulfide

Description	Set – 36	Set – 37	Set – 38
Empty vial (g)	7.67	7.71	7.57
Diphenyl sulfide (g)	1.02	1.33	1.03
1-Hexene (g)	4.98	0	0
SIRAL®40 (g)	0.32	0.3	0
Total weight of reactor before reaction (g)	1113.4	1156.4	1130.5
Total weight of reactor after reaction ended (g)	1113.1	1156.2	1130.3
Weight recovery (wt%)	99.97	99.98	99.98
Total weight of reactor after gas product is out (g)	1113.0	1156.0	1130.3
Weight of gas sample (g)	0.1	0.2	0

The gas GC result for gas sample collected after completion of reaction is presented in table 5.16.

Table 5.16 Composition of gas sample collected after reaction of diphenyl sulfide (N_2 free basis)

Compound name	Set – 36	Set – 37	Set – 38
CH_4 (wt%)	9.96	0.60	0.12
CO_2 (wt%)	0.01	0.07	0.05
Ethylene (wt%)	0.76	0.12	0.33
Ethane (wt%)	7.64	0.54	0.27
H_2S (wt%)	0.88	0.98	5.94
Propylene (wt%)	2.69	0.55	1.59
Propane (wt%)	2.74	0.50	0.35
i-Butane (wt%)	6.24	0.07	1.87
n-Butane (wt%)	0	0.50	0.77
2-Butane (wt%)	2.78	2.12	22.30
i-Pentane (wt%)	1.78	1.30	7.36
n-Pentane (wt%)	0.49	0.50	2.06
Hexenes (wt%)	63.95	92.14	56.97
n-Hexane (wt%)	0.82	1.30	21.79
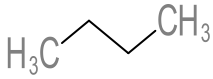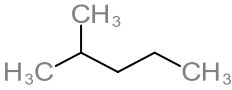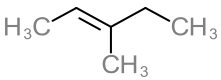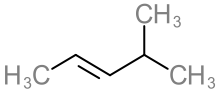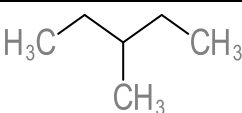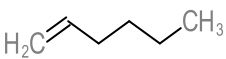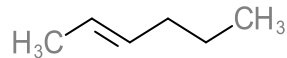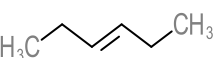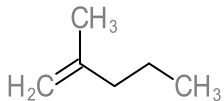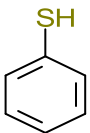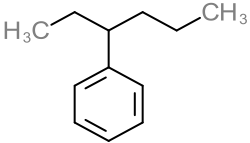
The plot of GC – MSD result of analysis of liquid product from three sets of reaction of diphenyl sulfide along with numbered peaks are presented in figure 5.6.
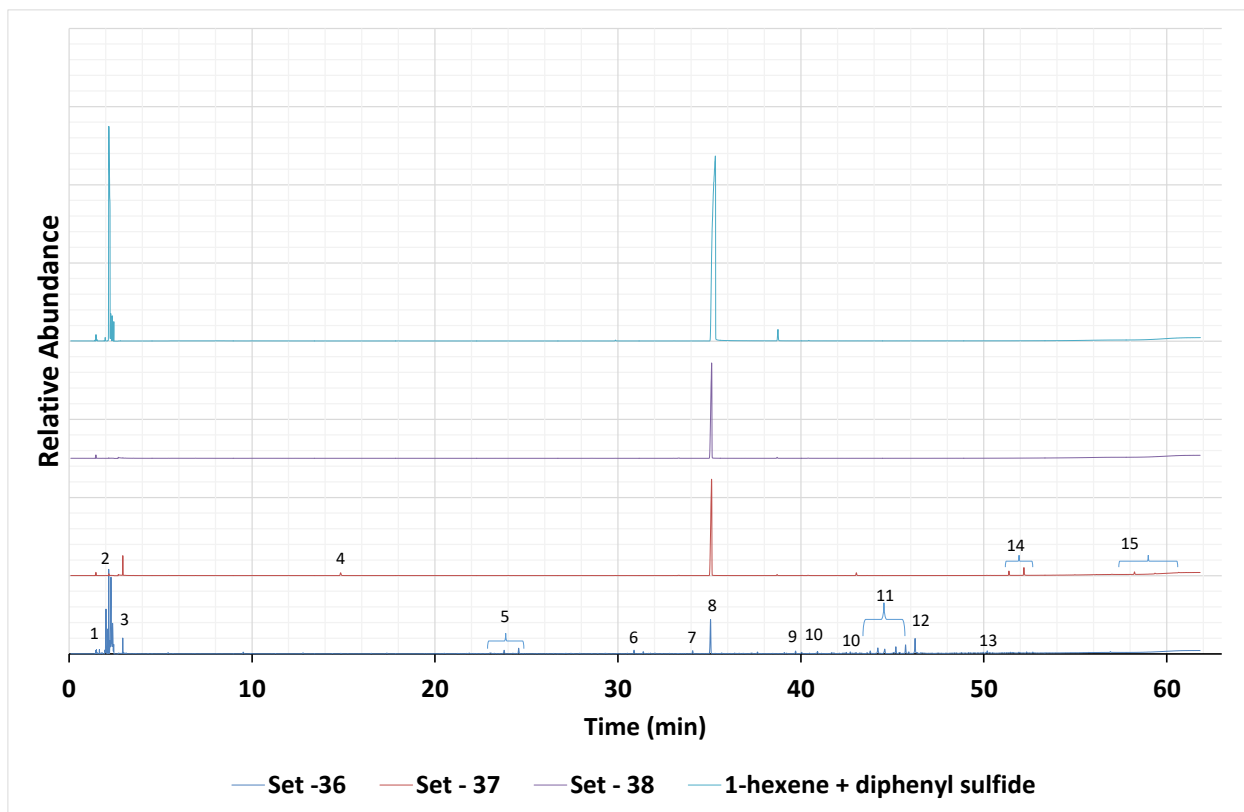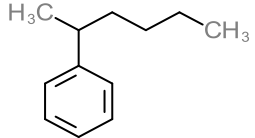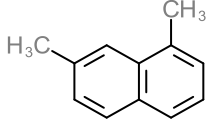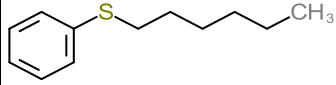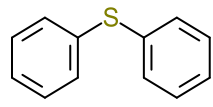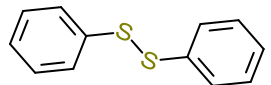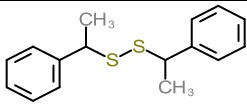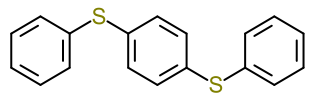
Figure 5.6 GC-MSD chromatogram for the reaction of diphenyl sulfide with 1-hexene over SIRAL® 40 catalyst.

The list of molecular structures identified and their retention time in the reaction product is given in table 5.17. Molecular structure presented in table 5.17 corresponds to one of the possible isomer of the compound identified. It is possible that multiple retention times were observed for one molecule presented in table 5.17. The relative concentration of each of identified molecule is given in table 5.17.

Table 5.17 List of molecules identified in the liquid product after reaction of diphenyl sulfide along with retention time and relative concentration

Peak number	Structure	Name	Retention time (min)	Relative Concentration (wt%)		
				Set-36	Set-37	Set-38
1		Butane	1.50	0.31	-	-
1		2-methyl-pentane	1.66	0.44	-	-
2		3-methyl 2-pentene	1.97	0.53	-	-
2		4-methyl-2-pentene	2.04	8.79	-	-
2		3-methyl pentane	2.11	3.79	-	-
2		1-Hexene	2.17	15.60	0.60	-
2		2-hexene	2.29	27.58	-	-
2		3-hexene	2.38	7.85	-	-
2		2-methyl 1-pentene	2.45	1.59	-	-
3		Benzene	2.94	2.35	5.70	-
4		Benzenethiol	14.85	-	1.96	-
5		3 – hexanylbenzene	23.78	1.18	-	-

#	Structure	Name	Retention time	Col A	Col B	Col C
5		2 - hexanylbenzene	24.58	1.61	-	-
6		1,7- Dimethyl naphthalene	30.89	1.07	-	-
7		n – hexyl phenyl sulfide	34.09	0.93	-	-
8		Diphenyl sulfide	35.07	10.96	81.84	100
9	Not Identified	NI	39.71	0.81	-	-
10		Diphenyl disulfide	40.39, 43.03	-	2.89	-
	Not Identified	NI	40.91	0.73	-	-
11	Not Identified	NI	43.80 – 45.73	9.20	-	-
12		Bis – (phenylethyl) disulfide	46.25	3.78	-	-
13	Not Identified	NI	50.19	0.88	-	-
14		1,4- Bis(phenylsulfanyl)benzene	51.37, 52.19	-	5.56	-
15	Not Identified	NI	58.24, 60.65	-	1.44	-

As was anticipated, diphenyl sulfide is thermally stable (set – 38) and no conversion products were observed after reaction in the absence of a catalyst. The reaction of diphenyl sulfide over the catalyst was interesting, because it demonstrated that the acid catalyst could lead to some conversion (set – 37), with single ring aromatics and addition products being observed in the liquid product (table 5.17). In the presence of 1-hexene (set – 36), the formation of heavier addition products (>51 min retention time) was suppressed and various aromatic alkylation products were observed in the liquid product.

5.4. Discussion

This work was inspired by the previous work by Mao[1], where asphaltenes conversion was attributed to C-S bond cleavage when reacted with propylene in presence of SIRAL®40 catalyst. Therefore the discussion section is more focused on the C-S bond cleavage that can be attributed to the presence of olefin (1-hexene) along with SIRAL®40 catalyst at 325 °C temperature. Based on the molecules identified in the liquid products hypothetical reaction path was created for each organosulfur compound. Formation of product molecules is briefly explained based on previous work by researchers. Detailed mechanisms of reaction path have not been provided.

The results are discussed separately for each organosulfur compound. Olefin isomerization on acid catalysts are widely used chemistry in hydrocarbon industry. Similar results are obtained in this work when the olefin (1-hexene) was heated in presence of SIRAL®40 catalyst. Since 1-Hexene was used with each organosulfur compound, reactions of 1-hexene independent of the presence of organosulfur compound has been discussed in section 5.4.1. These reactions are common for all acid catalyzed reactions involving 1-hexene with organosulfur compounds.

As it is mentioned in section 5.3 part of liquid was found outside the glass vial. This raises a valid concern regarding the contact between reactants and catalyst during reaction period. Similar valid concerns also arise from the explanation in section 5.2.1 when all reaction ingredients were placed inside the glass vial and catalyst settled at the bottom of vial and liquid ingredients were above the catalyst layer. The noticeable difference between the liquid product composition of four sets of reaction of each organosulfur compounds helps in concluding that reactants and catalyst were in contacts during the reaction time however the contact was transport restricted. The current work was mainly focused on understanding the C-S bond scission in presence of 1-hexene and catalyst without any emphasis on reaction kinetics.

5.4.1. Reaction of 1-hexene over SIRAL® 40 catalyst

Reaction of 1-Hexene over SIRAL® 40 catalyst at 325 °C is discussed in this section. 1-Hexene was present in two out of four sets of reactions for each organosulfur compounds. Based on molecules identified in liquid products, the reaction path for 1-Hexene has been drawn in figure 5.7.
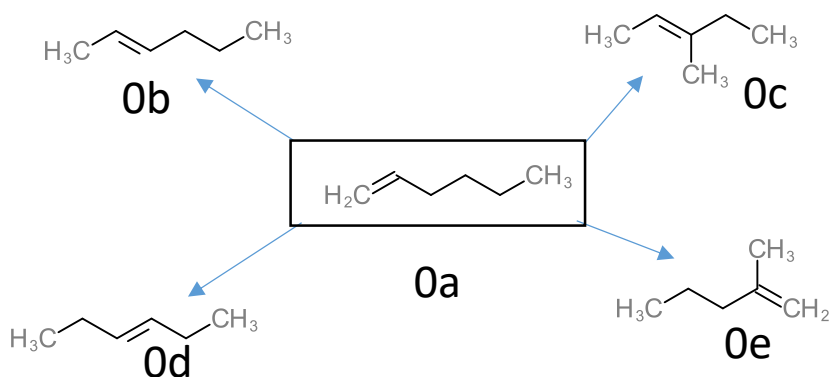
Figure 5.7 Hypothetical reactions for isomerization of 1-hexene in presence of SIRAL® 40 catalyst at 325 °C

5.4.2. Reaction of di-*n*-butyl sulfide (Set – 20, Set – 21, Set – 22, Set – 23)

The hypothetical reaction paths for di-*n*-butyl sulfide are shown in figure 5.8. Comparison of chromatograms in figure 5.2 indicate that di-*n*-butyl sulfide doesn't react appreciably when heated alone to a temperature 325 °C. Detection of molecules other than starting materials was observed only in set – 20, set – 21 and set – 22 reactions. Detection of H_2S in gas phase product indicate the cleavage of both C-S bond in di-*n*-butyl sulfide. The formation of butanethiol (**1a**) and butene (**1b**) in reaction set – 20 to 22 can be speculated to occur as the first step of reaction. Formation of ethanethiol and ethylene has been observed upon heating diethyl sulfide at 496 °C.[2] Similar products were observed after reaction of di-*n*-butyl sulfide in this work. Formation of **1a** and **1b** indicate the occurrence of thermal decomposition of di-*n*-butyl sulfide. But non-detection of **1a** and **1b** upon heating di-*n*-butyl sulfide only (in Set – 23 reaction), indicate that presence of catalyst and olefin facilitate the reaction at 325 °C. The role of catalyst can be understood as lowering the temperature requirement for this reaction. Formation of **1g**, **1h** and **1m** indicate the replacement of four carbon chain with the 6 carbon chain in both set – 20 and set – 22 reaction indicate that presence of catalyst is not mandatory for replacing four carbon chain with six carbon chain at reaction temperature of 325 °C. The scission of C-S bond in di-*n*-butyl sulfide is observed. However formation of new C-S bond is also observed. Similar reactions are relevant to the asphaltene conversion as observed by Mao.[1]

Formation of **1n** indicate the dimerization of **1a** with elimination of hydrogen. Since no hydrogen was detected in gas product, it is probably consumed in saturation of olefins which are formed by dimerization of olefins. This reaction is indicated a formation of **1p** and **1q** from dimerization of **1c**. These reactions are facilitated by catalyst. Dimerization of olefin over acid catalyst has been studied well.[3, 4] Compound **1f** is also formed by dimerization of mercaptans

147

(**1e**). Branched chain mercaptans (**1e**) are formed by recombination reaction between H_2S and branched olefin (**1c**).
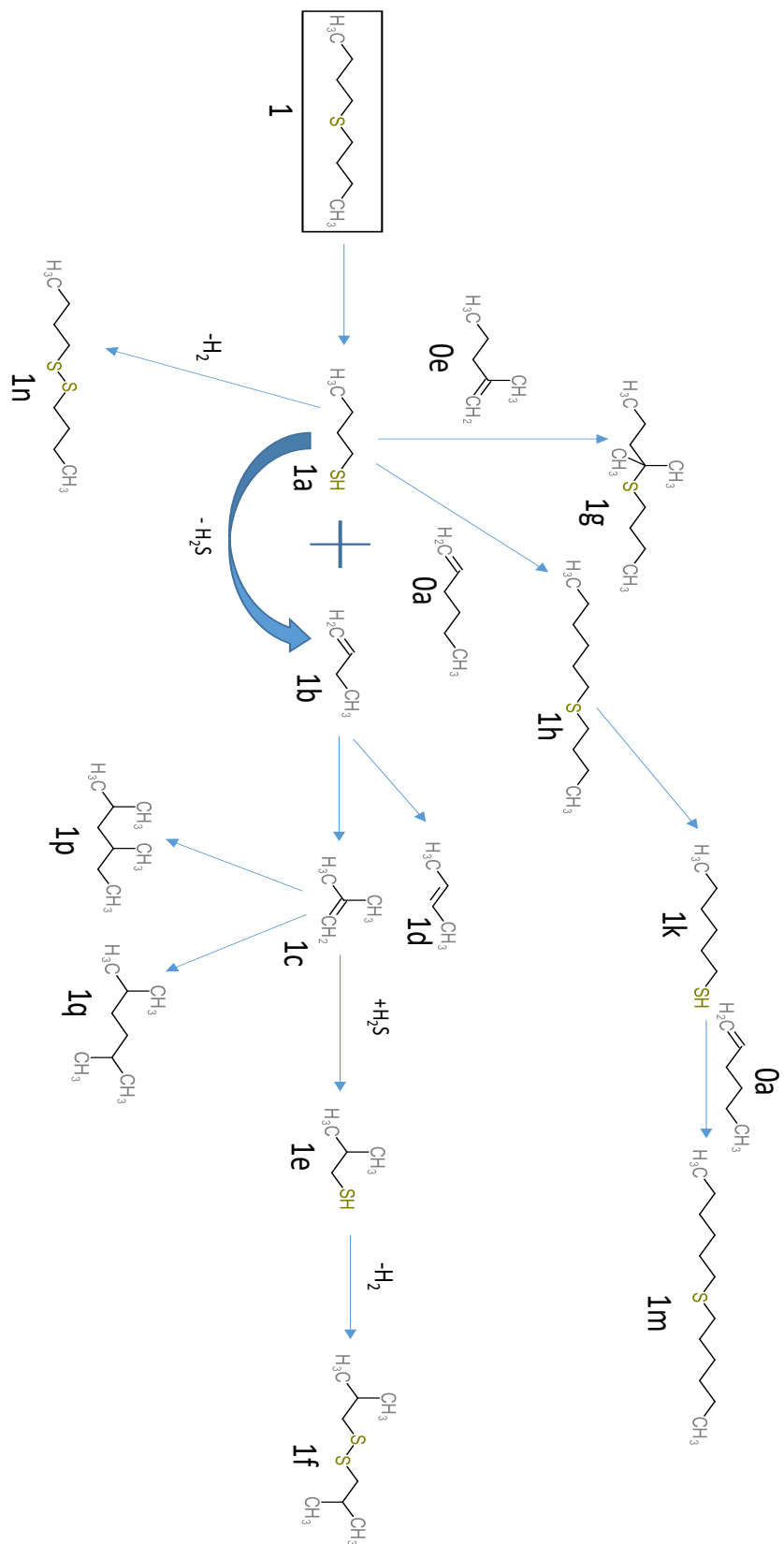
Figure 5.8 Hypothetical reaction path for reaction of di-*n*-butyl sulfide

5.4.3. Reaction of tetrahydrothiophene (Set – 24, Set – 25, Set – 26, Set – 27)

Depending upon the molecules identified in the liquid product after reaction, hypothetical reaction paths were created as presented in figure 5.9.
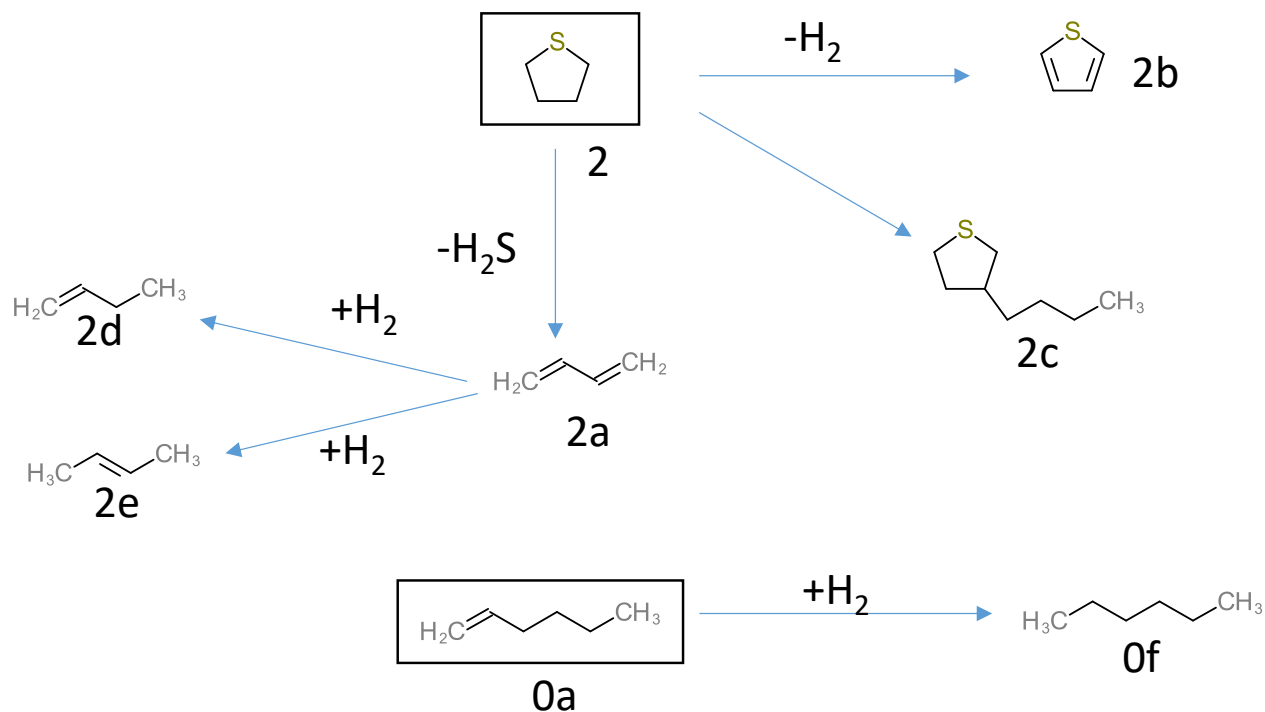
Figure 5.9 Hypothetical reaction path for reaction of tetrahydrothiophene

Isomerization reactions of 1-hexene are detailed in section 5.4.1 when acid catalyst is present with 1-hexene. Detection of H_2S indicate the cleavage of C-S bond in tetrahydrothiophene. The reaction products in set – 24 and set – 26 reactions indicate that tetrahydrothiophene remains unaffected by the presence of olefin. Tetrahydrothiophene, when heated alone at 325 °C doesn't decompose appreciably as evident from the chromatogram presented in figure 5.3. Presence of catalyst SIRAL®40 facilitates the formations of similar molecules as observed by Xia et al.[5] Formation of both 1, 3- butadiene and thiophenes has been concluded by Xia, et al.[5] by thermal

decomposition. No detection of 1, 3 – butadiene in this work can be attributed to partial saturation of diolefin and resulting into butene (**2d,** and **2e**) which is detected in liquid product. This saturation of diolefin is facilitated by SIRAL®40 catalyst. It is more likely that catalytic decomposition does not proceed through **2a**, but though the formation of an olefinic thiol first. Since few sulfur-containing products from the conversion of tetrahydrothiophene were observed in the liquid and likely remained mainly on the catalyst, it is likely that ring-opening would lead to further acid catalyzed addition reactions leading to the formation of much heavier sulfur-containing products. Some indirect evidence can be seen as **2c**.

Detection of saturated hexane (**0f**) can also be attributed to the saturation of 1-hexene (**0a**) consuming hydrogen. No reaction between 1-hexene and tetrahydrothiophene was observed. However the detection of **2c** indicate that olefins with four carbon can attach to the tetrahydrothiophene. This indicates that butene reacts with tetrahydrothiophene in presence of SIRAL®40 whereas no direct evidence was presented that 1-hexene reacts in the same way. The four carbon chain is attached to tetrhydrothiophene and C-S bond remains intact.

5.4.4.   Reaction of benzyl phenyl sulfide (Set – 28, Set – 29, Set – 30, Set – 31)

Hypothetical reaction path was created using the compounds identified in the liquid product after reaction of benzyl phenyl sulfide. Reaction path in shown in figure 5.10.

The chromatogram in figure 5.4 indicates that cleavage of C-S bond in benzyl phenyl sulfide (BPS) is mainly because of thermal reactions. Set – 31 reaction involved heating benzyl phenyl sulfide (BPS) alone at temperature equals to 325 °C. Similar compounds are formed in set – 28, set - 29 and set – 30 reactions too. Compounds in reaction products of this work are similar to those observed in thermal reactions conducted by Katritzky[6] and colleagues. This indicates that

151

reactions of BPS is mainly driven by temperature. Non detection of BPS in liquid product indicate 100% conversion of BPS and scission of benzylic C-S bond is entirely complete. Detection of H_2S in all four sets of reactions indicate scission of both C-S bond in BPS.

Presence of olefin and catalyst facilitates additional reactions on BPS. Detection of **3g** in set – 28 and set – 30 reactions indicate that catalyst's presence is not necessary for the reaction however addition of isomerized olefin (as formation of **3h**) is possible only when catalyst is present. Six carbon chain added to aromatic rings are observed. Hexene can be added to the aromatic ring (peaks 6, 7 and 8 in table 5.11) as well as by addition to the sulfur (peak 10 in table 5.11).
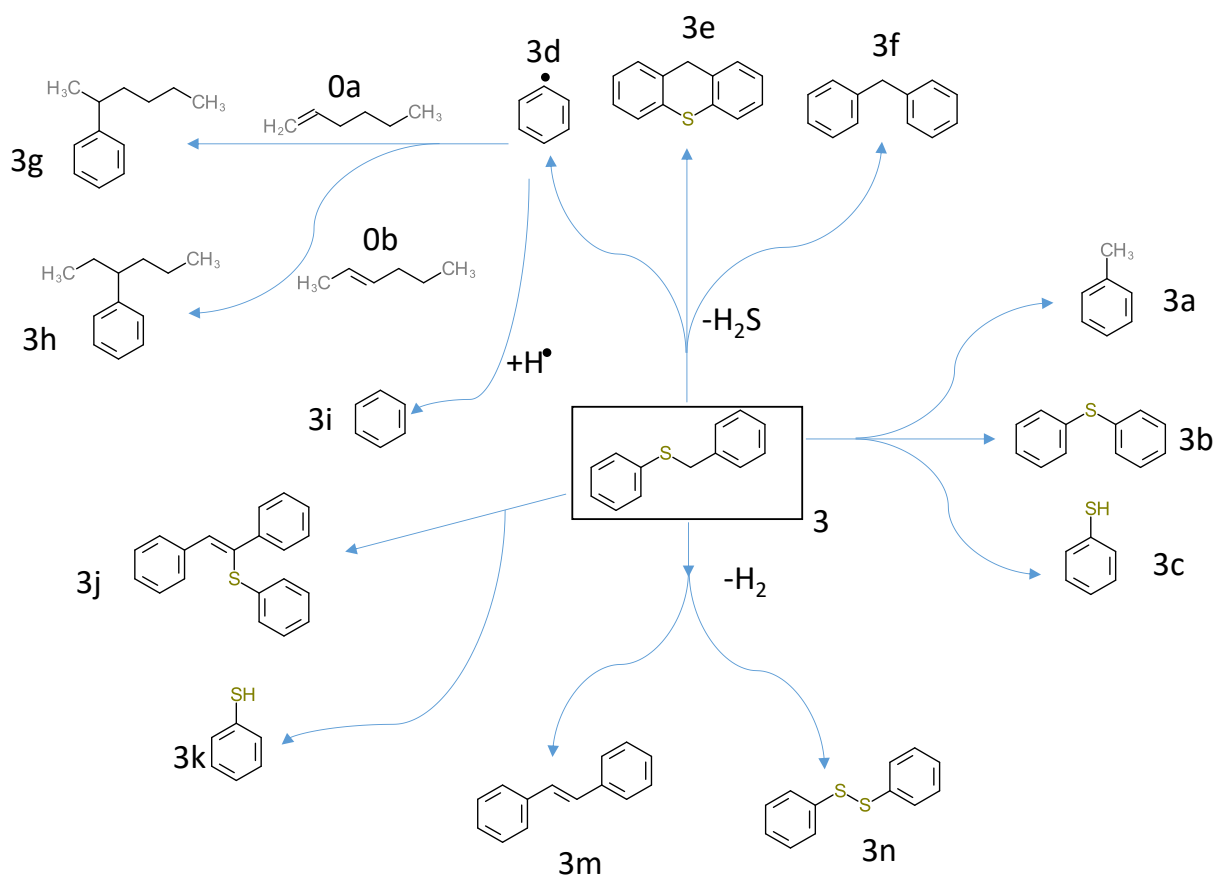
Figure 5.10 Hypothetical reaction paths for reaction of benzyl phenyl sulfide

5.4.5. Reaction of dibenzyl sulfide (Set – 32, Set – 33, Set – 34, Set – 35)

Reaction path has been drawn for the reaction of dibenzyl sulfide as presented in figure 5.11. Isomerization reactions of 1-hexene has been discussed in section 5.4.1.

Chromatogram shown in figure 5.5 indicate that dibenzyl sulfide (DBS) is not detected in the liquid product for all four sets of the reaction. Therefore it can be concluded that cleavage of both benzylic C-S bond is possible by heating it to 325 °C.
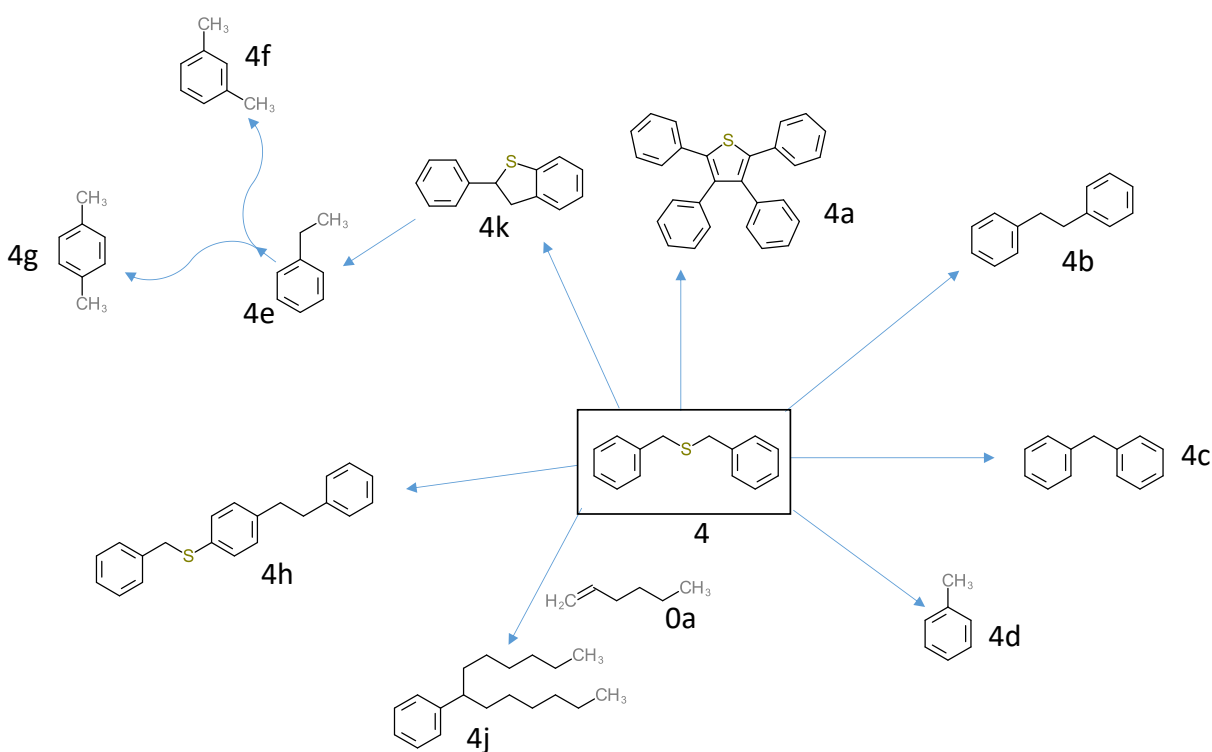
Figure 5.11 Hypothetical reaction path for reaction of dibenzyl sulfide

Formation of **4j** indicates the cleavage of C-S bonds followed by addition of two 1-hexene at the benzylic carbon. Products of thermal decomposition of dibenzyl sulfide have been presented by Horton[7] and Katritzky[6]. Similar molecules were observed in this work when dibenzyl sulfide was placed in presence of SIRAL®40 catalyst. Horton has demonstrated the formation of **4a** and **4k**

upon heating at 200^0C. In present work **4k** has not been detected. The formation of **4e** indicates that **4k** reacted quickly to form **4e**. Formation of **4f** and **4g** are in line with isomerization reactions observed for ethyl benzene by Hanson.[8] Some alkylation was observed on the aromatic ring (peak 6, table 5.14).

5.4.6. Reaction of diphenyl sulfide (Set – 36, Set – 37, Set – 38)

Reaction paths have been drawn for the reaction of diphenyl sulfide (DPS) as presented in figure 5.12. Isomerization reactions of 1-hexene have been discussed in section 5.4.1. Detection of H_2S indicates the cleavage of C-S bond in diphenyl sulfide. Product of thermal decomposition of diphenyl sulfide has been presented by Katritzky.[6] Detection of **5a, 5b, 5c, 5d, 5e** and **5f** in this work are similar to that observed by Katritzky.[6]
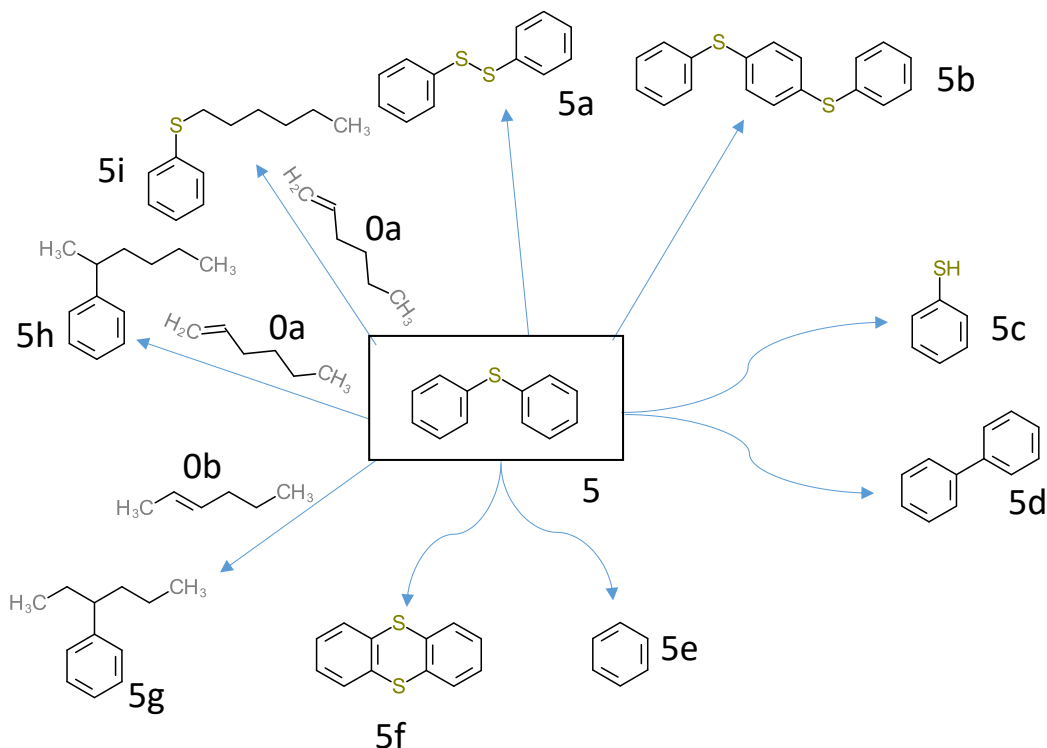
Figure 5.12 Hypothetical reaction paths for reaction of diphenyl sulfide

In addition to 1-hexene isomerization reactions, diphenyl sulfide reacts with 1-hexene and forms **5a, 5h** and **5i** as shown in figure 5.11. Isomerized 2-hexene (**0b**) reacts with diphenyl sulfide (**5**) to yield **5g**. Formation of **5g, 5h,** and **5i** indicates the cleavage of C-S bond in diphenyl sulfide and subsequent addition of six carbon chain in place of existing C-S bond.

5.5. Conclusion

Cleavage of C-S bond is observed when organosulfur compounds are heated in presence of acid catalyst. The presence of olefin (1-hexene) and acid catalyst (SIRAL®40) facilitates additional reactions. Main conclusions based on the results are presented below.

1. Catalyst and 1-hexene enabled C-S scission was observed in model organosulfur compounds. When 1-hexene was present addition of C_6 chain was also observed with model organosulfur compounds except for tetrahydrothiohene.

2. Presence of 1-hexene and catalyst facilitate significant C-S bond cleavage in case of aliphatic sulfide. In set – 23 reaction liquid product only di-*n*-butyl disulfide is detected when neither catalyst nor olefin was present.

3. Tetrahydrothiophene is fairly stable at reaction conditions employed in this study. Reaction between tetrahydrothiophene and 1 – hexene both in presence (set – 24) and absence (set – 26) of SIRAL®40 mainly resulted in isomerization of 1-hexene.

4. Benzyl phenyl sulfide and dibenzyl sulfide converts entirely to products in every set of reactions conducted in this study. No catalyst was needed for the thermal decomposition.

5. Benzyl phenyl sulfide transforms preferentially to diphenyl sulfide at the reaction conditions employed in this study. This indicates the formation of new C-S bond after scission of existing C-S bond.

155

6. Benzyl phenyl sulfide in presence of catalyst (set – 29) leads to formation of sulfur containing poly-aromatic compounds which is not present in case of similar reaction (set – 33) of dibenzyl sulfide.

7. Scission of C-S bond is observed in case of dibenzyl sulfide. Presence of catalyst results into formation of sulfur free molecules as evident in the molecules identified in liquid products of set - 32 and set – 33 reactions. Heating dibenzyl sulfide alone results into rearrangement of aromatic rings around the sulfur atom.

8. Diphenyl sulfide was found to be fairly stable at reaction conditions employed for this study.

5.6. References

1. Mao, X. Alkylation of asphaltenes; MSc thesis, University of Alberta, Edmonton, AB, Canada, **2015**

2. Faragher, W. F., Morrell, J. C., Comay, S. Thermal Decomposition of Organic sulfur Compounds. *Ind. Eng. Chem.* **1928**, vol 20, no. 5, 527-532.

3. Gee, J. C., Williams, S. T. Dimerization of linear olefins on Amberlyst® 15: Effects of chain length and double bond position. *J. Catal.* **2013**, 303, 1-8

4. O'Connor, C. T., Kojima, M. Alkene Oligomerization. Catal. Today **1990**, 6, 3, 329-349.

5. Xia, D., Tian, Y., Zhu, G., Xiang, Y., Luo, L., Huang, T. T. S. Theoretical and Experimental Studies on the Thermal Cracking of Tetrahydrothiophene, *Energy Fuels* **2007**, 21 (1), 1-6

6. Katritzky, A. R., Lapucha, A. R., Greenhill, J. V., Siskin, M. Aqueous High-Temperature Chemistry of Carbon- and Heterocycles. 13 Sulfides and Disulfides. *Energy Fuels* **1990**, 4, (5), 562-571

7. Horton, A. W. The Mechanism of the Reactions of Hydrocarbons with sulfur. *J. Org. Chem.* **1949,** 14 (5), 761-770.

8. Hanson, K. L., Engel, A. J. Kinetics of Xylene Isomerization over Silica-Alumina Catalyst. *AIChE J.* **1967**, 13 (2), 260-266

6. Final Conclusion and future work

This chapter presents the conclusions drawn from this work and provides some suggestions on future work. To put this into perspective it is useful to restate the objective for the work. The objective of this work was to explore C-S bond scission in organosulfur compounds using two approaches. The first approach was the reaction with methyl iodide and the second approach was reaction with an olefin in the presence of an acid catalyst.

6.1. Final Conclusions

The reaction of methyl iodide (CH_3I) with organosulfur compounds was investigated because CH_3I is capable of adding to aliphatic sulfur to form a sulfonium intermediate that decomposes to form the most stable carbocation. Following evidence in literature it was postulated that with approximately 30 % aliphatic sulfur in asphaltenes this would be a viable pathway for converting a fraction of asphaltenes into a sulfur-free and paraffin soluble oil. There were three aspects investigated that led to the conclusions reported here, namely, the influence of the type of solvent medium, the nature of reactions with model sulfur compounds, and the application of the reaction to the conversion of asphaltenes.

- THF and DMF, two promising solvents, were separately kept in contact with CH_3I at 75 °C for 24 hours. The reaction temperature was the same as was envisioned for the conversion of model compounds and asphaltenes. Only 3-ethyl-3-pentanol was detected in liquid product after reaction with THF. In case of DMF no reaction was observed. DMF was therefore selected as solvent for the model organosulfur compound study.

- Thioethers (both aliphatic and cyclic) react with CH_3I resulting in C-S bond cleavage.

- C-S bonds where the sulfur is directly attached to aromatic ring do not react with CH_3I as it was observed when Benzyl phenyl sulfide was reacted with CH_3I at the reaction condition in this work.

- Dibenzothiophene was reacted with CH_3I at ambient pressure and at elevated pressure. Dibenzothiophene remained unreacted in both cases.

- The reaction between CH_3I and asphaltenes proved ineffectual to convert asphaltenes into sulfur-free and paraffin soluble products. The separated solid product after reaction of asphaltenes with CH_3I was analyzed using TGA. The reaction affected the mass loss behavior of product in the range of 250 to 350 °C. Using the iodine content of the product sample before and after TGA, it can be inferred that the mass loss in sample during TGA is mainly due to removal of iodine. Some iodine remained in the product even after pyrolysis.

  The acid catalyzed conversion of asphaltenes in the presence of olefins was studied following on the promising results obtained in an earlier study. It was of interest to better understand the type of reactions that could have led to partial conversion of asphaltenes to paraffin soluble products. Different classes of model organosulfur compounds were studied to determine the relative contributions of thermal conversion and acid catalyzed conversion in the presence and absence of a model olefin.

- Presence of 1-hexene and catalyst facilitate significant C-S bond cleavage in case of aliphatic sulfide. When di-*n*-butyl sulfide was heated to 325 °C in absence of catalyst and 1-hexene, only di-*n*-butyl disulfide was detected as product. Acid catalyzed conversion in the presence of 1-hexene facilitated the cleavage of the C-S bonds and substitution of C_4 chains with C_6 chains.

- Tetrahydrothiophene was fairly stable at reaction conditions employed in this study. Reaction between tetrahydrothiophene and 1-hexene both in presence and absence of catalyst resulted mainly in isomerization of 1-hexene.

- Benzyl phenyl sulfide and dibenzyl sulfide convert entirely to products in every set of reactions that were conducted in this study. Benzyl phenyl sulfide transforms preferentially to diphenyl sulfide. This indicated the formation of new C-S bond after scission of existing C-S bond. Benzyl phenyl sulfide in the presence of the acid catalyst led to the formation of sulfur containing poly-aromatic compounds, which were not present in case of similar reaction of dibenzyl sulfide. Scission of C-S bond is observed in case of dibenzyl sulfide. Presence of catalyst results in the formation of sulfur free molecules as evident in the product molecules. Heating dibenzyl sulfide alone results in rearrangement of aromatic rings around sulfur atom.

- Diphenyl sulfide was found to be stable at reaction conditions employed for this study.

6.2. Suggestions for future work

Asphaltene is most complex class of hydrocarbon and continuous work on its conversion is never over emphasized. Based on this work following are the suggestions for future work.

- Methyl iodide is not effective in cleaving asphaltene into lower boiling hydrocarbon. Therefore asphaltene conversion using reaction with methyl iodide will not be investigated further.

- Alkylation reaction of asphaltenes with 1-hexene over SIRAL®40 catalyst should be further investigated for conversion of asphaltenes.

- Alkylation with 1-hexene on organosulfur compound should be further investigated with other acid catalysts. This will help in choosing appropriate acid strength for alkylation of asphaltene reaction.

- C-alkylation on aromatic carbon should be explored using organosulfur compounds such as dibenzyl sulfide and benzyl phenyl sulfide. Success of adding alkanes at aromatic carbon will increase the H:C ratio to a great extent.

BIBLIOGRAPHY

1. Alberta Energy Facts and statistics (http://www.energy.alberta.ca/OilSands/791.asp), (Accessed on 22 July, **2017**)

2. Ali, M. A.; Tatsumi, T.; Masuda, T. Development of Heavy Oil Hydrocracking Catalysts using Amorphous Silica-Alumina and Zeolites as Catalyst Supports. *Appl. Catal. A: General* **2002**, 233, 77-90.

3. Asaoka, S.; Nakata, S.; Shiroto, Y.; Takeuchi, C. Asphaltene Cracking in Catalytic Hydrotreating of Heavy Oils 2. Study of Changes in Asphaltene Structure during Catalytic Hydroprocessing, *Ind. Eng. Chem. Pro. Des. Dev.* **1983**, 22, 242-248.

4. Aske, N.; Kallevik, H.; Sjöblom, J. Determination of Saturate, Aromatic, Resin, and Asphaltenic (SARA) Components in Crude Oils by Means of Infrared and Near-Infrared Spectroscopy. *Energy Fuels* **2001**, 15, 1304-1312.

5. ASTM 6560-12; Standard Test Method for Determination of Asphaltenes (Heptane Insolubles) in Crude Petroleum and Petroleum Products. May **2012**

6. Brown, H. C.; Jungk, H. The Reaction of Benzene and Toluene with Methyl Bromide and Iodide in presence of Aluminium Bromide; Evidence for a Displacement Mechanism in the Methylation of Aromatic Compounds. *J. Am. Chem. Soc.* **1955**, 77, 5584-5589.

7. Cady, W. E.; Marschner, R. F.; Cropper, W. P. Composition of Virgin, Thermal, and Catalytic Naphthas from Mid-Continent Petroleum, *Ind. Eng. Chem.* **1952**, 44, 1859-1864.

8. Crick, F. What Mad Pursuit: A Personal View of Scientific Discovery; Alfred P. Sloan Foundation series. Basic Books: New York, **1988**; pp 150.

9. Faragher, W. F., Morrell, J. C., Comay, S. Thermal Decomposition of Organic sulfur Compounds. *Ind. Eng. Chem.* **1928**, vol 20, no. 5, 527-532.

10. Gee, J. C., Williams, S. T. Dimerization of linear olefins on Amberlyst® 15: Effects of chain length and double bond position. *J. Catal.* **2013**, 303, 1-8

11. Gray, M. R. Upgrading Oilsands Bitumen and Heavy Oil, 1st Edition; The University of Alberta Press: Edmonton, Alberta, **2015**.

12. Hanson, K. L., Engel, A. J. Kinetics of Xylene Isomerization over Silica-Alumina Catalyst. *AIChE J.* **1967**, 13 (2), 260-266

13. Hensen, E. J. M.; Poduval, D. G.; Magusin, P. C. M. M.; Coumans, A. E.; Van-Veen, J. A. R. Formation of Acid Sites in Amorphous Silica-Alumina, *J. Catal.* **2010**, 269, 201-218

14. Hofmann, I. C.; Hutchison, J.; Robson, J. N.; Chicarelli, M. I.; Maxwell, J. R. Evidence for Sulfide Links in a Crude Oil Asphaltene and Kerogens from Reductive Cleavage by Lithium in Ethylamine. *Org. Geochem.* **1992**, 19 (4-6), 371-387.

15. Horton, A. W. The Mechanism of the Reactions of Hydrocarbons with sulfur. *J. Org. Chem.* **1949**, 14 (5), 761-770.

16. Katritzky, A. R., Lapucha, A. R., Greenhill, J. V., Siskin, M. Aqueous High-Temperature Chemistry of Carbon- and Heterocycles. 13 Sulfides and Disulfides. *Energy Fuels* **1990**, 4, (5), 562-571

17. Kemp-Jones, A. V., and O. P. Strausz. Investigation of Possible Routes to Asphaltene in Nature. *Am. Chem. Soc. Div. Fuel Chem. Preprints* **1977**, 22 (3), 132-139.

18. Kenneth A. Gould, K. A. Chemical Depolymerization of Petroleum Asphaltenes. *Fuel* **1978**, 57, 756-762.

19. Lengyel, A.; Magyar, S.; Kalio, D.; Hancsók, J.; Catalytic Coprocessing of Delayed Coker Light Naphtha with Light Straight-Run Naphtha/FCC Gasoline, *Petrol. Sci. Technol.* **2010**, 28, 946-954.

20. Mao, X. Alkylation of Asphaltenes. MSc Thesis, University of Alberta, Edmonton, AB, Canada, **2015**.

21. Melpolder, F. W.; Brown, R. A.; Young, W. S.; Headington, C. E.; Composition of Naphtha from Fluid Catalytic Cracking, *Ind. Eng. Chem*. **1952**, 44 (5), 1142-1146.

22. Moschopedis, S. E.; Fryer, J. F.; Speight J. G. Investigation of Asphaltene Molecular Weights. *Fuel* **1976**, 55, 227-232.

23. Mullins, O. C.; Sheu, E. Y.; Fine Particle Society; American Chemical Society, Structures and Dynamics of Asphaltenes; Plenum Press: New York, **1998**.

24. Murray, P. M., Bellany, F., Benhamou, L., Bucar, D. K., Tabor, A. B., Sheppard, T. D. The Application of Design of Experiments (DoE) Reaction Optimization and Solvent Selection in the Development of New Synthetic Chemistry. *Org. Biomol. Chem.* **2016**, 14, 2373 – 2384.

25. NIST Chemistry WebBook, SRD 69. http://webbook.nist.gov/ (accessed on Nov 06, **2017**), Properties of methyl iodide.

26. O'Connor, C. T., Kojima, M. Alkene Oligomerization. *Catal. Today* **1990**, 6, 3, 329-349.

27. Papayannakos, N. Kinetics of Catalytic Hydrodesulfurization of a Deasphalted Oil and of the Asphaltenic and Non-Asphaltenic Fractions of a Petroleum Residue, *Appl. Catal.* **1986**, 24, 99-107

28. Payzant, J. D.; Mojelsky, T. W.; Strausz, O. P. Improved Methods for the Selective Isolation of Sulfide and Thiophenic Classes of Compounds from Petroleum. *Energy Fuels* **1989**, 3, 449-454.

29. Peng, P.; Morales-Izquierdo, A.; Hogg, A.; Strausz, O. P. Molecular Structure of Athabasca Asphaltene: Sulfide, Ether, and Ester Linkages. *Energy Fuels* **1997**, 11, 1171-1187.

30. Pomerantz, A. E., Seifert, S. J., Bake, K. D., Graddock, P. R., Mullins, O. C., Kodalen, B. G., Kirtley, S. M., and Bolin, T. B. Sulfur Chemistry of Asphaltenes from a Highly Compositionally Graded Oil Column. *Energy Fuels* **2013**, 27, 4604-4608.

31. Prado, G. H. C.; Klerk, A. D. Alkylation of Asphaltenes Using a FeCl3 Catalyst. *Energy Fuels* **2015**, 29, 4947−4955.

32. Reid, E. E. Organic Chemistry of Bivalent Sulfur. Vol. 2. Chemical Publishing Company, **1958**.

33. Savage, P. E.; Klein, M. T. Asphaltene Reaction Pathways. 2. Pyrolysis of n-pentadecylbenzen. *Ind. Eng. Chem. Res.* **1987**, 26, 488-494.

34. Schuler, B.; Meyer, G.; Peña, D.; Mullins, O.C.; Gross, L. Unraveling the Molecular Structure of Asphaltenes by Atomic Force Microscopy. *J. Am. Chem. Soc.* **2015**, 137, 9870−9876

35. Selker M. L. Kemp A. R. Reaction of Methyl Iodide with Sulfur Compounds. *Ind. Eng. Chem.* **1944,** 36 (January), 16-20.

36. Shaw, J. E. Molecular Weight Reduction of Petroleum Asphaltenes by Reaction with Methyl Iodide-Sodium Iodide. *Fuel* **1989**, 68, 1218-1220.

37. Sheu, E. Y.; Mullins, O. C. Asphaltenes: fundamentals and applications; Plenum Press: New York, **1995.**

38. Shigeru, O. Organic Chemistry of Sulfur. Plenum Press: New York, **1977**.

39. Siskin M.; Kelemen, S. R.; Eppig, C. P.; Brown, L. D.; Afeworki, M. Asphaltene Molecular Structure and Chemical Influences on the Morphology of Coke Produced in Delayed Coking. *Energy Fuels* **2006**, 20, 1227-1234.

40. Speight, J. G. Evidence for the type of Polynuclear Aromatic in Nonvolatile Fractions. In Polynuclear aromatic compounds; Ebert, L. B. Ed.; Advances in Chemistry Series; American Chemical Society: Washington, DC, **1987**.

41. Speight, J. G. Lange's Handbook of Chemistry. McGraw-Hill. 16th Edition, **2005**, Table -2.49, 2.470 - 2.494.

42. Speight, J. G.; Moschopedis, S. E. On the Polymeric Nature of Petroleum asphaltenes. *Fuel* **1980**, 59, 440-442.

43. Stull, D. R. Vapor pressure of Pure Substances Organic Compounds, *Ind. Eng. Chem.* **1947**, 39, 4, 517-540.

44. Takeuchi, C.; Fukui, Y.; Nakamura, M.; Shiroto, Y. Asphaltene Cracking in Catalytic Hydrotreating of Heavy Oils 1. Processing of Heavy Oils by Catalytic Hydroprocessing and Solvent Deasphalting, *Ind. Eng. Chem. Proc. Des. Dev.* **1983**, 22, 236-242.

45. Waldo, G. S.; Mullins, O. C.; Penner-Hahn, J. E.; Cramer, S. P. Determination of the Chemical Environment of Sulfur in Petroleum Asphaltene by X-ray Absorption, *Fuel* **1992**, 71, 53-56.

46. Wiehe, I. A. A phase-separation kinetic model for coke formation. *Ind. Eng. Chem. Res.* **1993**, 32, 2447-2454.

47. Wiehe, I. A. Process Chemistry of Petroleum Macromolecules; CRC Press: Boca Raton, **2008**.

48. Xia, D., Tian, Y., Zhu, G., Xiang, Y., Luo, L., Huang, T. T. S. Theoretical and Experimental Studies on the Thermal Cracking of Tetrahydrothiophene, *Energy Fuels* **2007**, 21 (1), 1-6

49. Zajac, G. W.; Sethi, N. K.; Joseph, J. T. Maya Petroleum Asphaltene Imaging by Scanning Tunneling Microscopy: Verification of Structure from ^{13}C and Proton Nuclear Magnetic Resonance. *Am. Chem. Soc., Div. Fuel Chem.* **1997**, 42, 423-426.

50. Zhao, A., Sparks, B. D., Kotlyar, L. S., and Chung, K. H. Reactivity of Sulphur Species in Bitumen Pitch and Residua during Fluid Coking and Hydrocracking. *Petrol. Sci. Technol.* **2002**, 20, 9-10, 1071-1085.